

STUDIES ON THE MOBILITY AND TRANSPORT OF
BARIUM PRESENT IN UNCONVENTIONAL
PETROLEUM PRODUCED WATER DISPOSED INTO
SALINE AQUIFERS

By

POUYAN LIALEKOL, EBRAHIMI

Bachelor of Science in Petroleum Exploration Engineering
Petroleum University of Technology
Abadan, Iran
2008

Master of Science in Petroleum Exploration Engineering
Sahand University of Technology
Tabriz, Iran
2011

Master of Science in Geology
Oklahoma State University
Stillwater, Oklahoma
2015

Submitted to the Faculty of the
Graduate College of the
Oklahoma State University
in partial fulfillment of
the requirements for
the Degree of
DOCTOR OF PHILOSOPHY
May, 2018

STUDIES ON THE MOBILITY AND TRANSPORT OF
BARIUM PRESENT IN UNCONVENTIONAL
PETROLEUM PRODUCED WATER DISPOSED INTO
SALINE AQUIFERS

Dissertation Approved:

Dr. Javier Vilcáez

Dissertation Adviser

Dr. Jim Puckette

Dr. Todd Halihan

Dr. David Lampert

ACKNOWLEDGEMENTS

Dedicated to:

My mother "Sima Moradi"



My father "Rouhollah Ebrahimi Lialekol"

“There are two things children should get from their parents: roots and wings”, Johann Wolfgang von Goethe. With these two things, I have been able to reach my goals in my life. Everything I have gained till now is because of the support from my parents. I thank my caring sisters, Simin, Samane, and Sara, and my brothers in law, Saber Mirzaee Ahandani and Kamyar Roshan for their love, support, and encouragement throughout my lifetime of education so far.

I would like to express my gratitude and special thanks to my Ph.D. adviser, Dr. Javier Vilcáez, for his guidance on the research study presented in my dissertation. He is knowledgeable, patient, and kind, and a wonderful human being. Sometimes the words cannot truly convey the message, and here is one of those moments. I can only say, I love my adviser and wish him the best things in his life.

“Deep in the sea are riches beyond compare. But if you seek safety, it is on the shore”, Idries Shah. I am very happy that I found Dr. Abdelsalam (my graduate coordinator at OSU) and Dr. Puckette (a member of my Ph.D. committee and my favorite professor at OSU) in the School of Geology at OSU. Thank you for your support and your open door policies.

I would like to extend my sincere thankfulness to my committee members Dr. Todd Halihan and Dr. David Lampert for their invaluable time and guidance. I would like to thank Dr. Tao Wu and Dr. Eliot Atekwana for helping me in designing the experiments and letting me use their laboratory equipment. I appreciate Dr. Estella Atekwana, Dr. Jack Pashin, and Dr. Michael Grammer for their continuous support during my studies at Oklahoma State University (OSU).

I would like to thank Dr. Milad Saidian, Dr. Hamid Rahnema, and Dr. Mahyar

Ghorbanian for counseling me about my studies at OSU and also about my future career. I also acknowledge all the support from my friends at OSU including Babak Shabani, Dr. Sahar Mohammadi, Dr. Mercy Achang, Cyrus Kian, Jenny Meng, Liang Xue, Ibukun Bode Omoleye, Tadesse Alemu, Micah Mayle, Luel Emishaw, and Afshin Aghayan. I would like to extend my gratitude to all the staff in School of Geology at OSU: Sandy Earls, Tim Sickbert, Tabitha Schneider, and lovely Heather Lindsey for their constant support. There are many other people at OSU and from other Schools who helped me to achieve my Ph.D., please forgive me if I forgot to mention your names. Last, but not least, I want to thank my Karate Master, Dr. Mansur Samadzadeh, for whose advice I am always thirsty in my life. As Shakespeare said, “I can no other answer make, but, thanks, and thanks, and ever thanks...”.

Name: POUYAN LIALEKOL, EBRAHIMI

Date of Degree: MAY, 2018

Title of Study: STUDIES ON THE MOBILITY AND TRANSPORT OF BARIUM
PRESENT IN UNCONVENTIONAL PETROLEUM PRODUCED
WATER DISPOSED INTO SALINE AQUIFERS

Major Field: GEOLOGY

Abstract:

Petroleum produced water (PPW) from unconventional oil and gas (UOG) in the USA contains heavy metals whose concentrations are in many cases hundreds of times above the USA drinking water standards. This poses an environmental risk as PPW injected into deep saline aquifers might migrate to underground source of drinking water (USDW).

For my dissertation, I have investigated the mobility and transport of barium (Ba) in sandstones and dolomites under the presence of guar gum and at typical concentrations of NaCl, Ca, and Mg in PPW from UOG reservoirs. Ba was selected because it constitutes the most common and abundant heavy metal found in the PPW from UOG reservoirs, guar gum was selected because it represents the most common organic additive used in viscosified fracturing fluids, and dolomites and sandstones were selected because they constitute the most common geological intervals containing saline aquifers where PPW is disposed in Oklahoma. To unveil the variables controlling the mobility and transport of Ba at deep saline aquifer conditions, I conducted batch and core-flooding experiments using powdered dolomites and sandstones (500-600 μm particles sizes), uniform synthetic and natural intact/fractured dolomite and sandstone core plugs (2.54 cm diameter and 4-10 cm length) at 22 and 60 °C. To interpret and understand the experimental results, I conducted computational studies using CrunchFlow and TOUGHREACT geochemical reactive transport simulators.

The results of the conducted experimental and computational studies revealed that brine salinity (NaCl) followed by the competition of cations (Ca and Mg) for binding sites, pH that results from dissolution/precipitation reactions of minerals, and to a less extent temperature control the sorption and thus the mobility of Ba in dolomites and sandstones. I found that presence of guar gum in PPW retards the transport of Ba through low permeability dolomites but not through high permeability sandstones. The higher Ba sorption levels attained in dolomites than in sandstones results in a faster transport of Ba through porous sandstones than through porous dolomites. However, the higher dispersion transport of Ba in fractured sandstones than in fractured dolomites can result in faster transport of Ba through fractured dolomites than through fractured sandstones.

The partition coefficients and reactive transport models proposed in this dissertation can be used to assess the risk of USDW contamination by Ba, on the case by case basis.

PUBLICATION DISSERTATION OPTION

This dissertation has been structured in two sections. The first section gives a brief outline of the dissertation and introduces the scientific question that we investigated in this research. This section also presents one manuscripts that have been published and two in review for publication.

Paper 1: Ebrahimi, P. and Vilcáez, J., 2018. “Unconventional Wastewater Disposal: Effect of Brine Salinity and Guar Gum on the Transport of Barium through Dolomite Rocks,” *Journal of Environmental Management*, (214), pp. 370–378.

<https://doi.org/10.1016/j.jenvman.2018.03.008>

Paper 2: Ebrahimi, P. and Vilcáez, J., 2018. “Petroleum Produced Water Disposal: Mobility and Transport of Barium in Sandstone and Dolomite Rocks,” *Science of the Total Environment*, (634), pp. 1054–1063.

<https://doi.org/10.1016/j.scitotenv.2018.04.067>

Paper 3: Ebrahimi, P. and Vilcáez, J., 2018. “Transport of Barium through Fractured Sandstone and Dolomite Rocks in Petroleum Produced Water Disposal,” to be submitted to *Science of the Total Environment*.

TABLE OF CONTENTS

Chapter	Page
ACKNOWLEDGEMENTS.....	iii
Abstract:.....	vi
PUBLICATION DISSERTATION OPTION.....	vii
TABLE OF CONTENTS.....	viii
LIST OF TABLES.....	xii
LIST OF FIGURES.....	xiii
CHAPTER I.....	1
INTRODUCTION.....	1
1.1. Motivation.....	1
1.2. Significance.....	4
1.3. Organization of the Dissertation.....	4
1.4. List of Publications.....	6
1.4.1. Published at or Submitted to Peer Reviewed Journals.....	6
1.4.2. Conference Proceedings and Abstracts.....	7
1.5. References.....	8
CHAPTER II.....	11
EFFECT of BRINE SALINITY and GUAR GUM on the TRANSPORT of BARIUM THROUGH DOLOMITE ROCKS: IMPLICATIONS for UNCONVENTIONAL OIL and GAS WASTEWATER DISPOSAL.....	11
2.1. Abstract.....	11
2.2. Introduction.....	13
2.3. Materials.....	16
2.3.1. Dolomite rock samples.....	16
2.3.1.1. Powdered rocks.....	19

2.3.1.2. Uniform synthetic core plugs.....	20
2.3.1.3. Natural core plugs.....	21
2.3.2. Brine solution.....	21
2.4. Methods.....	21
3.1. Batch experiments.....	21
3.2. Core-flooding experiments.....	22
2.5. Results and discussions.....	24
4.1. Effect of salinity and guar gum on the sorption of Ba on dolomite.....	24
4.2. Modeling of Ba sorption on dolomite.....	29
4.3. Effect of salinity and guar gum on the transport of Ba through dolomite rocks.....	37
2.6. Conclusions.....	42
2.7. Acknowledgements.....	44
2.8. References.....	44
CHAPTER III.....	51
PETROLEUM PRODUCED WATER DISPOSAL: MOBILITY and TRANSPORT of BARIUM in SANDSTONE and DOLOMITE ROCKS.....	51
3.1. Abstract.....	51
3.2. Introduction.....	52
3.3. Materials and methods.....	55
3.3.1. Sandstone and dolomite rock samples.....	55
3.3.2. Powdered rocks.....	57
3.3.3. Natural rock cores.....	58
3.3.4. Uniform Synthetic rock cores.....	58
3.3.5. Produced water.....	59
3.3.6. Batch sorption experiments.....	59
3.3.7. Core-flooding experiments.....	60
3.4. Results and discussion.....	60
3.4.1. Sorption of Ba in dolomites and sandstones.....	60
3.4.1.1. Effect of temperature.....	61

3.4.1.2. Effect of salinity.....	64
3.4.1.3. Effect of cations competition	65
3.4.1.4. Effect of guar gum	68
3.4.1.5. Effect of pH.....	71
3.4.2. Transport of Ba through sandstone and dolomite	75
3.4.3. Modeling of Ba transport through dolomite and sandstone	80
3.5. Conclusions.....	87
3.6. Acknowledgements.....	88
3.7. References.....	88
CHAPTER IV	92
TRANSPORT of BARIUM through FRACTURED SANDSTONE and DOLOMITE ROCKS in PETROLEUM PRODUCED WATER DISPOSAL.....	92
4.1. Abstract.....	92
4.2. Introduction.....	93
4.3. Materials	96
4.3.1. Natural Porous Rocks with/without Synthetic Fractures	96
4.3.2. Synthetic Petroleum Produced Water	98
4.4. Experimental Setup.....	98
4.5. Results and Discussion	100
4.6. Conclusions.....	115
4.7. Acknowledgment	116
4.8. References.....	116
CHAPTER V	120
CONCLUSIONS AND RECOMMENDATIONS	120
5.1. Conclusions.....	121
5.1.1. Effect of brine salinity and guar gum on the transport of barium through dolomite rocks: implications for unconventional oil and gas wastewater disposal.....	121
5.1.2. Petroleum produced water disposal: mobility and transport of barium in sandstone and dolomite rocks	122

5.1.3. Transport of Barium through Fractured Sandstone and Dolomite Rocks in Petroleum Produced Water Disposal.....	123
5.2. Recommendations for Future Studies	124
VITA.....	1

LIST OF TABLES

Table	Page
Table 2. 1. Surface complexation reactions of dolomite after Pokrovsky et al. (1999).....	30
Table 2. 2. Initial conditions for surface complexation simulations	31
Table 2. 3. Aqueous phase equilibrium complexation reactions.	32
Table 3. 1. Properties of prepared synthetic rock cores.	58
Table 3. 2. Composition of water solutions, obtained equilibrium Ba sorption, and partition coefficients (K_d).	61
Table 3. 3. Injection and initial conditions used to simulate the transport of Ba through dolomite and sandstone rock cores.	82
Table 3. 4. Transport properties of the synthetic rock cores.	82
Table 3. 5. Aqueous phase equilibrium complexation reactions.	82
Table 4. 1. Core plug properties and solution composition used in core flooding experiments. Ba concentration kept constant at 100 mg/L.	100

LIST OF FIGURES

Figure	Page
Fig 2. 1. Graphical abstract	12
Fig 2. 2. Arbuckle outcrop, Missouri	16
Fig 2. 3. Analysis of dolomite rocks collected from outcrops of the Arbuckle formation. (A) X-ray powder diffraction (XRD) analysis and (B) Micro-CT scan analysis.	18
Fig 2. 4. Scanning electron microscope (SEM) analysis of dolomite rocks collected from outcrops of the Arbuckle formation.....	19
Fig 2. 5. Uniform synthetic core plug preparation: (1) Powdering dolomite rocks, (2) Sieving, (3) Mixing with deionized water, (4) and (5) Front and bottom views of the mold, (6) Uniaxial compaction apparatus, and (7) Uniform synthetic dolomite core plug wrapped with aluminum foil.....	20
Fig 2. 6. Batch experiment setup.	22
Fig 2. 7. Core-flooding experimental setup: (1) Water tank, (2) Dual piston Chrom Tech-HPLC pump, (3) Hand pump, (4) Floating piston accumulator containing brine, (5) Confining pump, (6) Pressure transducer, (7) Hassler type core holder, (8) Chronometer, (9) Water tank, (10) Fraction collector, (11) Confining pressure port, (12) Viton sleeve, (13) Fluid injection/production port..	23
Fig 2. 8. Batch sorption experimental results. (A) Effect of brine salinity on the sorption of Ba (100 mg/L) using 500-600 μm particle size, (B) Effect of Mg (1,000 mg/L) and Ca (5,000 mg/L) on the sorption of Ba (100 mg/L) using 150-212 μm particle size. (C) Effect Mg (1,000 mg/L), Ca (5,000 mg/L) and brine salinity (90,000 mg-NaCl/L) on the sorption of Ba (100 mg/L) using 150-212 μm particle size.....	25
Fig 2. 9. Batch sorption experimental results. Effect of guar gum (GG) on the sorption of Ba (100 mg/L) on dolomite using 500-600 μm particle size. At brine salinities of (A) 0 mg-NaCl/L, (B) 18,000 mg-NaCl/L, (C) 90,000 mg-NaCl/L, and (C) 180,000 mg-NaCl/L.	28
Fig 2. 10. Comparison between experimental and simulated results. (A) Sorption isotherms of Ba on dolomite, and (B) pH profiles at brine salinities of 0 and 18,000 mg-NaCl/L, using 500-600 μm particle size.	33
Fig 2. 11. Simulation results. (A) Concentration profiles of hydration sites on dolomite, (B) Concentration profiles of Ca, Mg and Ba in solution, (C) Concentration profiles of chloro-complexes of Ca and Ba in solution, and (D) Saturation index profile. At a brine salinity of 18,000 mg-NaCl/L, and using 500-600 μm particle size.....	35

Fig 2. 12. Breakthrough curves of Ba through natural dolomite core plugs at a brine injection rate is 0.05 ml/min. (A) Effect of brine salinity in the absence of guar gum (GG), (B) Effect of guar gum at a brine salinity of 18,000 mg-NaCl/L, and (C) Pressure build up at the inlet of the core-holder at a brine salinity of 18,000 mg-NaCl/L and 50 mg-GG/L.....	38
Fig 2. 13. Breakthrough curves of Ba through synthetic dolomite core plugs at a brine injection rate is 0.05 ml/min. (A) Effect of flow properties at a brine salinity of 180,000 mg-NaCl/L and 0 g/L of guar gum (GG), (B) Effect of brine salinity in the absence of guar gum (0 mg-GG/L), and (C) and (D) Effect of guar gum at a brine salinity 180,000 mg-NaCl/L. 150-212 and 500-600 μ m particle size: 25% porosity and 9.6 mD permeability. 500-600 μ m particle size: 29.6% porosity and 13.7 mD permeability.....	41
Fig 3. 1. Graphical abstract.....	52
Fig 3. 2. Thin-section photomicrograph and XRD analysis of sandstone (A and C) and dolomite (B and D) samples used in this study.....	57
Fig 3. 3. Representative batch sorption experimental results: Effect of salinity and temperature on Ba sorption on dolomite and sandstone (500-600 μ m particle size).....	64
Fig 3. 4. Effect of cations (Ca and Mg) competition, salinity (NaCl), and temperature on the sorption of Ba on dolomite and sandstone.....	68
Fig 3. 5. Effect of guar gum (GG), salinity (NaCl) and temperature on the sorption of Ba on sandstone and dolomite.....	71
Fig 3. 6. Representative pH profiles of batch sorption experiments: Effect of temperature and rock type on pH.....	74
Fig 3. 7. Breakthrough curves of Ba through synthetic dolomite (P1) and sandstone (P2) cores (Table 3.1) at 22 °C. Injection flow rate of the solution of different compositions is 0.05 mL/min.	76
Fig 3. 8. Breakthrough curves of Ba through synthetic dolomite (P1) cores (Table 3.1) at 60 °C. Injection flow rate of the solution of different compositions is 0.05 mL/min.	78
Fig 3. 9. Breakthrough curves of Ba through natural dolomite and sandstone cores at 22 °C. Injection flow rate of the solution of different compositions is 0.05 mL/min.	79
Fig 3. 10. Hassler type core-holder used for experiments, and simulation of the core-flooding experiments of Ba transport through a dolomite core: Equilibrium Ba sorption distribution.....	85
Fig 3. 11. Experimental versus numerical breakthrough curves of Ba transport through porous dolomite and sandstone cores.	86
Fig. 4. 1. Graphical abstract.....	93
Fig. 4. 2. Representative core plug, synthetic fractures and photomicrograph analysis of sandstone and dolomite	97
Fig. 4. 3. Core-flooding experimental setup: (1) Water tank, (2) Dual piston Chrom Tech-HPLC pump, (3) Hand pump, (4) Floating piston accumulator containing brine, (5) Confining pump, (6) Pressure transducer, (7) Hassler type core holder, (8) Chronometer, (9) Water tank, (10) Fraction collector, (11) Confining pressure port, (12) Viton sleeve, (13) Fluid injection/production port..	99

Fig. 4. 4. Core flooding experiments results using intact and fractured sandstone and dolomite plugs..... 105

Fig. 4. 5. Discretization of the fractured core plug. The central mesh (orange color) is representative of a fracture line with permeability and porosity of fracture..... 110

Fig. 4. 6. Experimental versus numerical breakthrough curves of Ba transport through intact/fractured dolomite and sandstone cores..... 114

CHAPTER I

INTRODUCTION

1.1. Motivation

Recent development in horizontal drilling combined with hydraulic fracturing techniques have led to an increase in production from low permeable conventional and unconventional oil and gas (UOG) reservoirs (Ebrahimi, 2015, Jaiswal et al., 2014). Flowback and produced water (wastewater) from UOG reservoirs contains heavy metals whose concentrations are in many cases hundreds of times above the US drinking water standards (Chapman et al., 2012). High concentrations of heavy metals in wastewater, is due to the primary dissolution of formation salt and the direct communication of formation fluid into a more permeable hydraulic fractured zone (Blauch et al., 2009).

Injection of wastewater from gas shale into deep saline aquifers is a common management practice to prevent the pollution of underground sources of drinking water (USDW) with heavy metals. However, the common occurrence of permeable pathways (e.g. induced and natural fractures) overlying deep saline aquifers is raising serious concerns regarding the possibility of USDW contamination with heavy metals due to the lateral and upward migration of wastewater. Recent studies claim that the upward migration of brine has caused the pollution of USDW by heavy metals (Button, 2010). Definitive evidence, however, is constrained to isotopic composition analysis of USDW which reflect the composition of deep formation brines.

The confirmation or rejection of increasingly growing claims regarding the pollution of USDW with heavy metals, requires a scientifically sound understanding of the variables and interactions that control the transport of heavy metals at deep geological formation conditions where wastewater is disposed. Our current knowledge regarding the transport of heavy metals through fractured and porous media is constrained to shallow subsurface environments. Fundamental differences between shallow and deep subsurface environments arise from the different reactivity and geochemical composition of the mineral phase, different porosity/permeability properties, different water phase composition, and different temperature and pressure conditions.

In general, the transport of heavy metals through a porous media is controlled by mechanical and chemical mechanisms. A mechanical mechanism is the result of solute transfer by advective, dispersive and diffusive movement along a rock with low and high permeability. A chemical mechanism is the result of transfer of a solute from the liquid phase to the solid phase because of the multiple chemical reactions between transporting fluid and the rock (Kazemi and Takbiri-Borujeni, 2015a, b, 2016). Our knowledge about the mechanical and chemical transport of heavy metals in deep saline aquifers injected with wastewater is very limited.

Wastewater is characterized by high total dissolved salt (TDS) levels and variable concentrations of organic compounds. TDS includes heavy metals (e.g., Ba, As, Se and Sr). Organic compounds in wastewaters could be sourced from fracturing fluids containing multiple organic additives such as solvents, viscosifiers, biocides, scale inhibitors, friction reducers, surfactants and other biodegradable organic additives. Information on the controlling variables of sorption processes of organic additives and heavy metals on carbonate minerals such as dolomites at temperature and pressure conditions of deep saline aquifers is currently not available in literature.

Among the many organic additives of fracturing fluids, viscosifiers are believed to play a major role on the transport of heavy metals through fractured and porous media of deep saline aquifers.

Viscosifiers are added to allow for better proppant suspension and transport into developing fractures, however it is very well-known that viscosifiers can also work as a sorbing or complexing phase increasing the mobility of heavy metals (Comba et al., 2011; Kocur et al., 2013; Krol et al., 2013; Xue and Sethi, 2012). Organic polymers such as carboxy-methyl-cellulose, starch, xanthan gum and guar gum are commonly used to improve mobility of inorganic oxidizers (e.g. nanoscale zerovalent iron) in shallow aquifers (Comba et al., 2011; Kocur et al., 2013; Krol et al., 2013; Tosco et al., 2014; Velimirovic et al., 2012; Xue and Sethi, 2012). A common treatment to reduce the organic matter content in gas shale wastewater is biodegradation. However, contrary to expectations, because of the high salt content of wastewater which inhibits microbial activity, a complete removal of viscosifiers such as guar gum using biological methods is difficult to achieve (Doudoroff, 1940; Kaith et al., 2015; Lester et al., 2013).

This dissertation focuses on the transport of Ba through fractured and porous media of sandstone and dolomite rocks in brine containing guar gum at deep geological formation conditions (high pressure and high temperature) of disposal wells. I selected Ba because it is the most common and abundant heavy metal found in wastewater. Reported concentrations of Ba in wastewater from major shale gas plays including the Utica-Point Pleasant, Marcellus, Woodford, Fayetteville, Bakken, Barnett, Haynesville-Bossier, Eagle Ford, and Niobrara shales ranges from 3.6-15,700 mg/L (McBroom, 2013; Rozell and Reaven, 2012), which is considerably higher than the maximum admissible level of Ba in drinking water (2 mg/L) (EPA, 2016). I selected guar gum because it represents the most important organic additive used in viscosified fracturing fluids. And I selected dolomite and sandstone because they constitute the most common geological intervals containing saline aquifers where produced water is disposed in Oklahoma (Murray, 2015).

1.2. Significance

The gas production from shale formations in the USA, including Woodford, has been increasing dramatically from about 1 trillion cubic feet (tfc) in 2006 to more than 9.7 tfc in 2012 (Kuwayama et al., 2015). Nine out of ten natural gas wells in the USA are hydraulically fractured. Subsequently, the volume of lostwater and wastewater including their fracturing chemicals and heavy metals has been increasing. This poses environmental risk as wastewater might migrate from deep subsurface toward USDW. If organic additives of fracturing fluids such as guar gum ease the upward migration of heavy metals toward USDW, the risk of USDW contamination could increase dramatically.

To date, the role of fracturing polymers (i.e. guar gum), salinity, divalent cations (Ca, Mg), temperature, rock composition and presence of fractures in the transport of heavy metals at deep geological formation conditions of disposal wells are not known. This dissertation leads to an understanding of how the transport of Ba could be affected by guar gum, high salinity, presence of Ca and Mg, temperature, rock composition and presence of fractures at high pressure and temperature conditions of sandstone and dolomite saline aquifers. This understanding allows the assessment of the feasibility to USDW contamination by Ba subject to wastewater.

1.3. Organization of the Dissertation

This research has an experimental and a computational component. The ultimate goal of the dissertation was to develop a combined experimental and computational approach to predict and prevent the contamination of USDW by Ba contained in wastewater disposed into deep saline aquifers.

To reach this final goal, I developed an understanding of the transport mechanism and interactions that govern the transport of heavy metals in deep dolomite saline aquifers. This was done by conducting batch and core-flooding experiments. Batch experiments were conducted to assess the Ba sorption capacity of sandstone and dolomite rocks under the presence of guar gum, high salinity and the most

common divalent ions (Ca, Mg) in wastewater, and core-flooding experiments were carried out to assess the effect of sorption on the transport of Ba through synthetic, intact and fractured sandstone and dolomite core plugs. Experiments were conducted at deep saline aquifer temperature (at 22 and 60 °C) and pressure conditions. The obtained information from batch and core-flooding experiments were used to formulate and calibrate a core-scale reactive transport model to predict the transport of Ba through fractured and porous sandstone and dolomite rocks. This research utilized flowback water from Woodford shale gas reservoirs, the sandstone rocks are from shallow cores (<300 m) drilled through the Raton Formation in the Las Animas County, Colorado, and the dolomite rocks are from outcrops of the Arbuckle Group, McDonald County, Missouri.

This thesis consists of four chapters. Chapters 2 through 4 are three articles that are already published or submitted to peer-reviewed journals. The main results and discussions of my research are presented in these chapters. In the following, I briefly explain the subject of each chapter and highlight the main problems that are addressed:

Chapter 1 is a general introduction for the dissertation and addresses motivation and significance of the dissertation.

Chapter 2 presents the results of batch and core flooding experiments to investigate the sorption and transport of Ba through dolomite rocks at salinities and guar gum concentrations relevant to unconventional oil and gas wastewater. The experimental results are illustrated using a sorption model that accounts for surface complexation reactions on hydration sites and the kinetic dissolution of dolomite.

Chapter 3 presents the results of batch and core flooding experiments to understand the effect of salinity (NaCl), competition of cations (Ca, Mg), temperature (22 and 60 °C), and organic fracturing additives (guar gum) on the sorption and transport of Ba in dolomites and sandstones. The measured

partition coefficients (K_d) from batch experiments are used in reactive transport modeling and calibrating the results of core flooding experiments.

Chapter 4 presents the results of core flooding experiments to understand the transport of Ba through fractured sandstone and dolomite at salinities related to the unconventional oil and gas produced water.

The obtained information from chapter 2-4 have significant implications in understanding and predicting the mobility and transport of Ba in deep dolomite and sandstone saline aquifers.

Chapter 5 summarizes the main conclusions of this thesis and provides future works and recommendations.

1.4. List of Publications

1.4.1. Published at or Submitted to Peer Reviewed Journals

1. **Ebrahimi, P.** and Vilcáez, J., 2018. “Transport of Barium through Fractured Sandstone and Dolomite Rocks in Petroleum Produced Water Disposal,” to be submitted to Science of the Total Environment on May 2018.

2. **Ebrahimi, P.** and Vilcáez, J., 2018. “Petroleum Produced Water Disposal: Mobility and Transport of Barium in Sandstone and Dolomite Rocks,” Science of the Total Environment, (634), pp. 1054–1063. <https://doi.org/10.1016/j.scitotenv.2018.04.067>

3. **Ebrahimi, P.** and Vilcáez, J., 2018. “Unconventional Wastewater Disposal: Effect of Brine Salinity and Guar Gum on the Transport of Barium through Dolomite Rocks,” Journal of Environmental Management, (214), pp. 370–378. <https://doi.org/10.1016/j.jenvman.2018.03.008>

1.4.2. Conference Proceedings and Abstracts

1. Vilcáez, J., **Ebrahimi, P.** and Shabani, B. “Coupling the Disposal Of CO₂ and Produced Water From UOG Reservoirs Into Conventional Depleted Oil Reservoirs,” South-Central Section - 52nd Annual Meeting, Little Rock, Arkansas, 2018.
2. **Ebrahimi, P.** and Vilcáez, J. “Transport of Barium through Dolomite Rocks under the Presence of Guar Gum and Brine Salinities of Hydraulic Fracturing Wastewater,” AGU Annual Fall Meeting, New Orleans, Louisiana, 2017. [2017AGUFM.B11B1663E](#)
3. **Ebrahimi, P.** and Vilcáez, J. “Fate of Barium in Unconventional Wastewater Disposal through Dolomite Rocks,” 36th NABG Annual Technical Conference, Atlanta, Georgia, 2017.
4. **Ebrahimi, P.** and Vilcáez, J. “The Impact of Salinity and Guar Gum on the Transport of Barium through Fracturing Wastewater Disposal Sites in Deep Dolomite Saline Aquifers,” SPWLA Annual Symposium, Oklahoma City, Oklahoma., 2017.
5. **Ebrahimi, P.** and Vilcáez, J. “Experimental and Modeling Results of Barium Transport Through Dolomite under the Presence of High Salinity and Guar Gum of Fracturing Wastewater,” AAPG Mid-Continent Section Meeting, Oklahoma City, Oklahoma, 2017.
6. **Ebrahimi, P.** and Vilcáez, J. “Effect of Viscosifiers on Sorption and Transport of Heavy Metals in Dolomite Rocks,” American Geophysical Union, Student Showcase, Online, 2016.
7. **Ebrahimi, P.** and Vilcáez, J. “Effect of Guar Gum on the Mobility of Barium in Disposal Wells of the Arbuckle Formation,” Annual Meeting, The Geological Society of America, Denver, Colorado, (48), No.7. 2016.
8. **Ebrahimi, P.** and Vilcáez, J. “The Fate of Elevated Levels of Barium in Fracturing Wastewater Disposal Wells,” AAPG/SEG Spring Expo, Houston, Texas, 2016.

1.5. References

Blauch, M. E., Myers, R. R., Moore, T., Lipinski, B. A., and Houston, N. A., Marcellus shale post-frac flowback waters-Where is all the salt coming from and what are the implications?, in Proceedings SPE Eastern Regional Meeting 2009, Society of Petroleum Engineers.

Button, R. D., 2010, The Marcellus Shale and Public Health: University of Pittsburgh.

Chapman, E. C., Capo, R. C., Stewart, B. W., Kirby, C. S., Hammack, R. W., Schroeder, K. T., and Edenborn, H. M., 2012, Geochemical and strontium isotope characterization of produced waters from Marcellus Shale natural gas extraction: *Environmental Science & Technology*, v. 46, no. 6, p. 3545-3553.

Comba, S., Di Molfetta, A., and Sethi, R., 2011, A comparison between field applications of nano-, micro-, and millimetric zero-valent iron for the remediation of contaminated aquifers: *Water, Air, & Soil Pollution*, v. 215, no. 1-4, p. 595-607.

Doudoroff, M., 1940, Experiments on the adaptation of *Escherichia coli* to sodium chloride: *The Journal of general physiology*, v. 23, no. 5, p. 585-611.

Ebrahimi, P. L., 2015, Mechanistic models of unconventional reservoirs: Oklahoma State University.

Jaiswal, P., Varacchi, B., Ebrahimi, P., Dvorkin, J., and Puckette, J., 2014, Can seismic velocities predict sweet spots in the Woodford Shale? A case study from McNeff 2–28 Well, Grady County, Oklahoma: *Journal of Applied Geophysics*, v. 104, p. 26-34.

Kaith, B. S., Sharma, R., and Kalia, S., 2015, Guar gum based biodegradable, antibacterial and electrically conductive hydrogels: *International journal of biological macromolecules*, v. 75, p. 266-275.

Kazemi, M., and Takbiri-Borujeni, A., 2015a, An analytical model for shale gas permeability: *International Journal of Coal Geology*, v. 146, p. 188-197.

-, Predicting gas apparent permeability of shale samples: A novel analytical approach, in *Proceedings SPE Annual Technical Conference and Exhibition 2015b*, Society of Petroleum Engineers.

-, Effect of adsorption in flow of gases in organic nanopores: A molecular dynamics study 2016, *Unconventional Resources Technology Conference (URTEC)*.

Kocur, C. M., O'Carroll, D. M., and Sleep, B. E., 2013, Impact of nZVI stability on mobility in porous media: *Journal of contaminant hydrology*, v. 145, p. 17-25.

Krol, M. M., Oleniuk, A. J., Kocur, C. M., Sleep, B. E., Bennett, P., Xiong, Z., and O'Carroll, D. M., 2013, A field-validated model for in situ transport of polymer-stabilized nZVI and implications for subsurface injection: *Environmental science & technology*, v. 47, no. 13, p. 7332-7340.

Kuwayama, Y., Olmstead, S., and Krupnick, A., 2015, Water quality and quantity impacts of hydraulic fracturing: *Current Sustainable/Renewable Energy Reports*, v. 2, no. 1, p. 17-24.

Lasaga, A. C., 1984, Chemical kinetics of water - rock interactions: *Journal of Geophysical Research: solid earth*, v. 89, no. B6, p. 4009-4025.

Lester, Y., Yacob, T., Morrissey, I., and Linden, K. G., 2013, Can we treat hydraulic fracturing flowback with a conventional biological process? The case of guar gum: *Environmental Science & Technology Letters*, v. 1, no. 1, p. 133-136.

McBroom, M., 2013, *The Effects of Induced Hydraulic Fracturing on the Environment: Commercial Demands Vs. Water, Wildlife, and Human Ecosystems*, CRC Press.

Murray, K. E., 2015, Class II saltwater disposal for 2009–2014 at the annual - , state - , and county - scales by geologic zones of completion, Oklahoma: Okla. Geol. Surv. Open-File Rept. OF5-2015, p. 1-12.

Rozell, D. J., and Reaven, S. J., 2012, Water pollution risk associated with natural gas extraction from the Marcellus Shale: Risk Analysis, v. 32, no. 8, p. 1382-1393.

Tosco, T., Gastone, F., and Sethi, R., 2014, Guar gum solutions for improved delivery of iron particles in porous media (Part 2): Iron transport tests and modeling in radial geometry: Journal of contaminant hydrology, v. 166, p. 34-51.

Velimirovic, M., Chen, H., Simons, Q., and Bastiaens, L., 2012, Reactivity recovery of guar gum coupled mZVI by means of enzymatic breakdown and rinsing: Journal of contaminant hydrology, v. 142, p. 1-10.

Xue, D., and Sethi, R., 2012, Viscoelastic gels of guar and xanthan gum mixtures provide long-term stabilization of iron micro- and nanoparticles: Journal of nanoparticle research, v. 14, no. 11, p. 1239.

CHAPTER II

EFFECT of BRINE SALINITY and GUAR GUM on the TRANSPORT of BARIUM THROUGH DOLOMITE ROCKS: IMPLICATIONS for UNCONVENTIONAL OIL and GAS WASTEWATER DISPOSAL

Pouyan Ebrahimi, Javier Vilcáez*

Boone Pickens School of Geology, Oklahoma State University, Stillwater, OK 74078, USA

2.1. Abstract

This research aimed to elucidate the effect of brine salinity and guar gum on the sorption and transport of Ba in dolomite rocks collected from the Arbuckle formation in Oklahoma, US. Guar gum represents the most important organic additive used in viscosified fracturing fluids, and Ba constitutes the most common and abundant heavy metal found in unconventional oil and gas (UOG) wastewater. Batch experiments conducted using powdered dolomite rocks (500-600 μm particle size) revealed that at brine salinities of UOG wastewater, chloro-complexation reactions between Ba and Cl ions and pH changes that results from dolomite dissolution are the controlling factors of Ba sorption on dolomite. Organo-complexation reactions between Ba and guar gum, and competition of Ba with common cations (Ca and Mg) for hydration sites of dolomite, play a secondary role. This finding is supported by core-flooding experiments conducted to analyze the transport of Ba through natural and synthetic dolomite core plugs of high flow properties. The

transport of Ba through dolomite rocks of high flow properties (25-29.6% porosity, 9.6-13.7 mD permeability), increases with increasing brine salinity (0-180,000 mg-NaCl/L), while the presence guar gum (50-500 mg/L) does not affect the transport of Ba. However, core-flooding experiments conducted using natural dolomite core plugs (6.5-8.6% porosity, 0.06-0.3 mD permeability), indicates that guar gum can clog the pore throats of tight dolomite rocks retarding the transport of Ba. The mechanism of Ba sorption on dolomite is represented by a sorption model that accounts for both surface complexation reactions on three distinct hydration sites ($>CaOH_o$, $>MgOH_o$, and $>CO_3Ho$), and the kinetic dissolution of dolomite. These results are important in understanding the fate of heavy metals present in UOG wastewater disposed into deep dolomite saline aquifers.

* Corresponding author, Telephone: +1-405-744-6361. Email: vilcaez@okstate.edu

Keywords: Unconventional oil and gas wastewater; Barium; Guar gum; Dolomite; Heavy metals transport

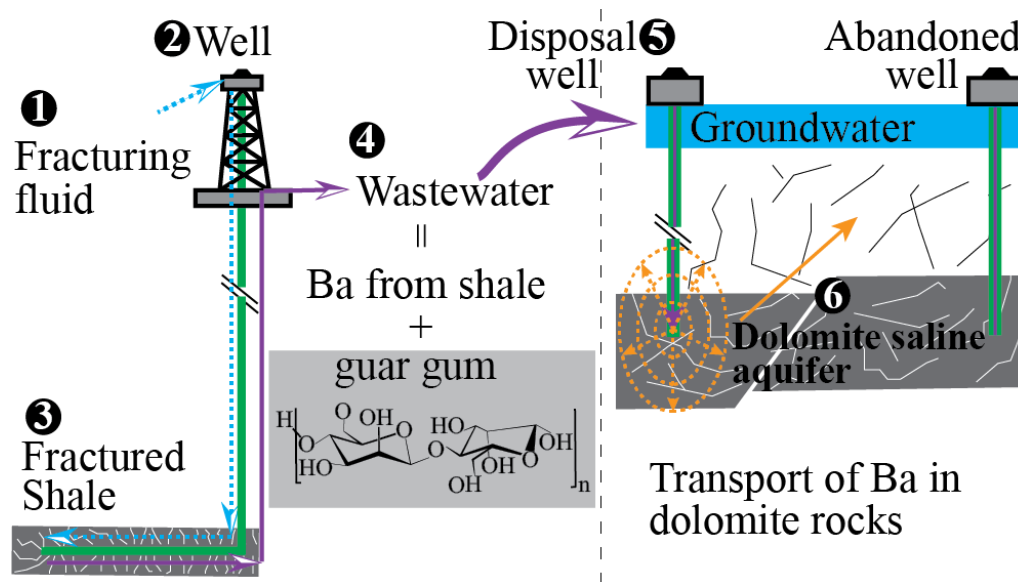


Fig 2. 1. Graphical abstract.

2.2. Introduction

Recent technological advances, combining horizontal drilling with hydraulic fracturing (HF) have led to a boom in the development of unconventional oil and gas (UOG) resources (including shale gas, coal bed methane, and tight oil) from low permeability formations (Arthur et al., 2009; Engle et al., 2014). HF involves the high-pressure injection of a fluid containing primarily water, proppant, and multiple organic additives such as solvents, viscosifiers, biocides, scale inhibitors, friction reducers, and surfactants (Ferrer and Thurman, 2015; Stringfellow et al., 2014). Typically, a large fraction of the injected HF fluid infiltrates to the geological formation, while only 10-15% of the HF fluid flows back to the surface when pressure is released (Jiang et al., 2014). The returning UOG wastewater, a combination of flowback and produced water, is stored in tanks or impoundment pits at the surface for subsequent treatment or disposal into deep geological formations. UOG wastewater is characterized by high total dissolved solids (TDS), naturally occurring radioactive materials (NORM) (Rowan et al., 2011), and variable concentrations of organic compounds (Strong et al., 2013). TDS includes heavy metals (e.g., Ba, As, Se and Sr) whose concentrations are in many cases hundreds of times above the US drinking water standards (Engle and Rowan, 2014; Haluszczak et al., 2013). Organic compounds in UOG wastewaters could be sourced from the injected HF fluids (Akob et al., 2015; Cluff et al., 2014; Orem et al., 2014). Whereas, high concentrations of heavy metals in wastewater might be due to the primary dissolution of fracture-filling and/or pore-filling evaporite minerals, or due to the direct communication of basinal brine into a more permeable hydraulic fracture zone (Blauch et al., 2009; Renock et al., 2016).

To prevent the contamination of underground sources of drinking water (USDW), UOG wastewater is frequently disposed into deep saline aquifers (Lutz et al., 2013). However, the common occurrence of permeable pathways (e.g., induced and natural fractures) overlying deep saline aquifers is raising serious concerns regarding the possibility of USDW contamination with

contaminants present in UOG wastewater (Dresel and Rose, 2010; EPA, 2012; Gadhamshetty et al., 2015; Gregory et al., 2011; Warner et al., 2012).

In order to be able to determine the physical feasibility of USDW contamination with contaminants present in UOG wastewater disposed into deep saline aquifers, a sound understanding of the factors controlling the transport of each of type of contaminant (heavy metals, NORMs and organic compounds) is needed. This research aims to elucidate the controlling factors of heavy metals transport through dolomite rocks under the presence of organic HF additives.

In general, the transport of heavy metals is to a large extent controlled by sorption (surface complexation) reactions (Appelo and Postma, 2005; Dokhani et al., 2016) of which very little is currently known for dolomite saline aquifers where UOG wastewater is commonly disposed. Among many physical and chemical factors that can affect the transport of heavy metals, organic additives such viscosifiers remaining in UOG wastewater, and brine salinity (TDS > 10,000 mg/L), is hypothesized plays an important role in the transport of heavy metals through porous media of dolomite saline aquifers injected with OUG wastewater.

This hypothesis is based on the fact that viscosifiers, which are added to allow for better proppant suspension and transport into developed fractures (Elsner and Hoelzer, 2016), have been reported to increase the mobility of heavy metals through shallow aquifers by acting as a sorbing or complexing phase (Comba et al., 2011; Kocur et al., 2013; Krol et al., 2013; Xue and Sethi, 2012). In fact, this property of viscosifiers (e.g., carboxy-methyl-cellulose, xanthan gum, and guar gum), is commonly used to improve the mobility of nanoscale zerovalent iron (NZVI) and remediate many organic contaminants (Comba et al., 2011; Gastone et al., 2014; Kocur et al., 2013; Krol et al., 2013; Phenrat et al., 2007; Tosco et al., 2014; Velimirovic et al., 2012; Xue and Sethi, 2012). Increasing brine salinity (0 - 29,220 mg/L) has been reported to increase the mobility of heavy metals (Cu, Cd, Zn, Pb and Zn) through soil materials (Acosta et al., 2011; Zhao et al., 2013).

However, the effect of brine salinity on the transport of heavy metals under the presence of organic HF additives (e.g., viscosifiers) is currently unknown.

Literature survey highlights lack of published work on the transport of heavy metals at through deep saline aquifers. Published work on the transport of heavy metals is constrained to shallow aquifers. Fundamental differences between shallow and deep saline aquifers arise from the different reactivity and geochemical composition of the mineral phase, different flow (porosity/permeability) properties and different water phase composition. This research aims to elucidate the effect guar gum and brine salinity on the transport of Ba through dolomite rocks at brine salinities of OUG wastewater. Guar gum represents the most common organic additive used in viscosified fracturing fluids. Contrary to expectations, a complete biodegradation of guar gum contained in UOG wastewater is difficult to achieve due to the high salinity of UOG wastewater that greatly decreases the activity of microbes (Lester et al., 2013). For the sake of simplicity, among the many heavy metals found in UOG wastewater, the focused of this research is on the transport of Ba, which is the most common and abundant heavy metal found in UOG wastewater (EPA, 2016; Rozell and Reaven, 2012).

Because of the discrete nature of fractures which can facilitate the upward migration of UOG wastewater, it is apparent that the transport of heavy metals through porous media connecting natural fractures plays an important role. Hence, this research aims to first understand the factors controlling the transport of heavy metals through porous dolomite rocks. With this aim, batch experiments were conducted to understand the effect of brine salinity and guar gum on the sorption of Ba on dolomite, whereas core-flooding experiments were conducted to analyze the effect of brine salinity and guar gum on the transport of Ba through natural and synthetic dolomite core plugs of homogeneous flow (porosity/permeability) properties.

2.3. Materials

2.3.1. Dolomite rock samples



Fig 2. 2. Arbuckle outcrop, Missouri.

Dolomite rocks used in this research were collected from outcrops of the Arbuckle formation (Fig. 2.2) where wastewater from oil and gas production is disposed in Oklahoma (Gadhamshetty et al., 2015). Fig. 2.3 shows representative X-rays diffraction (XRD) and Fig. 4 represents the scanning electron microscopy (SEM), and micro-CT scan analysis conducted on collected rocks. Analyses revealed that Arbuckle dolomite rocks are composed of 97% dolomite and the rest is quartz and calcite (Fig. 2.3A), grain size is 0.125-0.5 mm (red polygons in Fig. 2.4A), diameter of pores (yellow polygons in Fig. 2.4B) is <0.5 mm, and that pores are poorly connected to each other (Fig. 2.3B). Collected rocks were used to prepare three types of rocks: powdered rocks of uniform size, natural core plugs, and synthetic core plugs of uniform flow properties. Powdered rocks were used

to conduct batch experiments, whereas synthetic and natural core plugs were used to conduct core-flooding experiments.

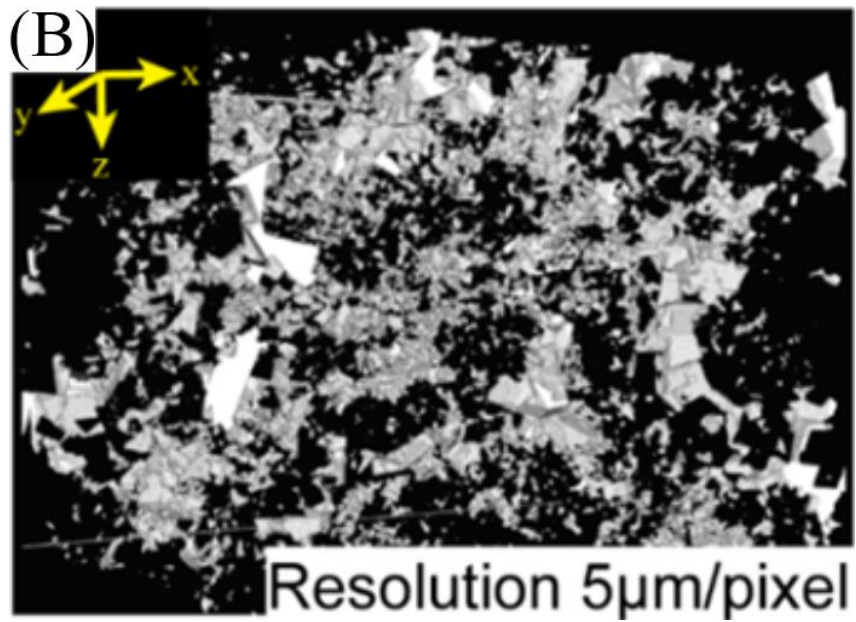
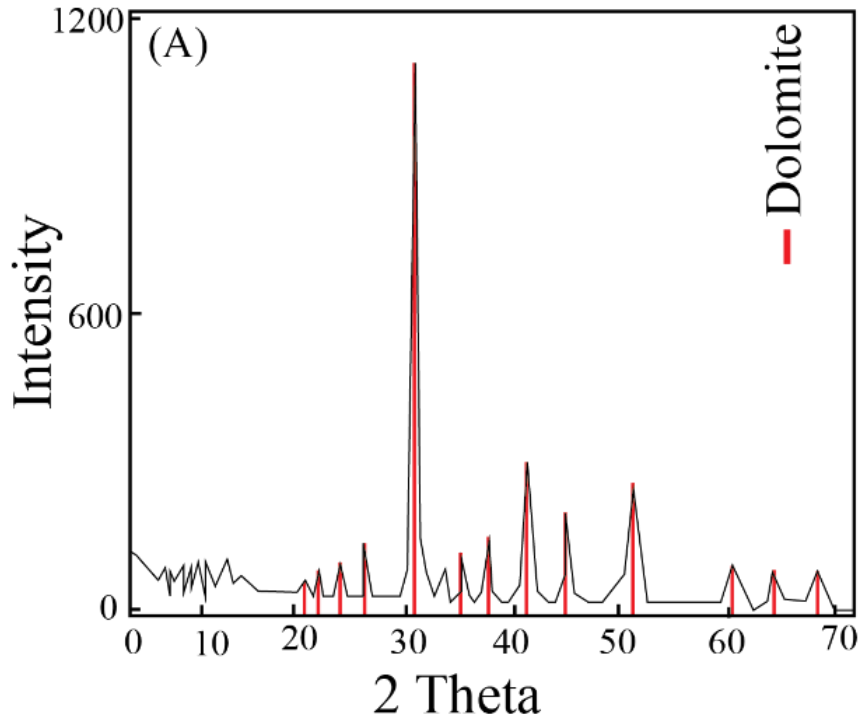
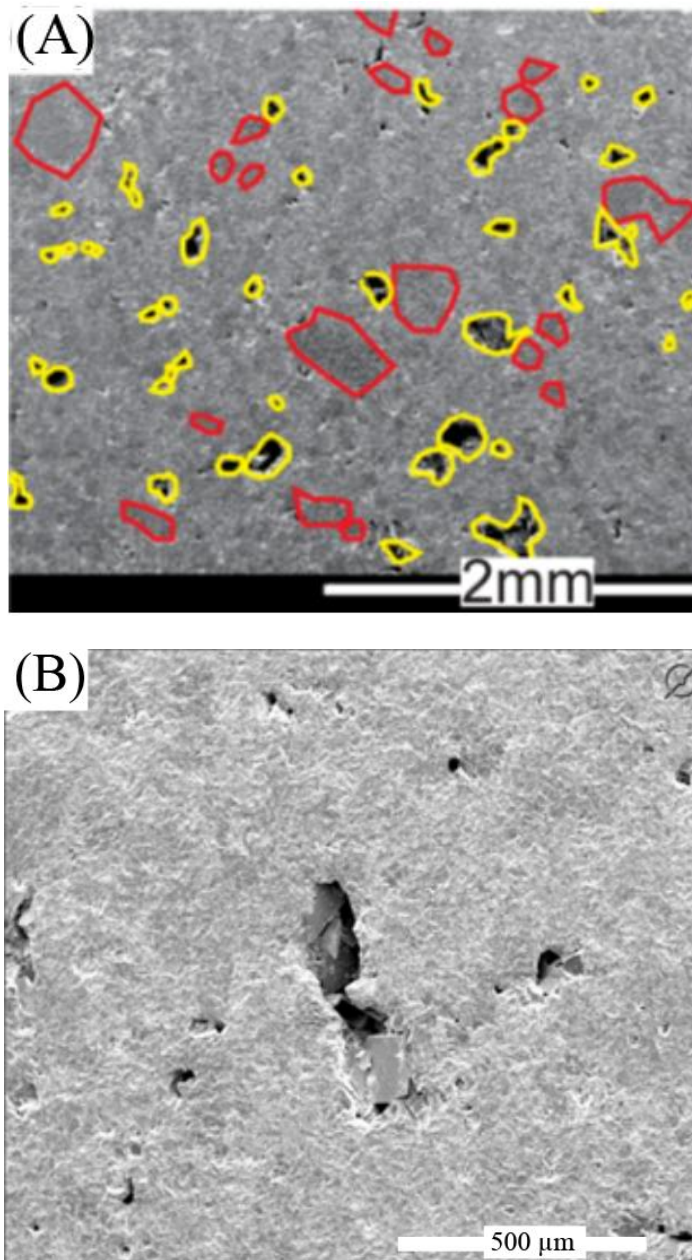


Fig 2. 3. Analysis of dolomite rocks collected from outcrops of the Arbuckle formation. (A) X-ray powder diffraction (XRD) analysis and (B) Micro-CT scan analysis.



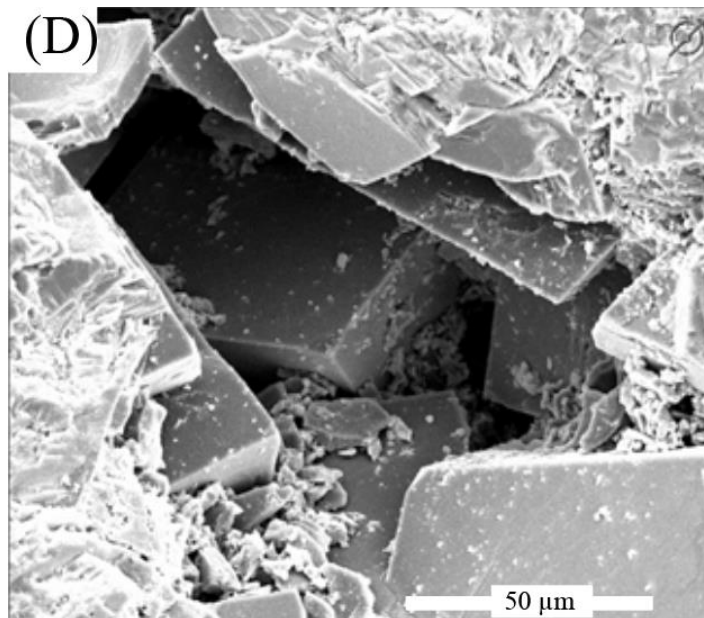
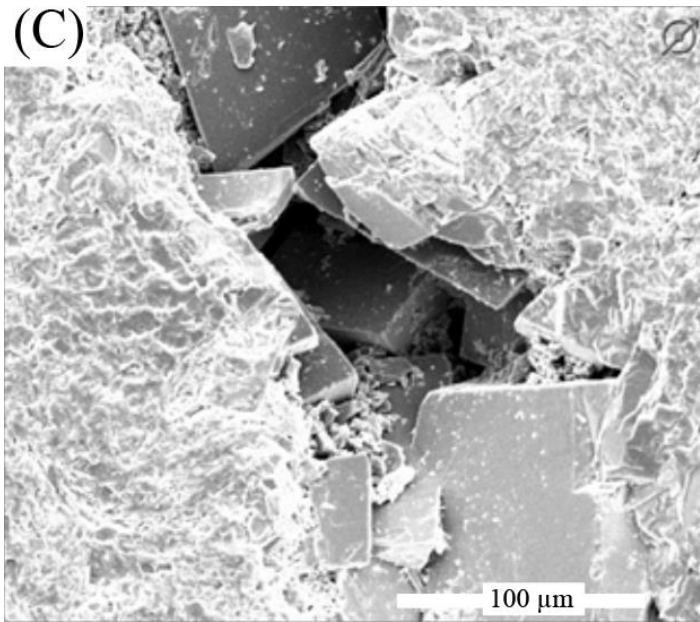


Fig 2. 4. Scanning electron microscope (SEM) analysis of dolomite rocks collected from outcrops of the Arbuckle formation.

2.3.1.1. Powdered rocks

Powdered dolomite were sieved to obtain 150-212 and 500-600 μm particles sizes. Dust from the sieved particles was removed by using an ultrasonic bath with deionized water.

2.3.1.2. Uniform synthetic core plugs

Natural dolomite rocks are tight heterogeneous porous media. In order to be able to conduct reproducible core-flooding experiments, homogeneous synthetic core plugs of high flow (porosity and permeability) properties were prepared using a uniaxial compaction apparatus (Carver Laboratory Presses, Model 4387). The procedure consisted in mixing 90 g of powdered dolomite rocks of known particle size and 9 g of deionized water (10% of dolomite weight). The resulting aggregate is poured into a stainless steel mold and compressed at 34473.79 kPa for one hour using the uniaxial compaction apparatus (Fig. 2.5). Measured length, diameter, porosity and permeability values of the prepared synthetic core plugs are 10 cm, 2.54 cm, 25% and 9.73 mD for 150-212 μm particle size, and 10, 2.54 cm, 29.6% and 13.73 mD for 500-600 μm particle size, respectively.



Fig 2. 5. Uniform synthetic core plug preparation: (1) Powdering dolomite rocks, (2) Sieving, (3) Mixing with deionized water, (4) and (5) Front and bottom views of the

mold, (6) Uniaxial compaction apparatus, and (7) Uniform synthetic dolomite core plug wrapped with aluminum foil.

2.3.1.3. Natural core plugs

Core plugs of 2.54 cm diameter and 4 cm length were drilled from the collected dolomites to analyze the transport of Ba through tight natural dolomite rocks. Measured porosities and permeabilities of the natural dolomite core plugs were 5-9% and 0.06-0.4 mD, respectively.

2.3.2. Brine solution

For simplicity, a synthetic brine solution composed of NaCl, CaCl₂·2H₂O, MgCl₂·6H₂O and BaCl₂·2H₂O (all from Fisher Scientific with >99% purity) was used. Used NaCl, Ca, and Mg concentrations correspond to measured concentrations in produced water from oil and gas fields in Oklahoma. Guar gum was provided by PFP Technology that supplies additives to hydraulic fracturing and oilfield completion companies in the US. To ensure that guar gum molecules have been hydrated properly in the synthetic brine, guar gum was added to the synthetic brine 24 hours prior to its utilization.

2.4. Methods

3.1. Batch experiments

Batch experiments were conducted to assess the effect of guar gum and brine salinity composition (NaCl, Ca and Mg) on the sorption of Ba on dolomite. Pyrex glass bottles were filled with 100 ml of synthetic brine and 40 g of powdered dolomite (Fig. 2.6). The initial concentration of Ba in all experiments was 100 mg/L. A mechanical orbital shaker was used to ensure well mixing between the powder dolomite and brine containing Ba and guar gum. To determine the sorption isotherm of Ba on dolomite, brine samples were collected periodically up to 300 minutes. Ba, Ca and Mg

concentrations in collected brine samples were measured by Inductively Coupled Plasma-Optical Emission Spectrometry (ICP-OES) analysis. Since pH is known to affect the sorption of heavy metals on minerals (Ghaemi et al., 2011; Pehlivan et al., 2009), pH changes in the brine solution was monitored through all experiments. The sorption percentage of Ba on dolomite was calculated according to:

$$\text{Sorption (\%)} = \frac{C_i - C_f}{C_i} \times 100 \quad (1)$$

where C_i and C_f are the initial and final Ba concentrations in the brine solution.



Fig 2. 6. Batch experiment setup.

3.2. Core-flooding experiments

Core-flooding experiments using a Hassler Type core holder (RCH-series of Core Laboratories) were conducted to assess the effect of brine salinity and guar gum on the transport of Ba through porous dolomite rocks at ambient temperature and a confining pressure of 20684.27 kPa. To emulate wastewater injection into a saline aquifer, prior to the injection of the synthetic brine

solution containing Na, Cl, Ca, Mg, Ba and/or guar gum, the core plug was saturated with a brine solution containing only NaCl. The synthetic brine solution was injected using a dual piston Chrom Tech-HPLC pump at constant rate of 0.05 ml/min in all core-flooding experiments. The inlet pressure of the core holder was measured using a Rosemount pressure transducer with a scale resolution of 0.48 kPa and the effluent was collected in 0.5 ml volumes every 10 minutes for 60 hours using an automated fraction collector. Collected samples were analyzed for their Ba, Ca, and Mg content by ICP-OES analysis. The core flooding setup is shown in the Fig. 2.7.

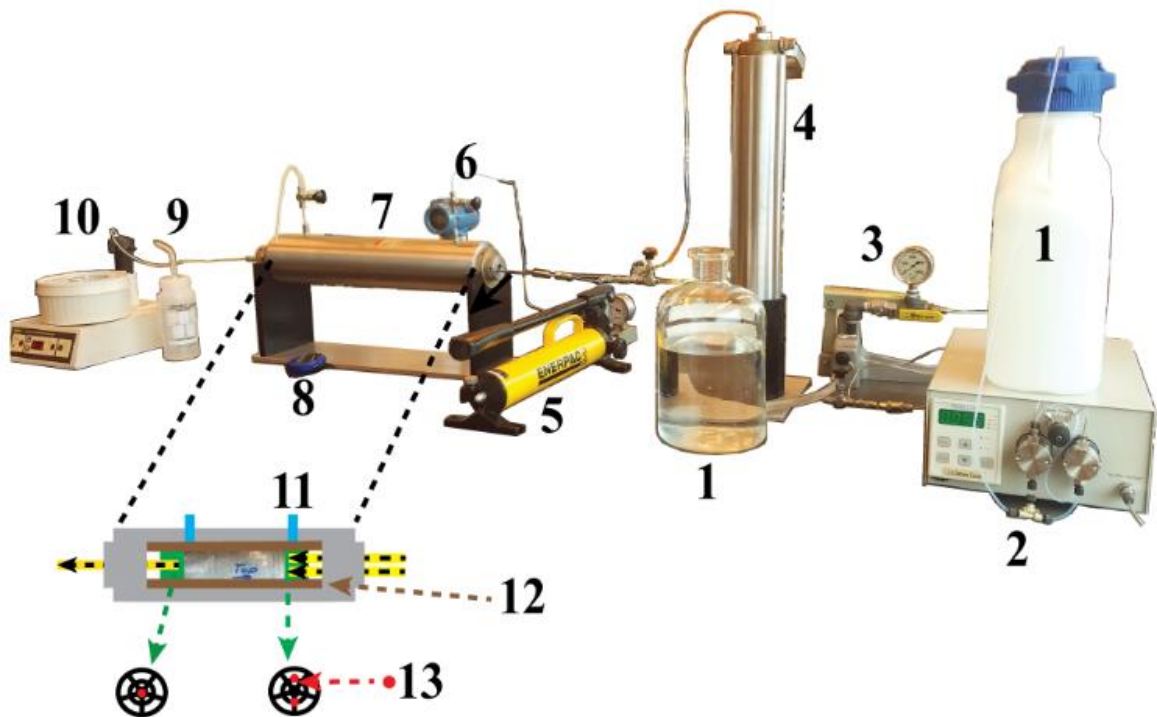
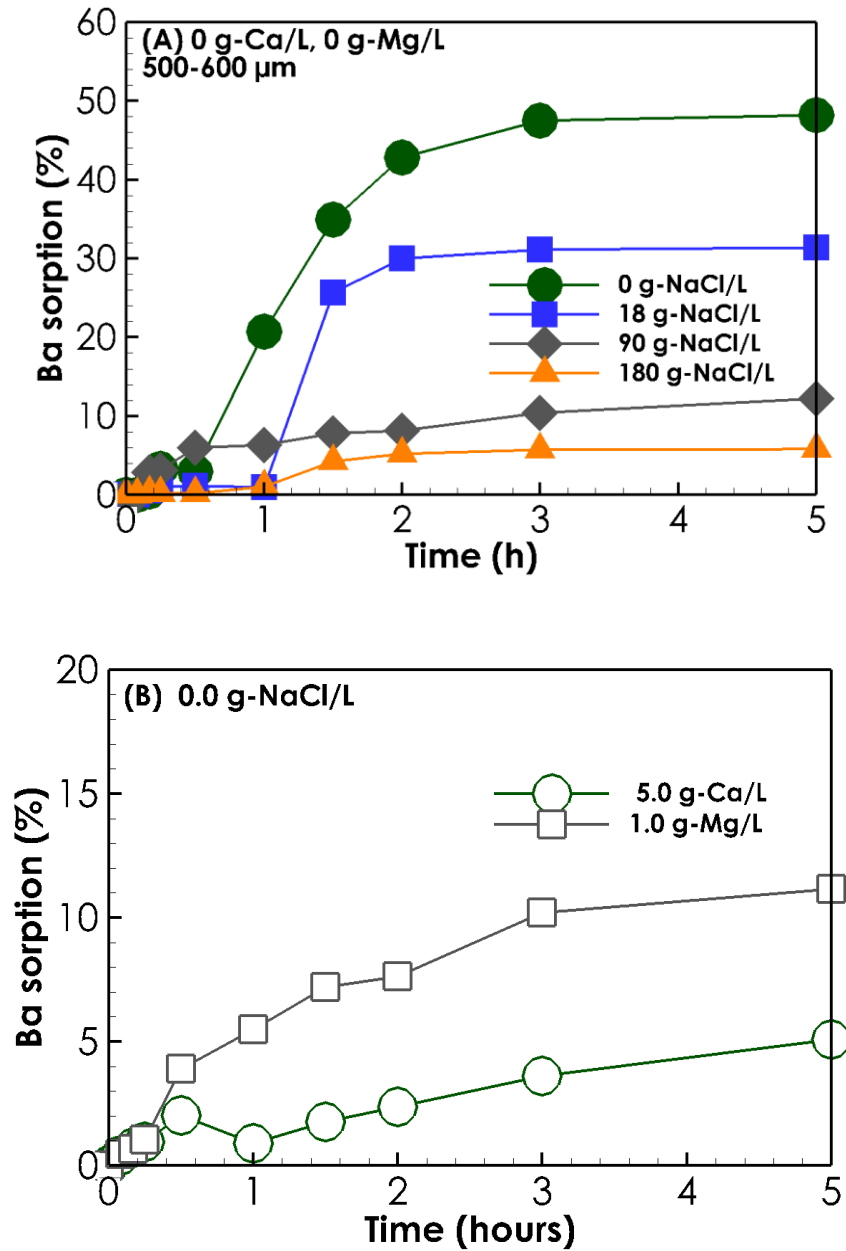


Fig 2. 7. Core-flooding experimental setup: (1) Water tank, (2) Dual piston Chrom Tech-HPLC pump, (3) Hand pump, (4) Floating piston accumulator containing brine, (5) Confining pump, (6) Pressure transducer, (7) Hassler type core holder, (8) Chronometer, (9) Water tank, (10) Fraction collector, (11) Confining pressure port, (12) Viton sleeve, (13) Fluid injection/production port.

2.5. Results and discussions

4.1. Effect of salinity and guar gum on the sorption of Ba on dolomite

This section describes the results of batch experiments conducted to analyze the effect of brine salinity composition and guar gum on Ba sorption on dolomite which has not been assessed before.



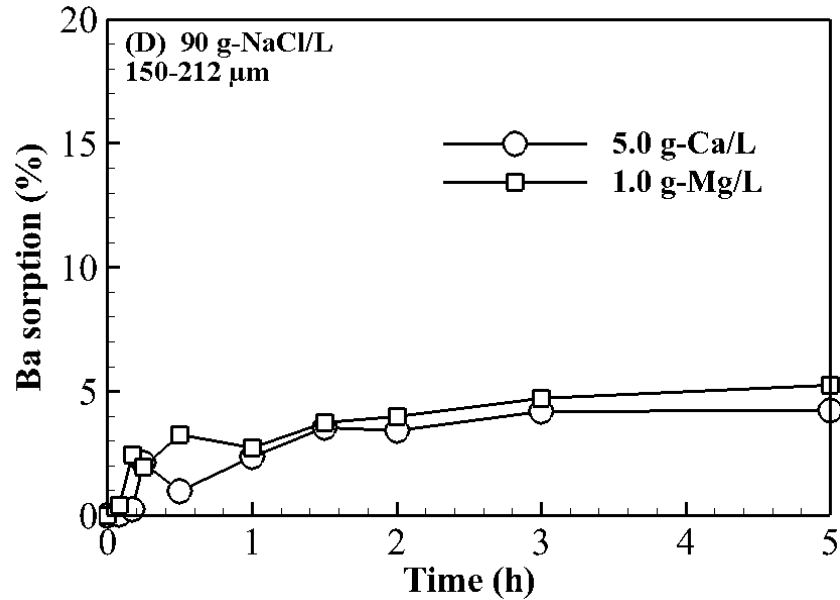


Fig 2. 8. Batch sorption experimental results. (A) Effect of brine salinity on the sorption of Ba (100 mg/L) using 500-600 μm particle size, (B) Effect of Mg (1,000 mg/L) and Ca (5,000 mg/L) on the sorption of Ba (100 mg/L) using 150-212 μm particle size. (C) Effect Mg (1,000 mg/L), Ca (5,000 mg/L) and brine salinity (90,000 mg-NaCl/L) on the sorption of Ba (100 mg/L) using 150-212 μm particle size.

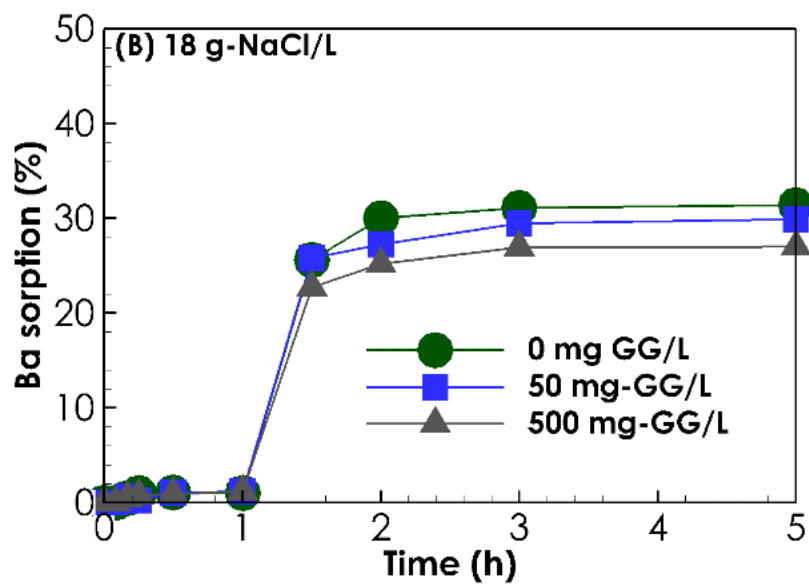
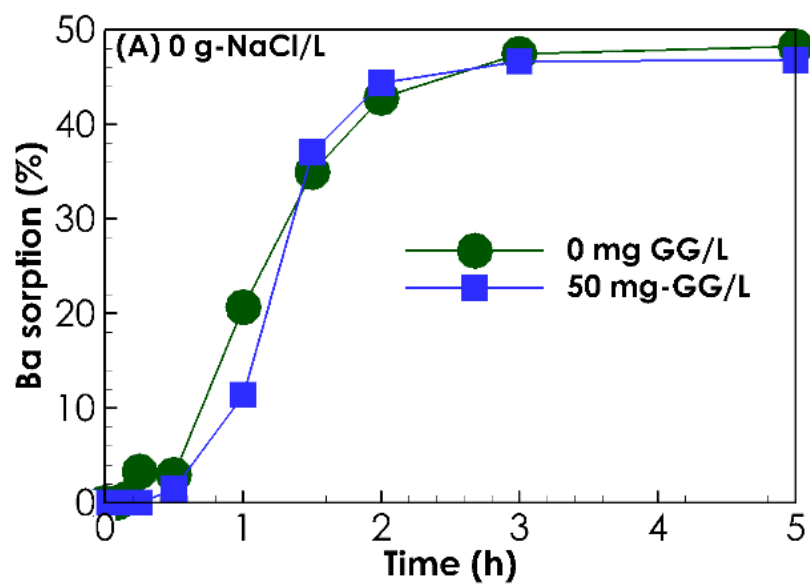
Fig. 2.8 shows representative sorption isotherms of Ba on dolomite at different brine salinity compositions. A comparison between sorption isotherms obtained with brine salinities of 0, 18,000, 90,000 and 180,000 mg-NaCl/L (Fig. 2.8A), reveals that Ba sorption on dolomite decreased with increasing brine salinity. The equilibrium sorption of Ba with 0 mg-NaCl/L is >45%, whereas with a brine salinity of 180,000 mg-NaCl/L is <5%. The effect of brine salinity in reducing Ba sorption on dolomite is explained by the following chloro-complexation reaction (Acosta et al., 2011; Hatje et al., 2003):



where the formed $\text{Ba}(\text{Cl})^+$ is less prone to be electrostatically attracted than Ba^{2+} by negatively charged hydration sites of dolomite.

At a brine salinity of 0 mg-NaCl/L, the presence of Mg (1,000 mg/L) reduced Ba sorption on dolomite from 49% (Fig. 2.8A) to 11.35% (Fig. 2.8B), whereas the presence of Ca (5,000 mg/L) reduced Ba sorption on dolomite from 49% (Fig. 2.8A) to 5.74% (Fig. 2.8B). A decrease in Ba sorption due to the presence of Mg and Ca is explained by the competition among cations for negatively charged hydration sites of dolomite. Competition among cations for hydration sites is a common phenomenon which has been widely studied for many heavy metals including Cd, Cr, Cu, Ni, Pb, and Zn, and various type of soils and geological media (Selim, 2012). Its effect on Ba sorption on dolomite at Na, Cl, Ca, and Mg concentrations of UOG wastewater had not been assessed before.

Fig. 2.8C shows sorption isotherms obtained at a brine salinity of 90,000 mg-NaCl/L under the presence of Mg and Ca. Equilibrium sorption levels of Ba decreased from 12.26% (Fig. 2.8A) to 5.23% due to the presence of Mg, and to 4.25% due to the presence of Ca. A decrease in the sorption of Ba due to the presence of Mg and Ca, suggests that both the formation of chloro-complexes of cations and competition of cations for hydration sites, contribute to the reduction of Ba sorption on dolomite. However, the relatively small reduction in the equilibrium sorption levels caused by the presence of Ca or Mg, indicates that at brine salinities of UOG wastewater (e.g., 90,000 mg-NaCl/L), chloro-complexation reactions, and thus brine salinity controls Ba sorption on dolomite rather than competition of cations for hydration sites.



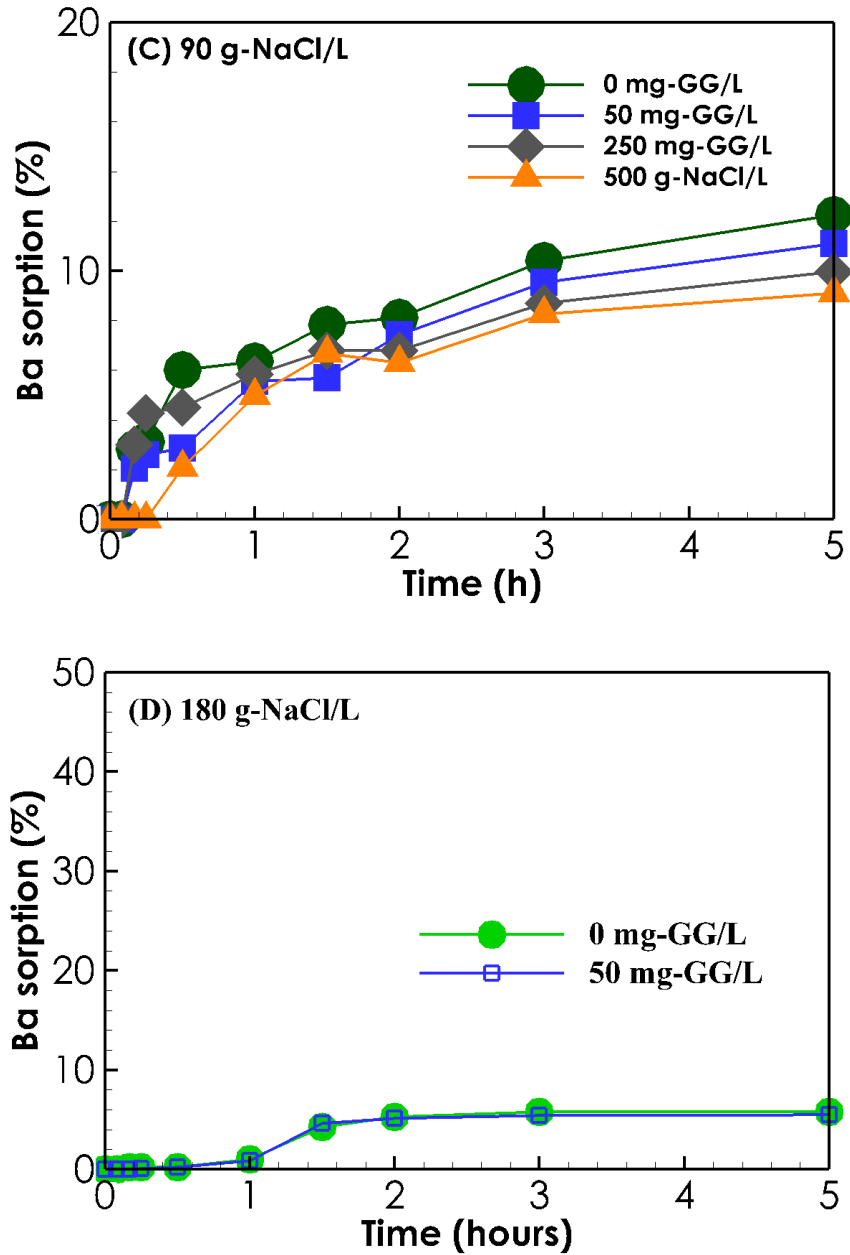


Fig 2. 9. Batch sorption experimental results. Effect of guar gum (GG) on the sorption of Ba (100 mg/L) on dolomite using 500-600 μm particle size. At brine salinities of (A) 0 mg-NaCl/L, (B) 18,000 mg-NaCl/L, (C) 90,000 mg-NaCl/L, and (C) 180,000 mg-NaCl/L.

Fig. 2.9 shows representative sorption isotherms of Ba on dolomite at three brine salinities and three guar gum concentrations. The equilibrium sorption of Ba on dolomite decreases with

increasing brine salinity regardless of the presence of guar gum in solution. These results indicate that guar gum at possible concentrations (50 - 500 mg/L) in UOG wastewater has a small effect in attenuating or promoting the sorption of Ba on dolomite. Sorption isotherms follow similar paths reaching similar equilibrium sorption levels, regardless of the presence of guar gum.

The small effect of guar gum on Ba sorption on dolomite might be due to chloro-complexation reactions between Ba and Cl ions (Eq. 2) which outcompete organo-complexation reactions between Ba and guar gum. Guar gum has many hydroxyl groups that can easily bond to cations such as Ba. For instance, guar gum is known to interact with zirconium through the formation of hydrogen and covalent bonds (Bahamdan, 2005). This property of guar gum has been suggested can be used to facilitate the transport of iron particles through soils (Gastone et al., 2014; Tosco et al., 2014).

4.2. Modeling of Ba sorption on dolomite

To confirm that at brine salinities of UOG wastewater, chloro-complexation reactions rather than organo-complexation reactions and competition of cations for hydration sites control Ba sorption on dolomite, a sorption model is formulated.

This model is formulated based on a previously surface complexation model (SCM) proposed for dolomite (Pokrovsky et al., 1999). This SCM was proposed based on surface titration and electrokinetic measurements using brine salinities up to 29,220 mg-NaCl/L. The validity of this SCM was verified through spectroscopic analysis (Pokrovsky et al., 2000), and it has been used before to explain the effect of pH on the sorption of phosphorous on dolomite (Xu et al., 2014). According to this SCM, surface complexation reactions can be written in terms of two primary hydration sites, $>MeOHo$, and $>CO_3Ho$, where Me is Ca or Mg and “>” indicates solid phase (Table 2.1).

Table 2. 1. Surface complexation reactions of dolomite after Pokrovsky et al. (1999)

Reaction on the surface of dolomite		Log K _{int} (25°C, [NaCl] = 0.0)	
		Ca	Mg
1	$> \text{CO}_3\text{H}^0 \leftrightarrow \text{CO}_3^- + \text{H}^+$	-4.8 ± 0.2	-4.8 ± 0.2
2	$> \text{CO}_3\text{H}^0 + \text{Me}^{2+} \leftrightarrow > \text{CO}_3\text{Me}^+ + \text{H}^+$	-1.8 ± 0.2	-2.0 ± 0.2
3	$> \text{MeOH}^0 \leftrightarrow > \text{MeO}^- + \text{H}^+$	-12 ± 2	-12 ± 2
4	$> \text{MeOH}^0 + \text{H}^+ \leftrightarrow > \text{MeOH}_2^+$	11.5 ± 0.2	10.6 ± 0.2
5	$> \text{MeOH}^0 + \text{CO}_3^{2-} + 2\text{H}^+ \leftrightarrow$ $> \text{MeHCO}_3^0 + \text{H}_2\text{O}$	24.0 ± 0.5	23.5 ± 0.5
6	$> \text{MeOH}^0 + \text{CO}_3^{2-} + \text{H}^+ \leftrightarrow > \text{MeCO}_3^- + \text{H}_2\text{O}$	16.6 ± 0.2	15.4 ± 0.2

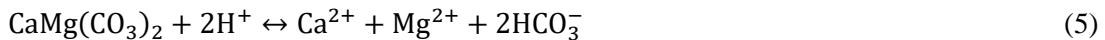
To account for the sorption of Ba, the following complexation reaction for Ba is added to the surface complexation reactions for Ca and Mg listed in Table 2.1:



with

$$K_{\text{int}} = \frac{[>\text{CO}_3\text{Ba}^+][\text{H}^+]}{[>\text{CO}_3\text{H}^0][\text{Ba}^{2+}]} \quad (4)$$

where K_{int} is the corresponding intrinsic stability constant, which is estimated by fitting the dependence of Ba sorption on brine salinity (Fig. 2.10A, 18 g-NaCl/L). Surface complexation reactions on dolomite are pH dependent, thus dolomite dissolution reaction needs to be accounted for in the model. The dissolution of dolomite reflected by an increase of pH in all conducted experiments is represented by the following reaction:



The kinetics of dolomite dissolution is represented by the transition state theory (TST) model (Lasaga, 1984):

$$-R_{\text{Dolomite}} = Ak_m [H^+] \left\{ 1 - \frac{[HCO_3^-]^2 [Ca^{2+}] [Mg^{2+}]}{[H^+] K_{eq}} \right\} \quad (6)$$

where k_m is the intrinsic rate constant, K_{eq} is the equilibrium constant of dolomite dissolution (Eq. (5)), and A is the surface area of dolomite.

The model is applied using CrunchFlow geochemical reactive transport simulator (Steeffel et al., 2005; Steefel and Molins, 2016). Table 2.2 summarizes initial conditions for the simulation of the batch sorption experiments conducted to assess the effect of brine salinity (Fig. 2.10A).

Table 2. 2. Initial conditions for surface complexation simulations

Species & parameters	Value
pH	6.0
Ca ²⁺	0-5,000 mg/L
Mg ²⁺	0-1,000 mg/L
Na ⁺	0-70,800 mg/L
Cl ⁻	Charge balance
HCO ₃ ⁻	P _{CO2} = 3.15×10 ⁻⁴ bar (Equilibrium)
Ba ²⁺	100 mg/L
>CaOH ^o	2×10 ⁻⁵ mol/m ² (Brady et al., 1999)
>MgOH ^o	2×10 ⁻⁵ mol/m ² (Brady et al., 1999)
>CO ₃ H ^o	2×10 ⁻⁵ mol/m ² (Brady et al., 1999)
Dolomite surface area	1 m ² /g (500-600 μm particle size)*
Dolomite volume fraction	0.13**
Log k_m	-9 mol/m ² /s (25°C) (Steeffel and Molins, 2016)
Log K_{eq}	2.525 (25°C) (Steeffel and Molins, 2016)
Log K_{int} (Eq. 4)	-2.33****

*Measured, **Calculated, ***Estimated (Fig. 2.10A, 18 g-NaCl/L)

Table 2.3 shows all aqueous phase complexation reactions with its corresponding equilibrium constants used for simulations.

Table 2. 3. Aqueous phase equilibrium complexation reactions.

Reaction	Log K (25°C)
$\text{OH}^- + \text{H}^+ \leftrightarrow \text{H}_2\text{O}$	13.991
$\text{CO}_2(\text{aq}) + \text{H}_2\text{O} \leftrightarrow \text{H}^+ + \text{HCO}_3^-$	-6.342
$\text{CO}_3^{2-} + \text{H}^+ \leftrightarrow \text{HCO}_3^-$	10.325
$\text{CaOH}^+ + \text{H}^+ \leftrightarrow \text{Ca}^{2+} + \text{H}_2\text{O}$	12.852
$\text{BaOH}^+ + \text{H}^+ \leftrightarrow \text{Ba}^{2+} + \text{H}_2\text{O}$	13.47
$\text{CaCO}_3(\text{aq}) + \text{H}^+ \leftrightarrow \text{Ca}^{2+} + \text{HCO}_3^-$	7.009
$\text{MgCO}_3(\text{aq}) + \text{H}^+ \leftrightarrow \text{HCO}_3^- + \text{Mg}^{2+}$	7.356
$\text{BaCO}_3(\text{aq}) + \text{H}^+ \leftrightarrow \text{Ba}^{2+} + \text{HCO}_3^-$	7.691
$\text{CaHCO}_3^+ \leftrightarrow \text{Ca}^{2+} + \text{HCO}_3^-$	-1.043
$\text{MgHCO}_3^+ \leftrightarrow \text{HCO}_3^- + \text{Mg}^{2+}$	-1.033
$\text{CaCl}^+ \leftrightarrow \text{Ca}^{2+} + 2\text{Cl}^-$	0.701
$\text{MgCl}^+ \leftrightarrow \text{Mg}^{2+} + \text{Cl}^-$	0.139
$\text{BaCl}^+ \leftrightarrow \text{Ba}^{2+} + \text{Cl}^-$	0.503
$\text{CO}_2(\text{g}) + \text{H}_2\text{O} \leftrightarrow \text{H}^+ + \text{HCO}_3^-$	-7.809

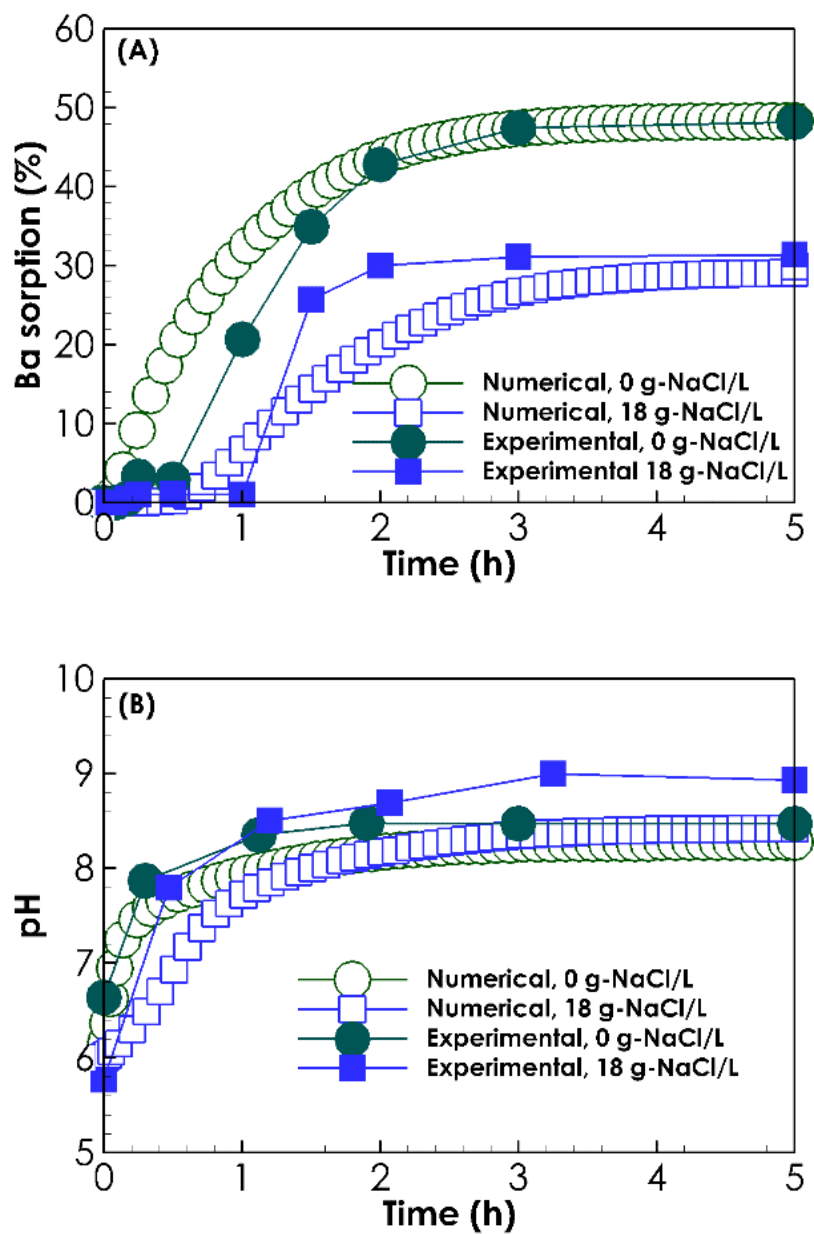
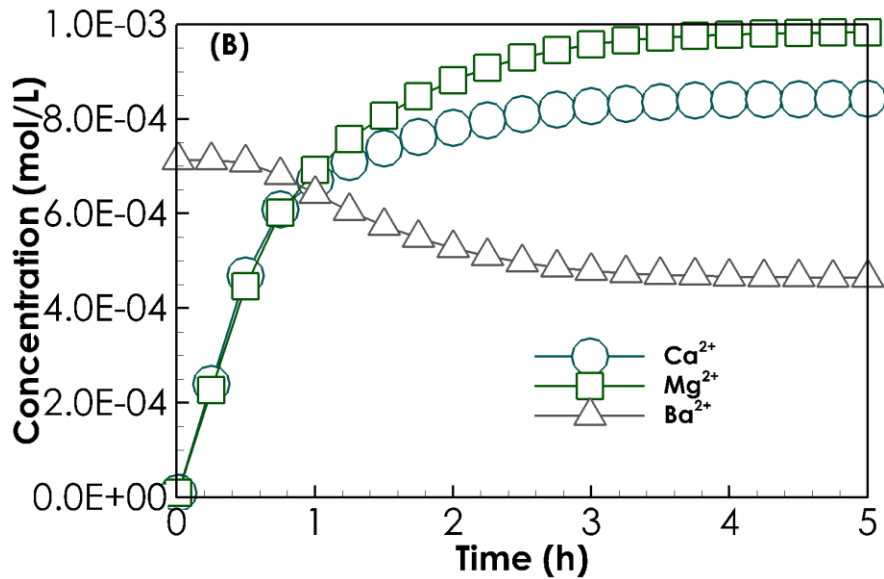
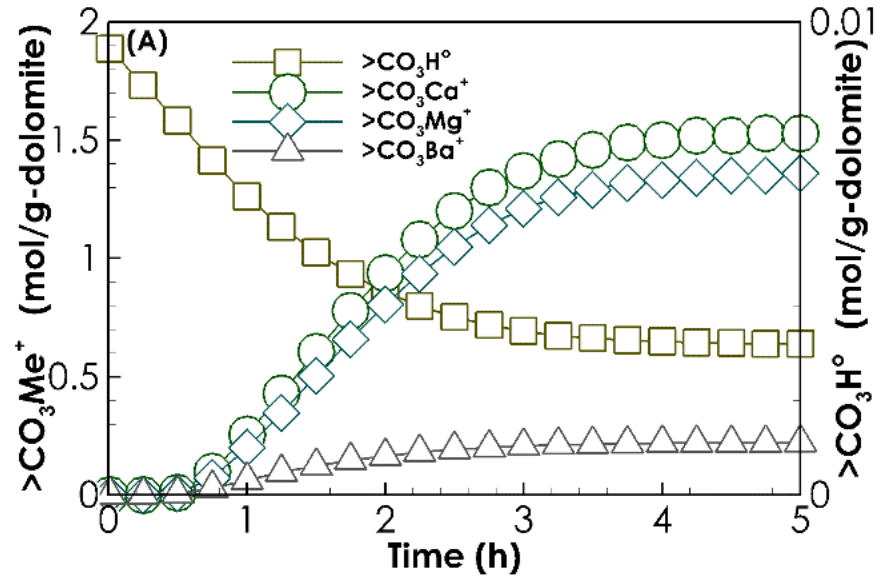


Fig 2. 10. Comparison between experimental and simulated results. (A) Sorption isotherms of Ba on dolomite, and (B) pH profiles at brine salinities of 0 and 18,000 mg-NaCl/L, using 500-600 μm particle size.

Fig. 2.10 compares experimental and simulated Ba sorption isotherms and pH profiles at two brine salinities (0 and 18,000 mg-NaCl/L). There is an excellent agreement between experimental and

simulated sorption isotherms of Ba, and pH profiles at both brine salinities. Differences during the initial stages of the reaction is attributed to the initial concentrations of hydration sites ($>CaOHo$, $>MgOHo$, and $>CO_3Ho$), which is unknown for Arbuckle dolomite. Employed initial concentration of hydration sites corresponds to pure dolomite (Brady et al., 1999).



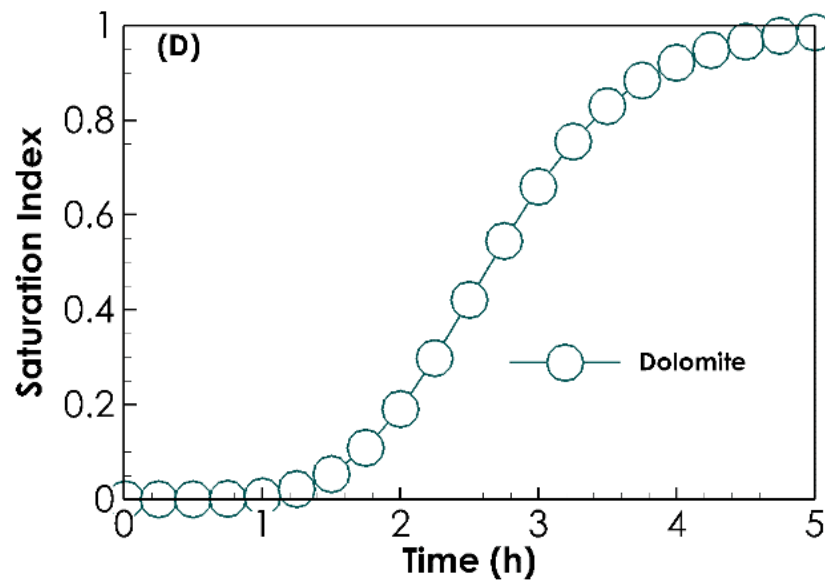
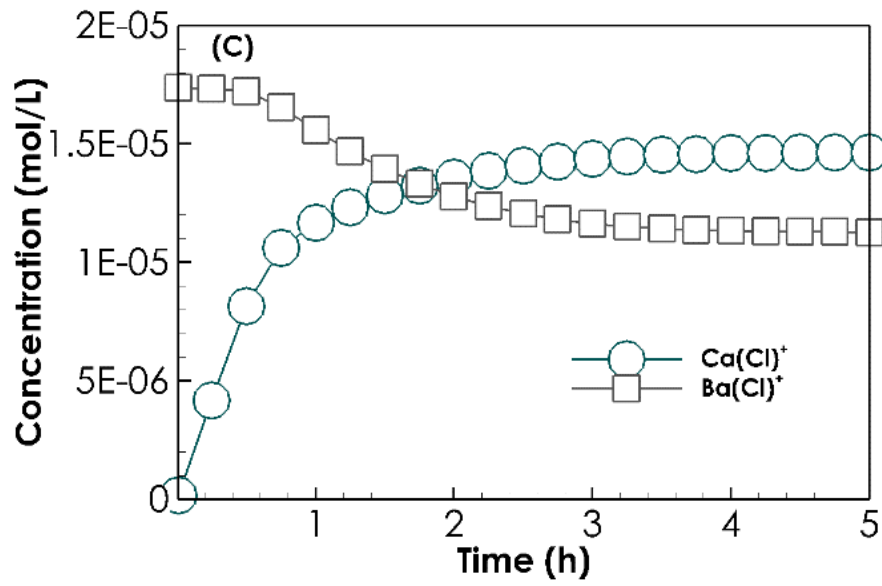


Fig 2. 11. Simulation results. (A) Concentration profiles of hydration sites on dolomite, (B) Concentration profiles of Ca, Mg and Ba in solution, (C) Concentration profiles of chloro-

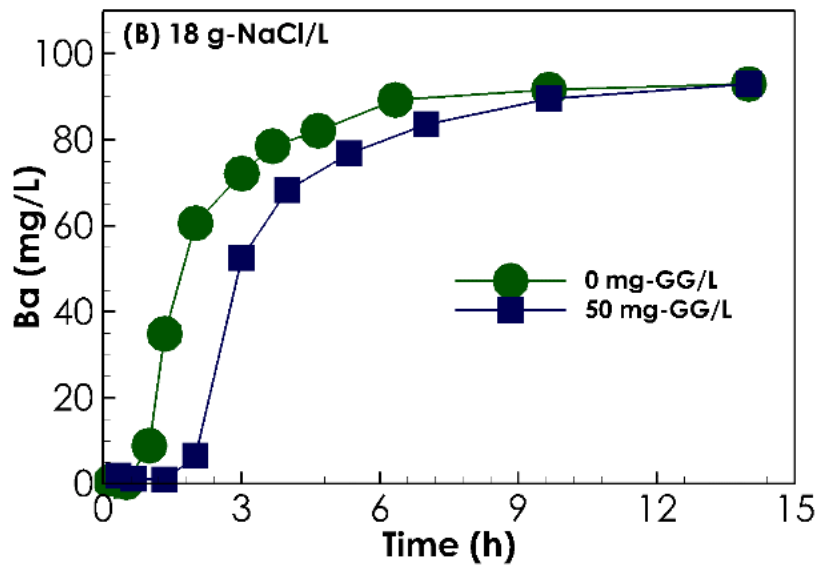
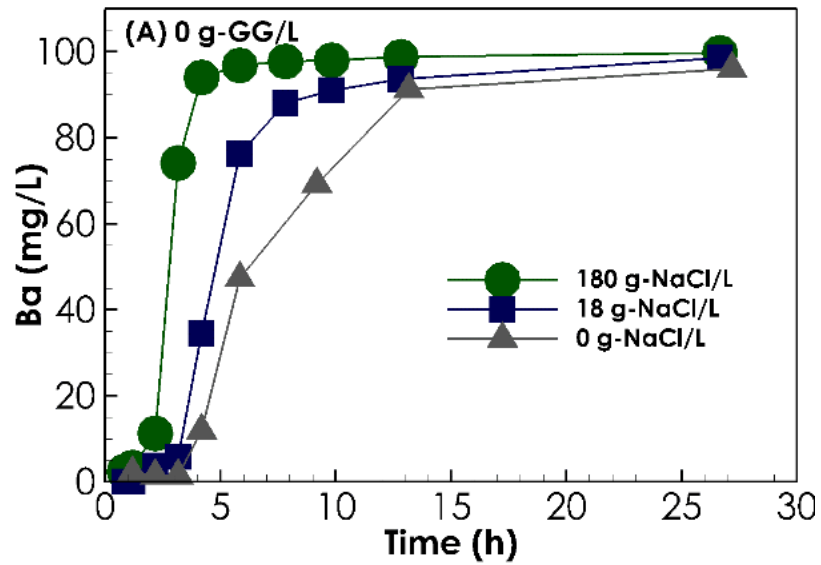
complexes of Ca and Ba in solution, and (D) Saturation index profile. At a brine salinity of 18,000 mg-NaCl/L, and using 500-600 μm particle size.

Fig. 2.11 shows simulated concentration profiles of $>\text{CaOHo}$ and $>\text{CO}_3\text{Ho}$ hydration sites on dolomite, and chloro-complexes of Ca and Ba in solution at a brine salinity of 18,000 mg-NaCl/L. Its corresponding Ba sorption isotherm and pH profile are shown in Fig. 2.11. Dolomite dissolution which increases the pH and the concentration of Ca and Mg in solution appears to play an important role in surface complexation reactions influencing Ba sorption on dolomite. An increase in pH due to the dissolution of dolomite promotes the sorption of Ba, Ca and Mg on dolomite (reaction 2 in Table 2.1), this is reflected by a decrease of $>\text{CO}_3\text{Ho}$ hydration sites, and an increase in the concentration of $>\text{CO}_3\text{Ba}^+$, $>\text{CO}_3\text{Ca}^+$, and $>\text{CO}_3\text{Mg}^+$ surface complexes (Fig. 2.11A). However, contrary to Ba whose concentration in the solution decreases due to its sorption on dolomite, the concentration of Ca and Mg in the solution increases due to dolomite dissolution (Fig. 2.11B). Apparently, the release of Ca and Mg cations from dolomite dissolution promotes the formation of $\text{Ca}(\text{Cl})^+$ and $\text{Mg}(\text{Cl})^+$ complexes, promoting the sorption of Ba on dolomite by decreasing the concentration of $\text{Ba}(\text{Cl})^+$ complex (Fig. 2.11C).

These results confirm that at brine salinities of UOG wastewater, chloro-complexation reactions rather than organo-complexation reactions and competition of cations for hydration sites control Ba sorption on dolomite. Moreover, the fact that an equilibrium sorption condition of Ba is concomitant with saturation index of dolomite close to 1.0 (Fig. 2.11D), reveals that besides brine salinity, dolomite dissolution is another important factor that determines the extent of Ba sorption on dolomite.

4.3. Effect of salinity and guar gum on the transport of Ba through dolomite rocks

This section describes the results of core-flooding experiments conducted to elucidate the effect of brine salinity and guar gum on the transport of Ba through natural and synthetic dolomite core plugs prepared following the procedure described in the materials section.



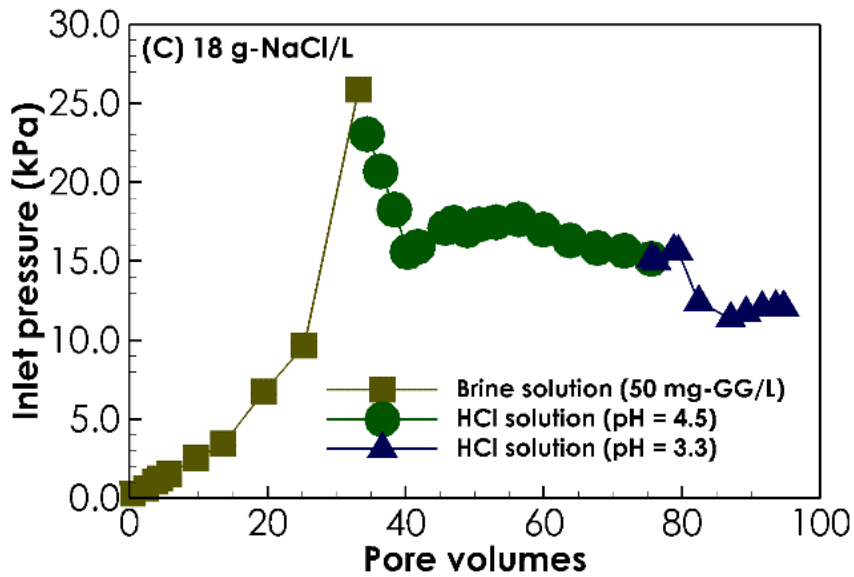


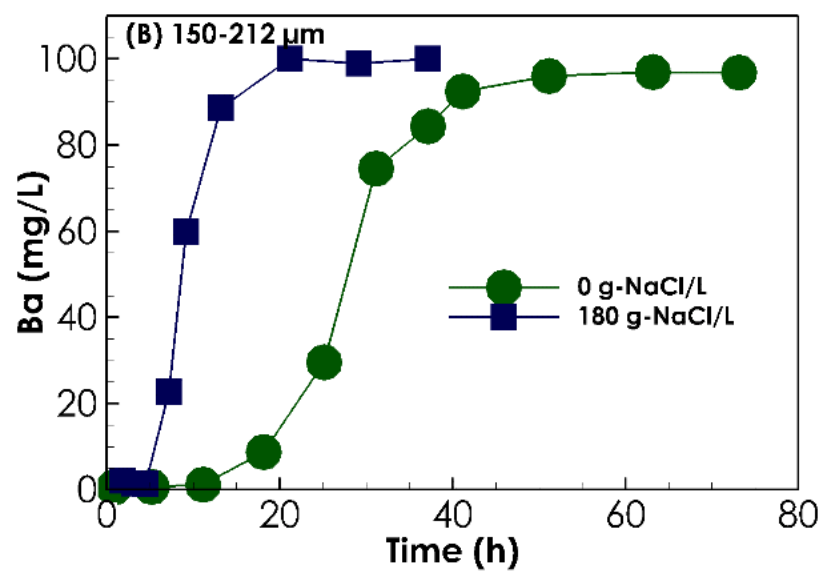
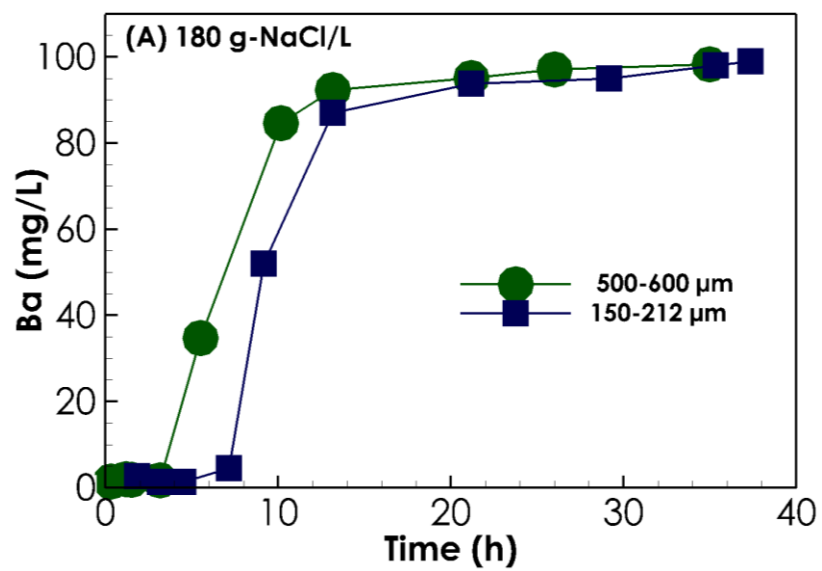
Fig 2. 12. Breakthrough curves of Ba through natural dolomite core plugs at a brine injection rate is 0.05 ml/min. (A) Effect of brine salinity in the absence of guar gum (GG), (B) Effect of guar gum at a brine salinity of 18,000 mg-NaCl/L, and (C) Pressure build up at the inlet of the core-holder at a brine salinity of 18,000 mg-NaCl/L and 50 mg-GG/L.

Fig. 2.12A compares breakthrough curves of Ba at three brine salinities (0, 18,000, and 180,000 mg-NaCl/L) in the absence of guar gum (0 mg/L). Porosity and permeability of the natural dolomite core plug used in the experiments were 5.3-8.7% and 0.06-0.1 mD, respectively. A longer breakthrough time with a brine salinity of 18,000 mg-NaCl/L (13 h) than with a brine salinity of 180,000 mg-NaCl/L (6 h) is in accordance with the batch sorption experimental results, where Ba sorption on dolomite decreased with increasing brine salinity and vice versa. This result suggests that Ba mobility might be higher in deep saline aquifers than in shallow aquifers where the maximum TDS concentration set by the Environmental Protection Agency (EPA) is 500 mg/L.

Fig. 2.12B compares the breakthrough curves of Ba obtained using natural dolomite core plugs at two guar gum concentrations (0 and 50 mg/L) and a brine salinity of 18,000 mg-NaCl/L. Porosity and permeability of the dolomite core plug were 6.4-7.2% and 0.3-0.4 mD, respectively. All other conditions were the same as in the previous core-flooding experiment conducted to assess the effect of brine salinity (Fig. 2.12A). The breakthrough time of Ba is shorter with 0 mg/L of guar gum than with 50 mg/L of guar gum, suggesting that guar gum retards the transport of Ba through tight dolomite rocks. The inlet pressure of the core holder was recorded, while the inlet pressure did not change in the experiments with 0 mg/L of guar gum, the inlet pressure in experiments conducted with 50 mg/L of guar gum gradually increased over time, suggesting that guar gum clogging the pore throats of dolomite acts as a sorbing or complexing phase for Ba.

Fig. 2.12C shows a representative inlet pressure profile recorded for experiments conducted with 50 mg/L of guar gum, the inlet pressure gradually increases from 1.138 kPa to 25.8 kPa. Subsequent injection of 60 pore volumes of diluted hydrochloric acid solution (pH of 4.5 and 3.3) could not restore the initial inlet pressure. This result confirms that guar gum plugs the pore throats of tight dolomite rocks and most likely acts as sorbing phase for Ba, retarding its transport.

To elucidate the effect of brine salinity and guar gum on the transport of Ba through dolomite porous media, additional core-flooding experiments were conducted using synthetic dolomite core plugs of high flow properties similar to that of shallow aquifers.



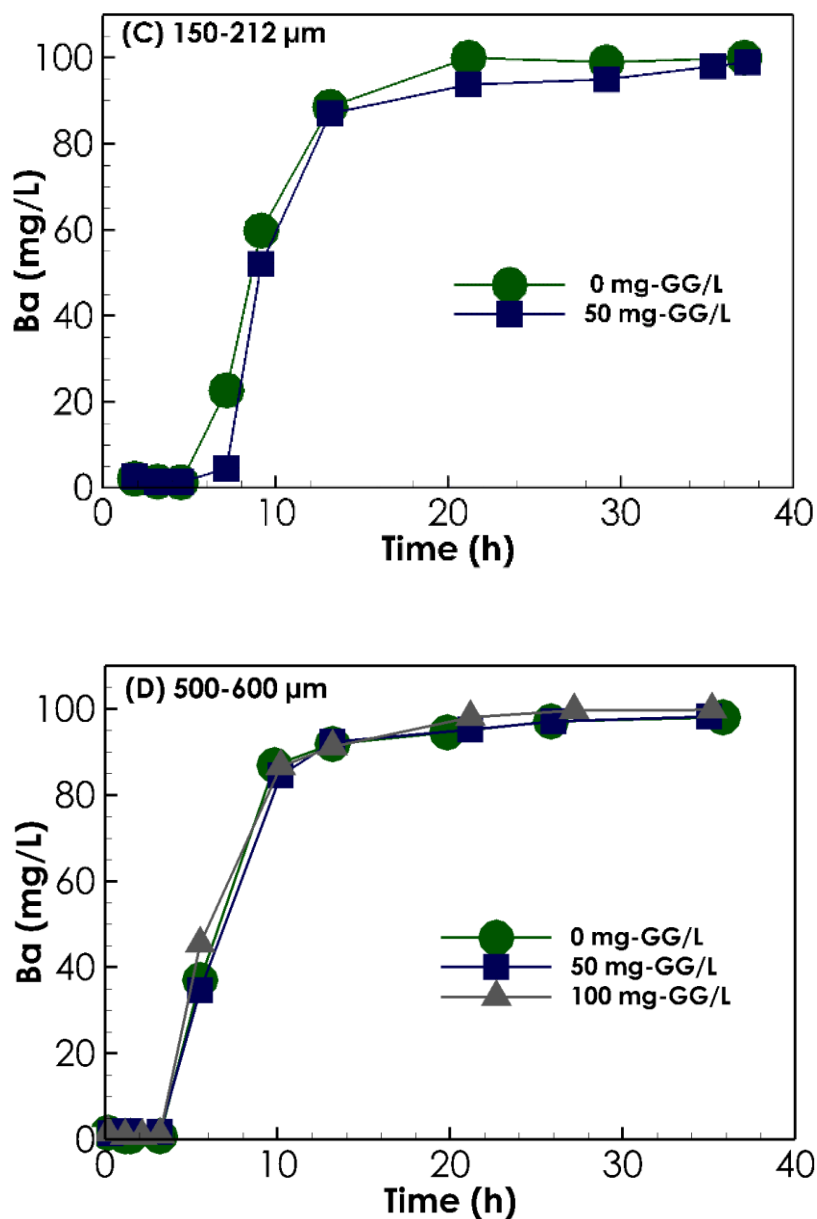


Fig 2. 13. Breakthrough curves of Ba through synthetic dolomite core plugs at a brine injection rate is 0.05 ml/min. (A) Effect of flow properties at a brine salinity of 180,000 mg-NaCl/L and 0 g/L of guar gum (GG), (B) Effect of brine salinity in the absence of guar gum (0 mg-GG/L), and (C) and (D) Effect of guar gum at a brine salinity 180,000 mg-NaCl/L. 150-212 and 500-600 μm particle size: 25% porosity

and 9.6 mD permeability. 500-600 μm particle size: 29.6% porosity and 13.7 mD permeability.

Fig. 2.13A compares the breakthrough curves of Ba obtained using synthetic dolomite core plugs prepared using 150-212 and 500-600 μm particle sizes at a brine salinity of 180,000 mg-NaCl/L. All other conditions were maintained the same to those used in the experiments using natural dolomite core plugs. As expected, at the same brine salinity the breakthrough time of Ba is slower through the core plug of 150-212 μm particle size (20 hours) than through the core plug of 500-600 μm particle size (10 hours). This is because of the surface area of porous media, which increases by decreasing the particle size of the synthetic dolomite core plug (Saidian et al., 2016).

Figure 2.13B compares the breakthrough curves of Ba through core plugs of 150-212 μm particle size at brine salinities of 0 and 180,000 mg-NaCl/L. The breakthrough time of Ba at a brine salinity of 180,000 mg-NaCl/L is 20 hours, whereas at a brine salinity of 0 mg-NaCl/L is 50 hours, confirming that brine salinity facilitates the transport of Ba through dolomite rocks by reducing its sorption on dolomite.

Figure 2.13C compares the breakthrough curves of Ba through core plugs of 150-212 μm particle size at a brine salinity of 180,000 mg-NaCl/L and guar gum concentrations of 0 and 50 mg/L. Breakthrough times at both guar gum concentrations (0 and 50 mg/L) are practically the same (20 hours), confirming that at flow properties of shallow aquifers, the effect of guar gum on the transport of Ba through dolomite porous media is small compared to the effect of brine salinity.

2.6. Conclusions

Batch and core-flooding experiments were conducted to assess the effect of brine salinity and guar gum on the sorption and transport of Ba in dolomite rocks collected from the Arbuckle formation in Oklahoma, US.

At brine salinities of UOG wastewater, Ba sorption on dolomite is controlled by chloro-complexation reactions between Ba and Cl ions, and pH changes that results from dolomite dissolution. Chloro-complexation reactions between Ba and guar gum, competition of Ba with common cations (Ca and Mg) for hydration sites of dolomite, play a secondary role. Ba sorption on dolomite decreases with increasing brine salinity and increases with increasing pH. This mechanism of Ba sorption on dolomite can be represented by a sorption model that accounts for both surface complexation reactions on three distinct hydration sites ($>CaOHo$, $>MgOHo$, and $>CO_3Ho$), and the kinetic dissolution of dolomite.

Although, guar gum does not affect the transport of Ba through dolomite rocks of high flow properties, guar gum can retard the transport of Ba through tight dolomite rocks of low flow properties by clogging the pore throats of dolomite.

Collectively, the results of these research indicate that as a consequence of high brine salinities of UOG wastewater, the mobility of heavy metals such as Ba in deep dolomite saline aquifers might be much higher than the mobility of heavy metals observed in shallow aquifers where brine salinity is <500 mg/L. Contrary to shallow aquifers where organic polymers such as guar gum increases the mobility of heavy metals (Mittal et al., 2015; Pal et al., 2014; Thakur et al., 2014), in deep dolomite saline aquifers injected with UOG wastewater of high brine salinities (18,000-180,000 mg/L), depending on the flow properties of the dolomite rock, organic polymers might play a secondary role on the transport of heavy metals through porous dolomite rocks.

These results have large implications toward the elucidation of the physical feasibility of USDW contamination with heavy metals present in UOG wastewater disposed into deep dolomite saline aquifers. Studies on the effect of temperature and transport of heavy metals through fractures will follow.

2.7. Acknowledgements

We thank Dr. James Puckette for his help on preparing and characterizing the rock samples, to Drs. Eliot Atekwana and Tao Wu for their help in the analytical methods, and the Society of Petrophysicists and Well Log Analysts (SPWLA) and Unconventional Resources Special Interest Group (URSIG) for their economic support.

2.8. References

Acosta, J.A., Jansen, B., Kalbitz, K., Faz, A., Martínez-Martínez, S., 2011. Salinity increases mobility of heavy metals in soils. *Chemosphere* 85, 1318-1324.

Akob, D.M., Cozzarelli, I.M., Dunlap, D.S., Rowan, E.L., Lorah, M.M., 2015. Organic and inorganic composition and microbiology of produced waters from Pennsylvania shale gas wells. *Applied Geochemistry* 60, 116-125.

Appelo, C.A.J., Postma, D., 2005. *Geochemistry, Groundwater and Pollution*. CRC Press.

Arthur, J.D., Langhus, B., Alleman, D., 2009. *Modern Shale Gas Development in the United States: A Primer*. US Department of Energy, Office of Fossil Energy.

Bahamdan, A., 2005. *Hydrophobic guar gum derivatives prepared by controlled grafting processes for hydraulic fracturing applications*. University of Arkansas at Little Rock.

Blauch, M.E., Myers, R.R., Moore, T., Lipinski, B.A., Houston, N.A., 2009. *Marcellus Shale Post-Frac Flowback Waters - Where is All the Salt Coming from and What are the Implications?* Society of Petroleum Engineers.

Brady, P.V., Papenguth, H.W., Kelly, J.W., 1999. Metal sorption to dolomite surfaces. *Applied Geochemistry* 14, 569-579.

Cluff, M.A., Hartsock, A., MacRae, J.D., Carter, K., Mouser, P.J., 2014. Temporal Changes in Microbial Ecology and Geochemistry in Produced Water from Hydraulically Fractured Marcellus Shale Gas Wells. *Environmental Science & Technology* 48, 6508-6517.

Comba, S., Di Molfetta, A., Sethi, R., 2011. A comparison between field applications of nano-, micro-, and millimetric zero-valent iron for the remediation of contaminated aquifers. *Water, Air, & Soil Pollution* 215, 595-607.

Dokhani, V., Yu, M., Bloys, J., 2016. Influence of Sorptive Tendency of Porous Medium on Hydraulic Properties of Shale, 50th US Rock Mechanics/Geomechanics Symposium. American Rock Mechanics Association.

Dresel, P.E., Rose, A.W., 2010. Chemistry and origin of oil and gas well brines in western Pennsylvania. Open-File Report OFOG 10, 01.00.

Elsner, M., Hoelzer, K., 2016. Quantitative survey and structural classification of hydraulic fracturing chemicals reported in unconventional gas production. *Environmental science & technology* 50, 3290-3314.

Engle, M.A., Cozzarelli, I.M., Smith, B.D., 2014. USGS investigations of water produced during hydrocarbon reservoir development, Fact Sheet, Reston, VA, p. 4.

Engle, M.A., Rowan, E.L., 2014. Geochemical evolution of produced waters from hydraulic fracturing of the Marcellus Shale, northern Appalachian Basin: A multivariate compositional data analysis approach. *International Journal of Coal Geology* 126, 45-56.

EPA, 2012. Study of the potential impacts of hydraulic fracturing on drinking water resources: progress report, EPA/601/R-12/011. Hydraulic Fracturing for Oil and Gas: Impacts from the Hydraulic Fracturing Water Cycle on Drinking Water Resources in the United States, www.epa.gov.

EPA, 2016. Hydraulic Fracturing for Oil and Gas: Impacts from the Hydraulic Fracturing Water Cycle on Drinking Water Resources in the United States, Main Report, in: EPA/600/R-16/236fa (Ed.). United States Environmental Protection Agency, www.epa.gov.

Ferrer, I., Thurman, E.M., 2015. Chemical constituents and analytical approaches for hydraulic fracturing waters. *Trends in Environmental Analytical Chemistry* 5, 18-25.

Gadhamshetty, V., Shrestha, N., Chilkoor, G., Bathi, J.R., 2015. Emerging Environmental Impacts of Unconventional Oil Development in the Bakken Formation in the Williston Basin of Western North Dakota, *Hydraulic Fracturing: Environmental Issues*. American Chemical Society, pp. 151-180.

Gastone, F., Tosco, T., Sethi, R., 2014. Guar gum solutions for improved delivery of iron particles in porous media (Part 1): Porous medium rheology and guar gum-induced clogging. *Journal of contaminant hydrology* 166, 23-33.

Ghaemi, A., Torab-Mostaedi, M., Ghannadi-Maragheh, M., 2011. Characterizations of strontium (II) and barium (II) adsorption from aqueous solutions using dolomite powder. *Journal of hazardous materials* 190, 916-921.

Gregory, K.B., Vidic, R.D., Dzombak, D.A., 2011. Water management challenges associated with the production of shale gas by hydraulic fracturing. *Elements* 7, 181-186.

Haluszczak, L.O., Rose, A.W., Kump, L.R., 2013. Geochemical evaluation of flowback brine from Marcellus gas wells in Pennsylvania, USA. *Applied Geochemistry* 28, 55-61.

Hatje, V., Payne, T.E., Hill, D.M., McOrist, G., Birch, G.F., Szymczak, R., 2003. Kinetics of trace element uptake and release by particles in estuarine waters: effects of pH, salinity, and particle loading. *Environment International* 29, 619-629.

Jiang, M., Hendrickson, C.T., VanBriesen, J.M., 2014. Life cycle water consumption and wastewater generation impacts of a Marcellus shale gas well. *Environmental science & technology* 48, 1911-1920.

Kocur, C.M., O'Carroll, D.M., Sleep, B.E., 2013. Impact of nZVI stability on mobility in porous media. *Journal of contaminant hydrology* 145, 17-25.

Krol, M.M., Oleniuk, A.J., Kocur, C.M., Sleep, B.E., Bennett, P., Xiong, Z., O'Carroll, D.M., 2013. A field-validated model for in situ transport of polymer-stabilized nZVI and implications for subsurface injection. *Environmental science & technology* 47, 7332-7340.

Lasaga, A.C., 1984. Chemical kinetics of water-rock interactions. *Journal of Geophysical Research: Solid Earth* 89, 4009-4025.

Lester, Y., Yacob, T., Morrissey, I., Linden, K.G., 2013. Can we treat hydraulic fracturing flowback with a conventional biological process? The case of guar gum. *Environmental Science & Technology Letters* 1, 133-136.

Lutz, B.D., Lewis, A.N., Doyle, M.W., 2013. Generation, transport, and disposal of wastewater associated with Marcellus Shale gas development. *Water Resources Research* 49, 647-656.

Mittal, H., Maity, A., Ray, S.S., 2015. Effective removal of cationic dyes from aqueous solution using gum ghatti-based biodegradable hydrogel. *International journal of biological macromolecules* 79, 8-20.

Orem, W., Tatu, C., Varonka, M., Lerch, H., Bates, A., Engle, M., Crosby, L., McIntosh, J., 2014. Organic substances in produced and formation water from unconventional natural gas extraction in coal and shale. *International Journal of Coal Geology* 126, 20-31.

- Pal, A., Nasim, T., Giri, A., Bandyopadhyay, A., 2014. Polyelectrolytic aqueous guar gum for adsorptive separation of soluble Pb (II) from contaminated water. *Carbohydrate polymers* 110, 224-230.
- Pehlivan, E., Özkan, A.M., Dinç, S., Parlayici, Ş., 2009. Adsorption of Cu 2+ and Pb 2+ ion on dolomite powder. *Journal of Hazardous Materials* 167, 1044-1049.
- Phenrat, T., Saleh, N., Sirk, K., Tilton, R.D., Lowry, G.V., 2007. Aggregation and sedimentation of aqueous nanoscale zerovalent iron dispersions. *Environmental Science & Technology* 41, 284-290.
- Pokrovsky, O.S., Mielczarski, J.A., Barres, O., Schott, J., 2000. Surface Speciation Models of Calcite and Dolomite/Aqueous Solution Interfaces and Their Spectroscopic Evaluation. *Langmuir* 16, 2677-2688.
- Pokrovsky, O.S., Schott, J., Thomas, F., 1999. Dolomite surface speciation and reactivity in aquatic systems. *Geochimica et Cosmochimica Acta* 63, 3133-3143.
- Renock, D., Landis, J.D., Sharma, M., 2016. Reductive weathering of black shale and release of barium during hydraulic fracturing. *Applied Geochemistry* 65, 73-86.
- Rowan, E.L., Engle, M.A., Kirby, C.S., Kraemer, T.F., 2011. Radium content of oil- and gas-field produced waters in the northern Appalachian Basin (USA)—Summary and discussion of data. U.S. Geological Survey Scientific Investigations Report 2011–5135.
- Rozell, D.J., Reaven, S.J., 2012. Water pollution risk associated with natural gas extraction from the Marcellus Shale. *Risk Analysis* 32, 1382-1393.

Saidian, M., Godinez, L.J., Prasad, M., 2016. Effect of clay and organic matter on nitrogen adsorption specific surface area and cation exchange capacity in shales (mudrocks). *Journal of Natural Gas Science and Engineering* 33, 1095-1106.

Selim, H.M., 2012. *Competitive Sorption and Transport of Heavy Metals in Soils and Geological Media*. CRC Press.

Steeffel, C.I., DePaolo, D.J., Lichtner, P.C., 2005. Reactive transport modeling: An essential tool and a new research approach for the Earth sciences. *Earth and Planetary Science Letters* 240, 539-558.

Steeffel, C.I., Molins, S., 2016. *CrunchFlow User's Manual*.

Stringfellow, W.T., Domen, J.K., Camarillo, M.K., Sandelin, W.L., Borglin, S., 2014. Physical, chemical, and biological characteristics of compounds used in hydraulic fracturing. *Journal of Hazardous Materials* 275, 37-54.

Strong, L., Gould, T., Kasinkas, L., Sadowsky, M., Aksan, A., Wackett, L., 2013. Biodegradation in Waters from Hydraulic Fracturing: Chemistry, Microbiology, and Engineering. *Journal of Environmental Engineering* 140, B4013001.

Thakur, S., Kumari, S., Dogra, P., Chauhan, G.S., 2014. A new guar gum-based adsorbent for the removal of Hg (II) from its aqueous solutions. *Carbohydrate polymers* 106, 276-282.

Tosco, T., Gastone, F., Sethi, R., 2014. Guar gum solutions for improved delivery of iron particles in porous media (Part 2): Iron transport tests and modeling in radial geometry. *Journal of contaminant hydrology* 166, 34-51.

Velimirovic, M., Chen, H., Simons, Q., Bastiaens, L., 2012. Reactivity recovery of guar gum coupled mZVI by means of enzymatic breakdown and rinsing. *Journal of contaminant hydrology* 142, 1-10.

Warner, N.R., Jackson, R.B., Darrah, T.H., Osborn, S.G., Down, A., Zhao, K., White, A., Vengosh, A., 2012. Geochemical evidence for possible natural migration of Marcellus Formation brine to shallow aquifers in Pennsylvania. *Proceedings of the National Academy of Sciences* 109, 11961-11966.

Xu, N., Chen, M., Zhou, K., Wang, Y., Yin, H., Chen, Z., 2014. Retention of phosphorus on calcite and dolomite: speciation and modeling. *RSC Advances* 4, 35205-35214.

Xue, D., Sethi, R., 2012. Viscoelastic gels of guar and xanthan gum mixtures provide long-term stabilization of iron micro-and nanoparticles. *Journal of Nanoparticle Research* 14, 1-14.

Zhao, S., Feng, C., Wang, D., Liu, Y., Shen, Z., 2013. Salinity increases the mobility of Cd, Cu, Mn, and Pb in the sediments of Yangtze Estuary: Relative role of sediments' properties and metal speciation. *Chemosphere* 91, 977-984.

CHAPTER III

PETROLEUM PRODUCED WATER DISPOSAL: MOBILITY and TRANSPORT of BARIUM in SANDSTONE and DOLOMITE ROCKS

Pouyan Ebrahimi, Javier Vilcáez*

Boone Pickens School of Geology, Oklahoma State University, Stillwater, OK 74078, USA

3.1. Abstract

To assess the risk of underground sources of drinking water contamination by Ba present in petroleum produced water disposed into deep saline aquifers, we examined the effect of salinity (NaCl), competition of cations (Ca, Mg), temperature (22 and 60 °C), and organic fracturing additives (guar gum) on the sorption and transport of Ba in dolomites and sandstones. We found that at typical concentration levels of NaCl, Ca, and Mg in petroleum produced water, Ba sorption in both dolomites and sandstones is inhibited by the formation of $Ba(Cl)^+$ complexes in solution and/or the competition of cations for binding sites of minerals. The inhibition of Ba sorption by both mechanisms is greater in dolomites than in sandstones. This is reflected by a larger decrease in the breakthrough times of Ba through dolomites than through sandstones. We found that the presence of guar gum has little influence on the sorption and thus the transport of Ba in both dolomites and sandstones. Contrary to most heavy metals, Ba sorption in both dolomites and sandstones decreases with increasing temperature, however the reducing effect of temperature on Ba sorption is relevant only at low salinity conditions. Higher inhibition of Ba sorption in dolomites

than in sandstones is due to the greater reactivity of dolomite over sandstone. The results of this study which includes the formulation of a reactive transport model and estimation of partition coefficients of Ba in dolomites and sandstones have significant implications in understanding and predicting the mobility and transport of Ba in deep dolomite and sandstone saline aquifers.

* Corresponding author, Telephone: +1-405-744-6361. Email: vilcaez@okstate.edu

Keywords: Petroleum produced water, Deep saline aquifers, Ba mobility, Guar gum, Salinity, Temperature.

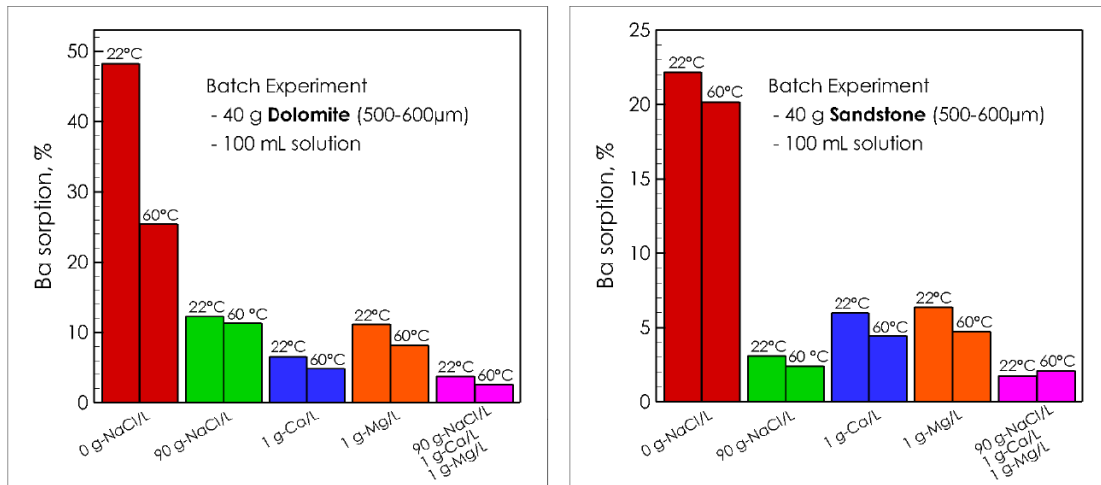


Fig 3. 1. Graphical abstract.

3.2. Introduction

Produced water from conventional and unconventional oil and gas (UOG) reservoirs generally contains higher levels of dissolved salts, organic chemicals, and heavy metals than the maximum contaminant levels (MCLs) established by the US Environmental Protection Agency (EPA) for drinking water (Yost et al., 2016). To prevent the contamination of surface and underground sources of drinking water (USDW), produced water is commonly disposed by injection into highly porous and permeable disposal sites below the lowermost USDW (Lutz et al., 2013). Depths of

disposal sites ranges from a few hundreds to thousands of meters and can correspond to different geological intervals. For instance in Oklahoma, USA, the shallowest depth of produced wastewater disposal has been reported to be 109 m, which corresponds to a sandstone interval of the Permian basin. Differently, the deepest depth for produced wastewater disposal has been reported to be 5,757m, which corresponds to a dolomitic interval of the Atokan-Morrowan basin (Murray, 2014). The produced water in Oklahoma is mostly disposed into dolomite intervals of the Arbuckle Group at a relatively median depth of 2,088 m (Murray, 2014). However, there are growing concerns regarding the possibility of USDW contamination by heavy metals present in produced water. This is because of the increase in the volumes of produced water disposed into the Arbuckle Group from 434 MMbbl in 2009 to >1046 MMbbl in 2014 (Murray, 2015), the common occurrence of wells with mechanical and cement failures, and the proximity of injection wells to basement faults which can facilitate the upward migration of disposed produced water.

Because it is important to assess the risk of USDW contamination by heavy metals due to the possible upward migration of disposed produced water through different geological intervals of different flow (porosity/permeability) and reactivity properties, this study aims to understand the variables controlling the sorption and transport of Ba in sandstones and dolomites, under the presence of guar gum, at typical concentrations of NaCl, Ca, and Mg in produced water from conventional and UOG reservoirs, and at both shallow and deep subsurface temperatures. Ba is selected because it constitutes the most common and abundant heavy metal found in the produced water from UOG reservoirs. Also, guar gum is selected because it represents the most common organic additive used in viscosified fracturing fluids (EPA, 2016; Hanes et al., 2003; Rozell and Reaven, 2012). Dolomites and sandstones are selected because they constitute the most common geological intervals containing saline aquifers where produced water is disposed in Oklahoma (Murray, 2015).

We focus on Ba sorption reactions because sorption process of heavy metals is generally accepted to be the most significant factor influencing the mobility of heavy metals in aquifers (Bradl, 2004). Sorption of heavy metals in aquifers depends on many factors including the mineral composition of the aquifer material, competition of binding sites of minerals, ionic strength and organic matter availability in the aqueous phase, and temperature (Landry et al., 2009). For instance, Reich et al. (2010) showed that the sorption of Pb is different on the surface of quartz and kaolinite. Temminghoff et al. (1995) found that by increasing the ionic strength from 0.003 to 0.3 mol/L, the sorption of Cd on sandy soil decreases by 60% for $\text{Ca}(\text{NO}_3)_2$ and by 25% for NaNO_3 . Acosta et al. (2011) showed that the concentrations of competing cations for sorption sites significantly affect the sorption of heavy metals. Strawn and Sparks (2000) showed that increasing the concentration of organic matter in the fluid results in decreasing the rate of Pb sorption on soil. Arias and Sen (2009) and Fan et al. (2009) showed that by increasing temperature, the sorption of Zn on kaolin decreases and sorption of Ni on attapulgite (a hydrated magnesium aluminum silicate) increases.

While many studies have been conducted to understand the variables controlling the sorption and transport of heavy metals commonly found in shallow freshwater aquifers (e.g., Cd, Pb, Cu, and Zn) (Lajçi et al., 2017), to our best knowledge no study has been conducted to understand the variables controlling the sorption and transport of heavy metals commonly found in produced water from UOG reservoirs (e.g., Ba, Sr, Se, and Ra) disposed into deep saline aquifers. Contrary to shallow aquifers which are characterized by close to ambient temperature, low salinity, and relatively low concentrations of organic matter conditions, deep saline aquifers injected with produced water are characterized by thermophilic temperatures, high salinity, and relatively high availability of organic matter derived from the use of organic fracturing additives (e.g., guar gum, polyacrylamide, and glutaraldehyde) for hydraulic fracturing.

Our experimental design which consisted of batch sorption and core-flooding approaches seeks to understand the variables controlling the sorption and transport of Ba in deep dolomite and

sandstone aquifers. Batch sorption experiments were implemented, on the one hand, to assess the effect of salinity (NaCl), guar gum, competition of cations (Ca and Mg), and temperature on Ba sorption in sandstones and dolomites. Core-flooding experiments were utilized, on the other hand, to analyze the effect of sorption reactions on the transport of Ba through the dolomites and sandstones.

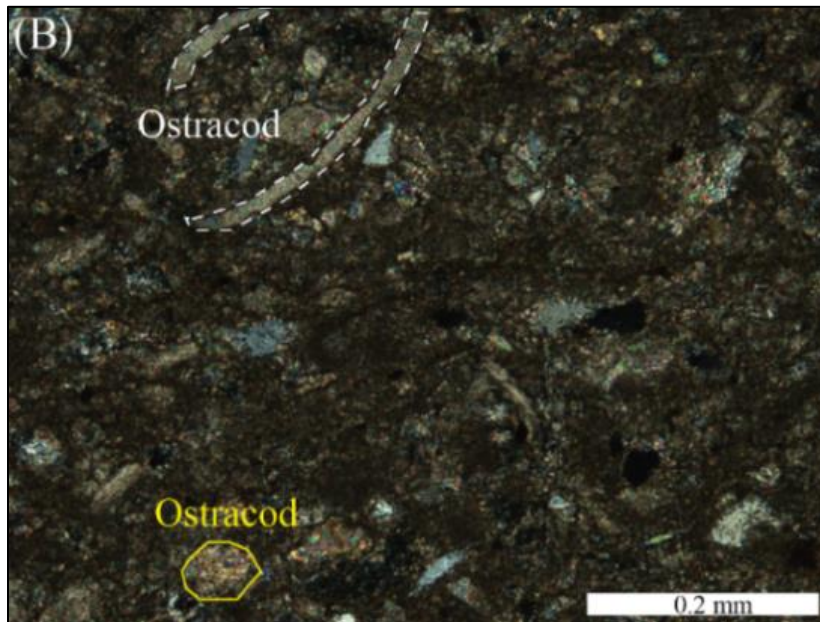
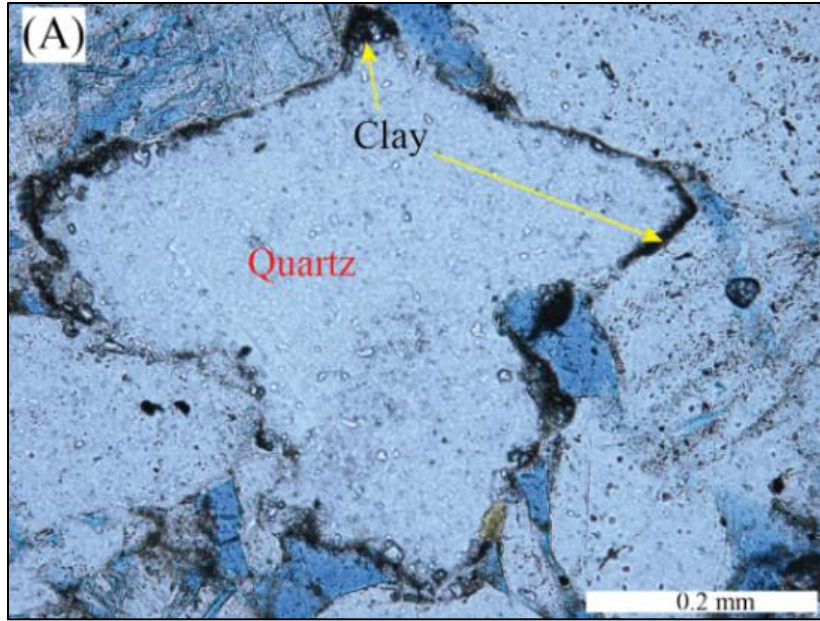
Obtained batch experimental results were used to calculate partition coefficients of Ba in the dolomites and sandstones, and core-flooding experimental results were used to verify a reactive transport model that can be used to bridge the gap between lab-scale batch sorption and core-flooding experimental results and field-scale applications to predict the transport of Ba from deep saline aquifers to USDW.

3.3. Materials and methods

3.3.1. Sandstone and dolomite rock samples

The sandstone samples used in this study are from shallow cores (<300 m) drilled through the Raton Formation in the Las Animas County, Colorado. The dolomite samples are from outcrops of the Arbuckle Group, McDonald County, Missouri.

Fig. 3.2 shows representative X-rays diffraction (XRD) and photomicrograph analysis conducted on the collected sandstone and dolomite samples. The sandstone sample has a quartz-dominated mineralogy with >98% quartz and <2% clay minerals (Fig. 3.2C). The quartz grain size is 0.1-1.2 mm, diameter of pores (blue sections) is 0.1-0.6 mm, and the clay minerals coat quartz grains and are found in inter-granular pores (Fig. 3.2A). The dolomite sample is mainly composed of dolomite mineral (>99%) (Fig. 3.2D) and the rest is calcite (ostracod and crinoid fossils) as well as quartz and silt (Fig. 3.2B). Both sandstone and dolomite samples were used to prepare powdered rocks, natural rock cores, and uniform synthetic rock cores by following the procedures described below.



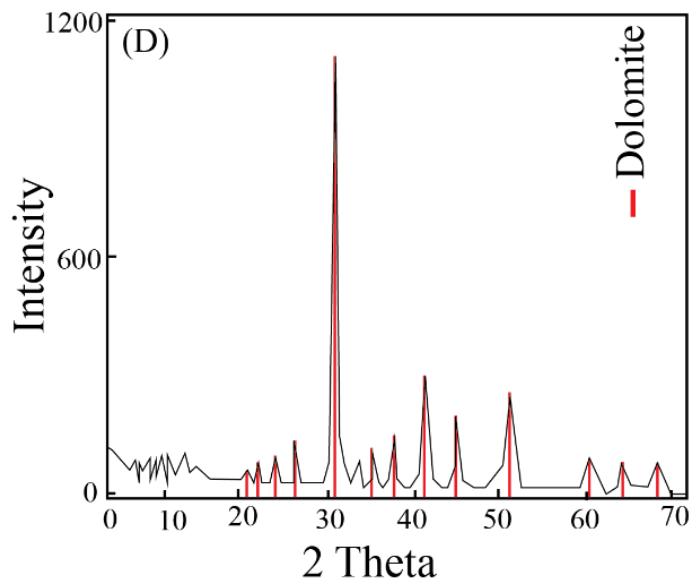
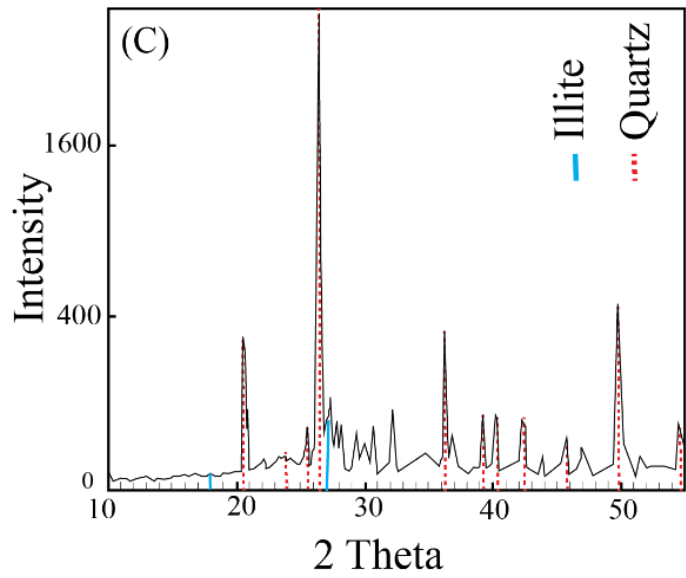


Fig 3. 2. Thin-section photomicrograph and XRD analysis of sandstone (A and C) and dolomite (B and D) samples used in this study.

3.3.2. Powdered rocks

The dolomite and sandstone samples were crushed and sieved to obtain 150-212 μm and 500-600 μm particles sizes. Prior to their utilization, dust from the sieved particles was removed by washing

five times with deionized water using an ultrasonic bath, and humidity from the wet particles was removed by drying ambient air.

3.3.3. Natural rock cores

Natural dolomites and sandstones have different flow and reactivity properties, in order to compare and analyze the transport of Ba through both rock types, core-flooding experiments were conducted using rock cores drilled from the sandstone and dolomite samples. Table 3.1 shows measured lengths, porosities and permeabilities of the natural dolomite and sandstone cores.

3.3.4. Uniform Synthetic rock cores

Natural sandstones and dolomites are heterogeneous porous media. In order to conduct reproducible core-flooding experiments, homogeneous synthetic rock cores were prepared using powdered sandstones and dolomites. The procedure consisted of mixing 3 g of deionized water and 77 g of powdered sandstones or dolomites. The resulting aggregate was poured into a stainless steel mold and compressed at 55.158 MPa for one hour using a uniaxial compaction apparatus (Carver Laboratory Presses, Model 4387). Measured lengths, porosities and permeabilities of the prepared synthetic rock cores are shown in Table 3.1.

Table 3. 1. Properties of prepared synthetic rock cores.

Core	Type	Grain size (μm)	Diameter (cm)	Length (cm)	Porosity (%)	Permeability (mD)
P1	Synthetic dolomite	150-212	2.54	10	25.0	9.7
P2	Synthetic sandstone	500-600	2.54	8.8	32.5	108.7
P3	Natural dolomite	~50-150	2.54	4-4.8	5.3-8.7	0.1-0.16
P4	Natural sandstone	~100-2,000	2.54	5.2	2.5-3.6	1-2.5

3.3.5. Produced water

Inductively coupled plasma-atomic emission spectroscopy (ICP-OES) analysis conducted on produced water from conventional and UOG reservoirs near Stillwater confirmed that produced water in Oklahoma is highly saline. Salinity ranges from 90 to 180 g/L, and it is mainly composed of NaCl (>93.5%), Ca (~5%) and Mg (~1%), and <0.5% of other elements (e.g., Fe, S, N). Based on this information and given the possibility of competition of Ca, Mg, and Ba for binding sites of minerals, we used synthetic produced water containing NaCl, CaCl₂·2H₂O, MgCl₂·6H₂O, and BaCl₂·2H₂O (all from Fisher Scientific with >99% purity). To assess the effect of guar gum, the prepared synthetic produced water was supplied with guar gum provided by PFP Industries LLC that supplies additives to hydraulic fracturing and oilfield completion companies in the USA. To ensure that guar gum molecules have been hydrated properly, the prepared synthetic produced water was supplied with guar gum 24 hours prior to its utilization (Habibpour and Clark, 2017).

3.3.6. Batch sorption experiments

Pyrex glass bottles were filled with 100 mL of synthetic produced water and 40 g of powdered (500-600 μm particle size) sandstones or dolomites. Reported concentrations of Ba in wastewater from major shale gas plays, including the Utica-Point Pleasant, Marcellus, Woodford, Fayetteville, Bakken, Barnett, Haynesville-Bossier, Eagle Ford, and Niobrara shales, ranges from 3.6-15,700 mg/L (McBroom, 2013; Rozell and Reaven, 2012). For comparison purpose, all experiments were conducted using a Ba concentration of 100 mg/L. Complete biodegradation of organic hydraulic fracturing additives such as guar gum is difficult to achieve due to the inhibitory effect of salinity on microbial activity (Lester et al., 2013). Assuming 90% biodegradation of possible guar gum concentrations (e.g., 500 mg/L) in produced water from UOG reservoirs, all experiments were conducted using a guar gum concentration of 50 mg/L. A mechanical orbital shaker was used to ensure mixing between the powdered rocks and the synthetic produced water containing Ba and

guar gum. Ba sorption on the powdered sandstones and dolomites was traced over time by ICP-OES analysis of solution samples collected periodically. Batch experiments ended when a steady state concentration of Ba in the bulk fluid was reached. pH is known to affect the sorption of heavy metals on minerals (Ghaemi et al., 2011), thus pH was also traced over time through all batch sorption experiments.

3.3.7. Core-flooding experiments

To emulate produced water injection into a saline aquifer, prior to the injection of the synthetic produced water containing NaCl, CaCl₂·2H₂O, MgCl₂·6H₂O, BaCl₂·2H₂O, and/or guar gum, the rock core was saturated with a synthetic produced water containing only NaCl. In all core-flooding experiments, the prepared synthetic produced water was injected using a dual piston Chrom Tech-HPLC pump at constant rate of 0.05 ml/min. The inlet pressure of the core holder was measured using a Rosemount pressure transducer with a scale resolution of 0.48 kPa and the effluent was collected in 0.5 mL volumes every 10 minutes for 60 hours using an automatic fraction collector. Collected samples were analyzed for their Ba, Ca, and Mg content by ICP-OES analysis.

3.4. Results and discussion

3.4.1. Sorption of Ba in dolomites and sandstones

Table 3.2 summarizes the composition of all synthetic produced waters used to assess the effect of salinity (NaCl), guar gum, competition of cations (Ca and Mg), and temperature on the sorption of Ba in dolomites and sandstones. Concentrations are representative of produced water from UOG reservoirs. As such, salinity in this study refers to the amount of NaCl in solution.

Table 3. 2. Composition of water solutions, obtained equilibrium Ba sorption, and partition coefficients (K_d).

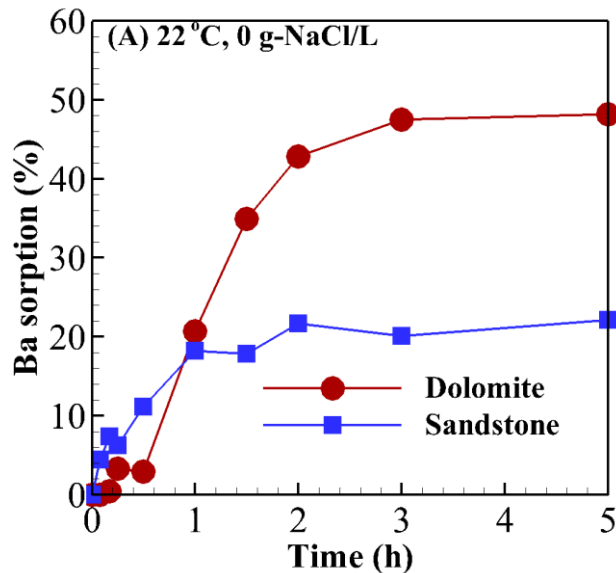
	T (°C)	NaCl (g/L)	Ca (g/L)	Mg (g/L)	GG ^a (mg/L)	Ba sorption (%)		K_d (L/Kg)	
						Dolomite	Sandstone	Dolomite	Sandstone
1	22	0.0	0.0	0.0	0.0	48.2	22.1	2.32	0.71
2	22	90	0.0	0.0	0.0	12.6	3.1	0.36	0.08
3	22	0.0	1.0	0.0	0.0	6.5	5.9	0.17	0.16
4	22	0.0	0.0	1.0	0.0	11.1	6.3	0.31	0.17
5	22	90	1.0	1.0	0.0	3.7	1.8	0.01	0.04
6	22	0.0	0.0	0.0	50	46.8	17.5	2.19	0.53
7	22	90	0.0	0.0	50	11.1	2.8	0.31	0.07
1	60	0.0	0.0	0.0	0.0	25.4	20.1	0.85	0.63
2	60	90	0.0	0.0	0.0	11.2	2.4	0.31	0.06
3	60	0.0	1.0	0.0	0.0	4.8	4.5	0.12	0.12
4	60	0.0	0.0	1.0	0.0	8.2	4.7	0.22	0.12
5	60	90	1.0	1.0	0.0	2.6	2.1	0.07	0.05
6	60	0.0	0.0	0.0	50	23.3	18.8	0.76	0.58
7	60	90	0.0	0.0	50	10.7	2.1	0.30	0.05

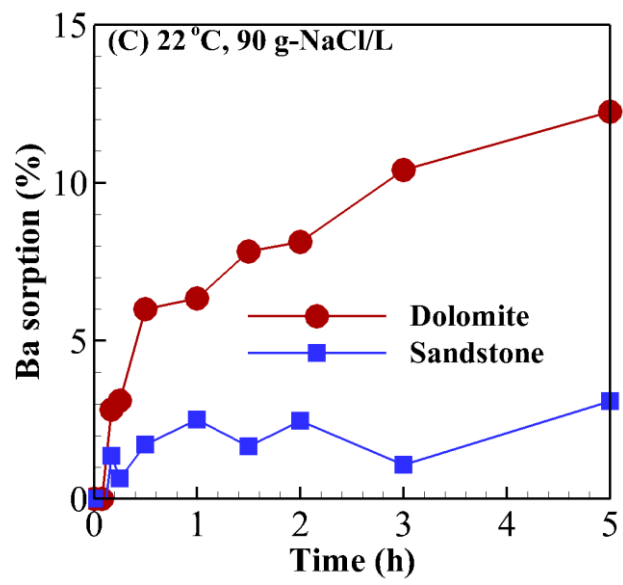
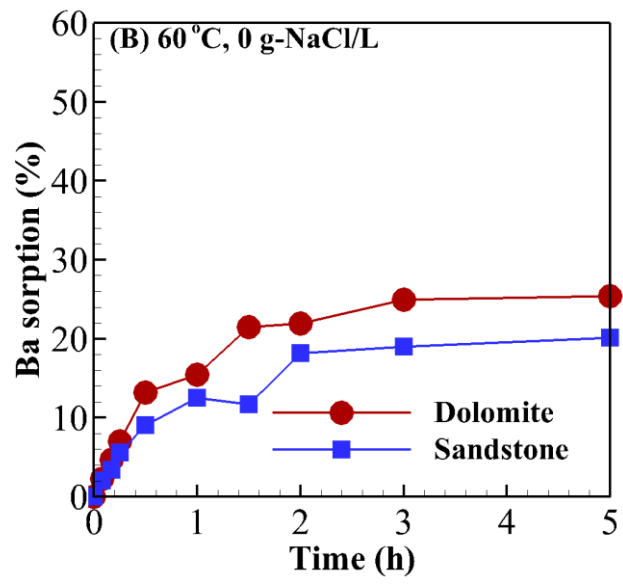
^a Guar gum

3.4.1.1. Effect of temperature

Figs. 3.3A&B compares Ba sorption on powdered dolomites and sandstones as function of time using water of zero salinity at 22 and 60 °C. At zero salinity, equilibrium Ba sorption on both dolomite and sandstone decreases with increasing temperature. Clearly, temperature exerts a stronger effect on the sorption of Ba on dolomite than on sandstone. While equilibrium Ba sorption

on dolomite decreases from 48.2 to 25.4% by increasing temperature from 22 to 60 °C (Fig. 3.3A), equilibrium Ba sorption on sandstone only decreases from 22.2 to 20.2% (Fig. 3.3B). A much lower equilibrium Ba sorption on sandstone than on dolomite at 22 °C, suggests a higher mobility of Ba in shallow freshwater sandstone aquifers than in shallow freshwater dolomite aquifers. Whereas, similar equilibrium Ba sorption levels on dolomite and sandstone obtained at 60 °C, suggests similar mobility of Ba in deep freshwater sandstone and dolomite aquifers. The observed effect of temperature on Ba sorption on powdered dolomite and sandstone rocks is in accordance with previous studies showing Ba sorption on magnesite decreases with increasing temperature probably due to the increase of thermal energy of sorbed Ba (Shahwan et al., 1998). However, the observed effect is opposite to the effect of temperature reported in studies about the sorption of Cu, Ni, and Zn on various soils (Sangiumsak and Punrattanasin, 2014; Xing et al., 2011), and Co, Sr, and Cs on marble (Hamed et al., 2016) where the sorption of these heavy metals increases with increasing temperature.





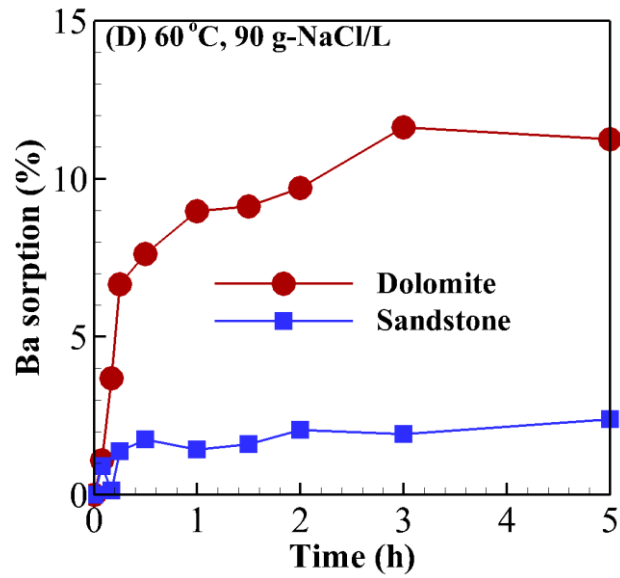


Fig 3. 3. Representative batch sorption experimental results: Effect of salinity and temperature on Ba sorption on dolomite and sandstone (500-600 μm particle size).

3.4.1.2. Effect of salinity

Figs. 3.3C&D compares Ba sorption on powdered dolomites and sandstones as function of time using saline water (90 g-NaCl/L) at 22 and 60 °C. At 90 g-NaCl/L salinity, equilibrium Ba sorption at both temperatures are practically the same; 12.6 and 11.2% on dolomite (Fig. 3.3C), and 3.1 and 2.4% on sandstone (Fig. 3.3D). Higher equilibrium Ba sorption levels at both temperatures on dolomite than on sandstone, suggest a higher mobility of Ba in sandstone saline aquifers than in dolomite saline aquifers.

A comparison between equilibrium Ba sorption using zero salinity water (Figs. 3.3A&B) and saline water (Figs. 3.3C&D) shows that increasing salinity from 0 to 90 g-NaCl/L greatly reduces the equilibrium Ba sorption on both dolomite and sandstone. At 22 °C, equilibrium Ba sorption decreased from 48.2 to 12.6% on dolomite, and from 22.2 to 3.1% on sandstone. Similarly at 60 °C, equilibrium Ba sorption decreased from 25.4 to 11.2% on dolomite, and from 20.1 to 2.4% on

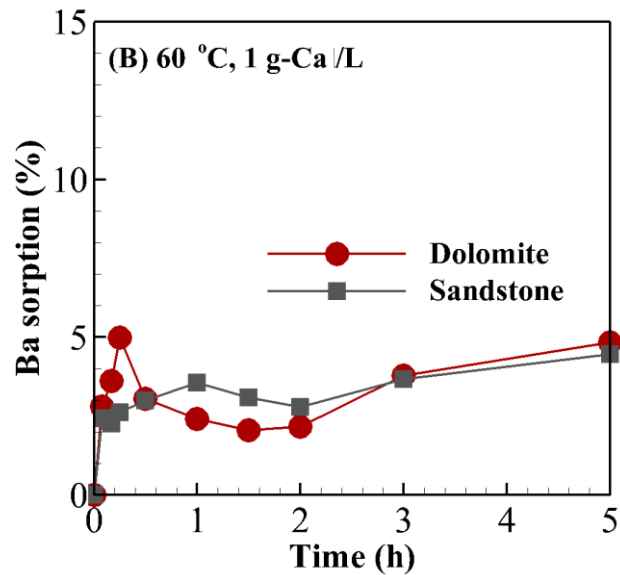
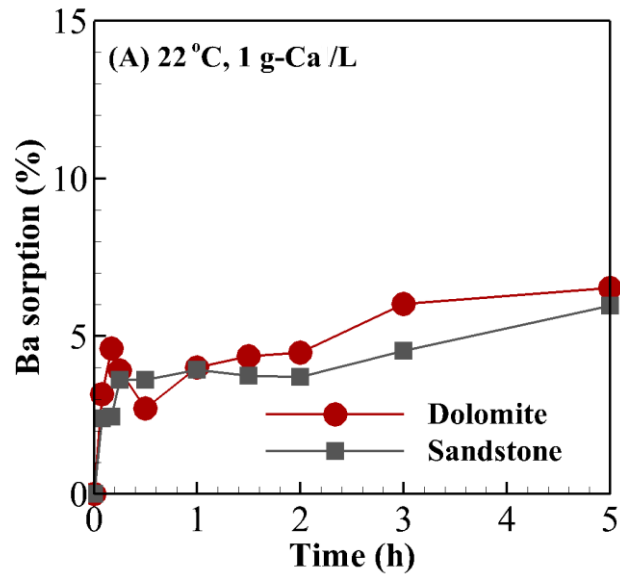
sandstone. These behaviors are in accordance with previous studies showing that salinity (NaCl) plays a major role on Ba sorption on dolomite. Formed $\text{Ba}(\text{Cl})^+$ complexes in solution are subjected to less electrostatic attraction than Ba^{2+} by negatively charged binding sites of minerals (Ebrahimi and Vilcáez, 2018). The new results presented in this study indicate that contrary to expectations, temperature plays a secondary role compared to salinity in inhibiting Ba sorption in both dolomites and sandstones.

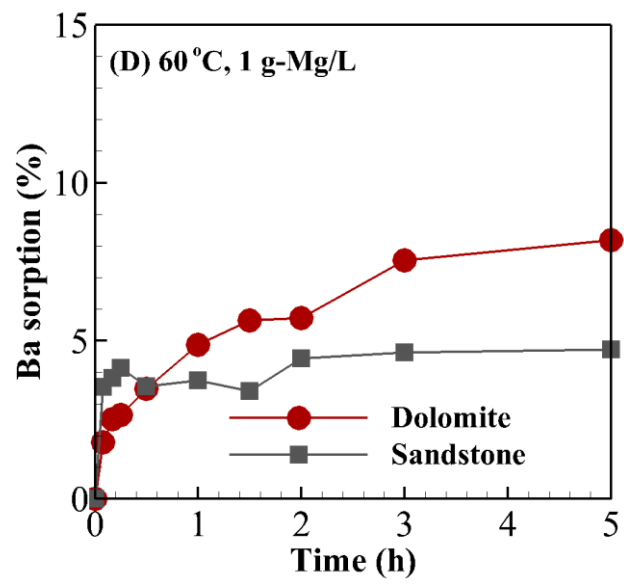
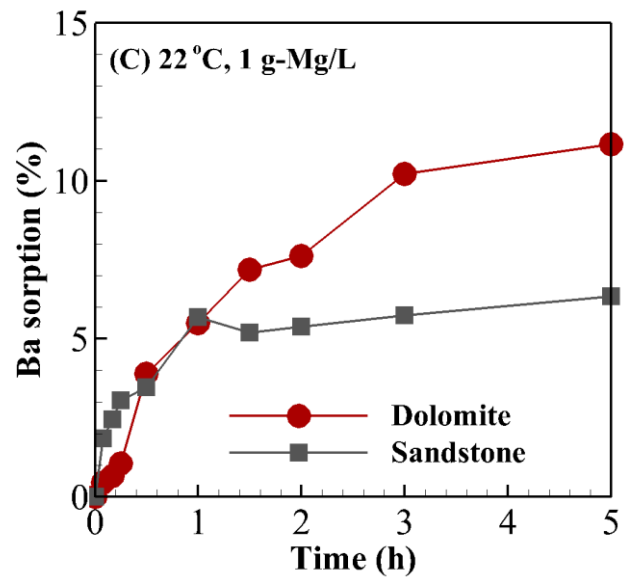
3.4.1.3. Effect of cations competition

Figs. 3.4A-D compares Ba sorption on powdered dolomites and sandstones as function of time at 22 and 60 °C using water containing Ca and Mg. At 1.0 g-Ca/L, equilibrium Ba sorption on dolomite and sandstone are 6.53 and 5.96% at 22 °C (Fig. 3.4A), and 4.83 and 4.46% at 60 °C (Fig. 3.4B), respectively. Whereas, at 1.0 g-Mg/L, equilibrium Ba sorption on dolomite and sandstone are 11.15 and 6.35% at 22 °C (Fig. 3.4C), and 8.18 and 4.72% at 60 °C (Fig. 3.4D), respectively. Equilibrium Ba sorption levels obtained using water containing Ca and Mg are much lower than the equilibrium Ba sorption levels obtained using zero salinity water (Figs. 3.3A&B), indicating that besides salinity that inhibits Ba sorption on dolomite and sandstone due to the formation of $\text{Ba}(\text{Cl})^+$ complexes, competition of Ba, Ca, and Mg for surface binding sites of minerals contributes to the inhibition of Ba sorption in deep dolomite and sandstone saline aquifers. Moreover, higher equilibrium Ba sorption levels on dolomite and sandstone with water containing Mg than with water containing the same concentration of Ca, reveals a preference of dolomite and sandstone for Ca sorption over Mg.

Figs. 3.4E&F show Ba sorption on powdered dolomites and sandstones as function of time at 22 and 60 °C using saline water (90 g-NaCl/L) containing both Ca and Mg (1.0 g/L). At 22 °C, equilibrium Ba sorption on dolomite and sandstone are 3.74 and 1.76% (Fig. 3.4E), whereas at 60 °C equilibrium Ba sorption on dolomite and sandstone are 2.6 and 2.1% (Fig. 3.4F), respectively.

Equilibrium Ba sorption levels obtained using saline water containing Ca and Mg are lower than the equilibrium Ba sorption levels obtained using saline water containing only NaCl (Figs. 3.3C&D). This indicates that competition of cations for surface complexation sites contributes to the inhibition of Ba sorption in dolomite and sandstone saline aquifers.





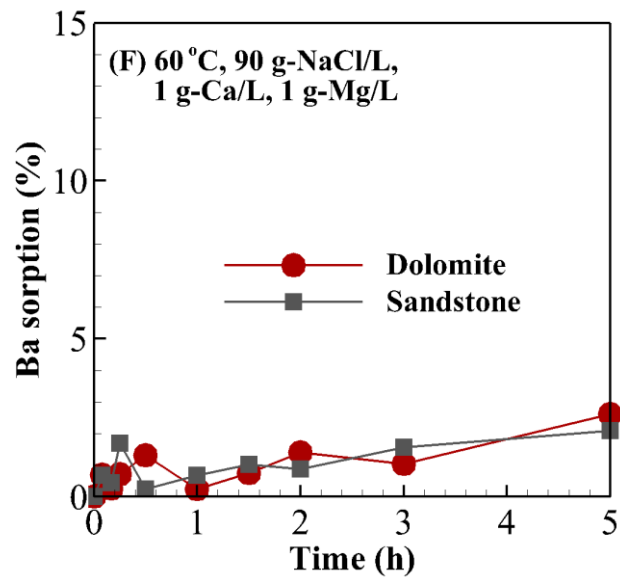
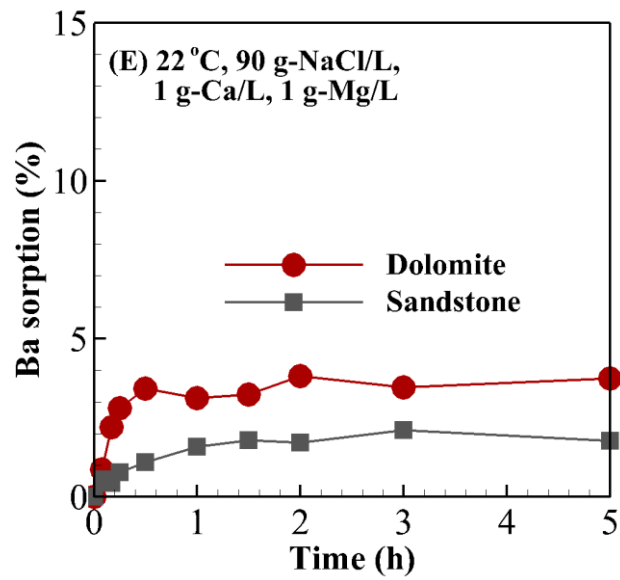
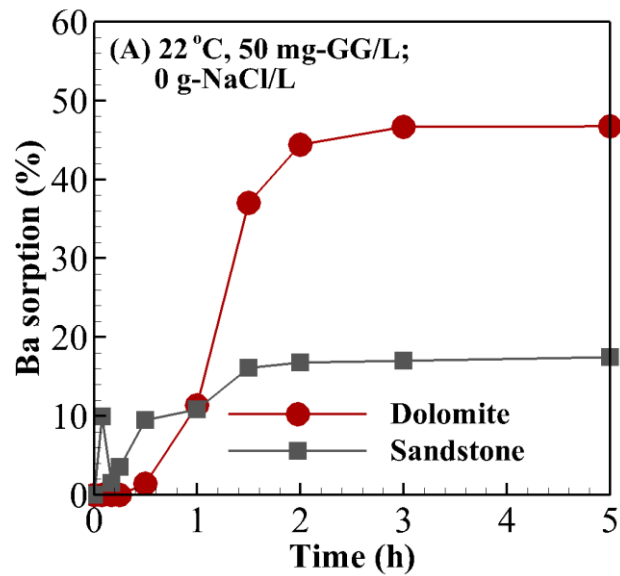


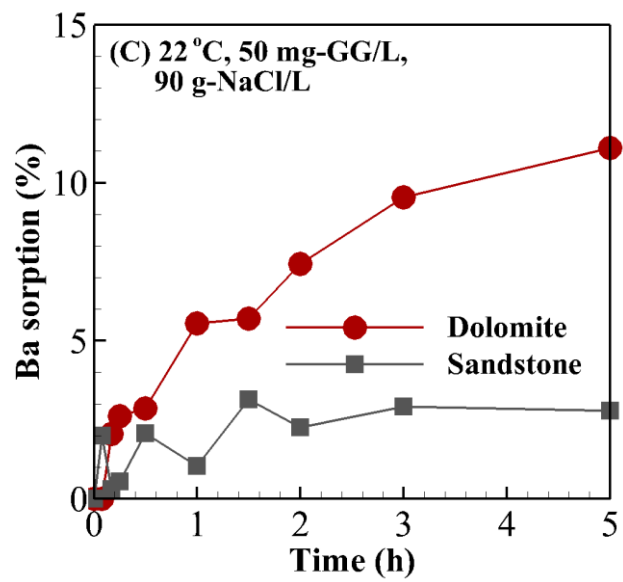
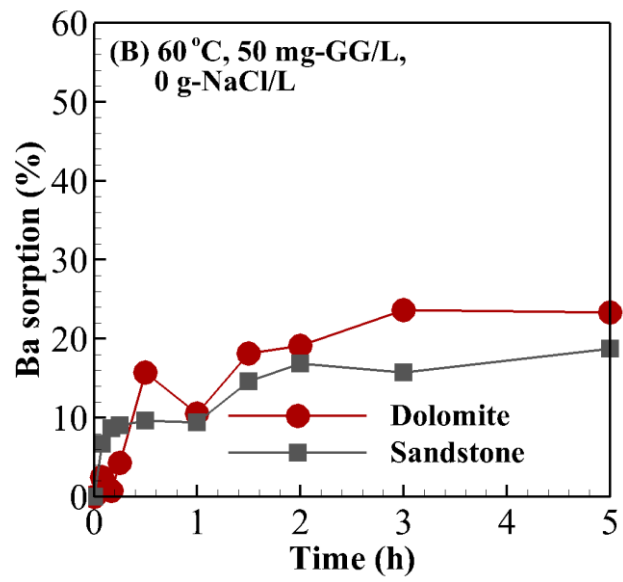
Fig 3. 4. Effect of cations (Ca and Mg) competition, salinity (NaCl), and temperature on the sorption of Ba on dolomite and sandstone.

3.4.1.4. Effect of guar gum

Figs. 3.5A-D compares Ba sorption on powdered dolomites and sandstones as function of time using zero salinity water and saline water (90 g-NaCl/L) containing guar gum at 22 and 60 °C. The

same as in batch sorption experiments conducted without the addition of guar gum, equilibrium Ba sorption on sandstone and dolomite decreases with increasing brine salinity and temperature. Equilibrium Ba sorption levels obtained under the presence of guar gum are practically the same equilibrium Ba sorption levels obtained without the addition of guar gum (Fig. 3.4). Hence, apparently guar gum at possible concentrations in produced water from hydraulically fractured UOG reservoirs has a very little effect on Ba sorption on dolomites and sandstones. These results are in agreement with previous studies showing that guar gum sorption on quartz, oxide minerals, and kaolinite is very small (<1% at different concentrations), and independent of pH and cations (Na, Ca, and Mg) availability (Ma and Pawlik, 2007). The results of this study indicates that this observation is valid not only for freshwater but also for saline water.





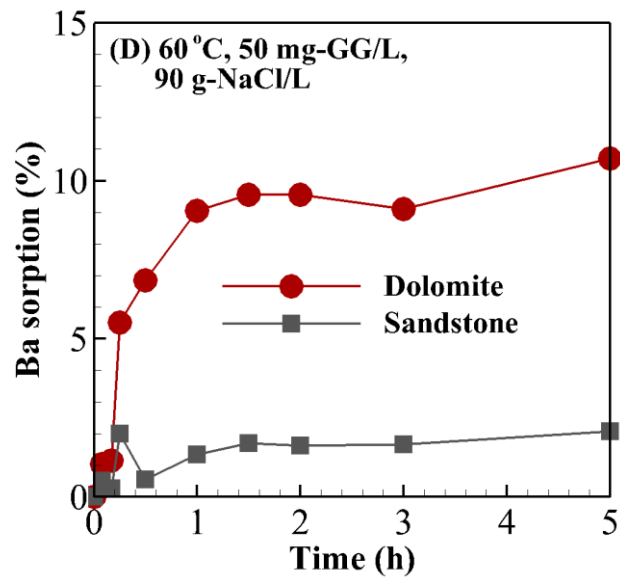


Fig 3. 5. Effect of guar gum (GG), salinity (NaCl) and temperature on the sorption of Ba on sandstone and dolomite.

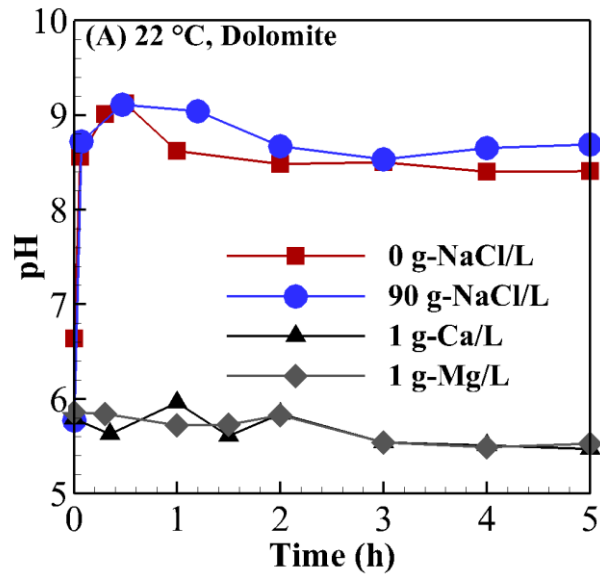
3.4.1.5. Effect of pH

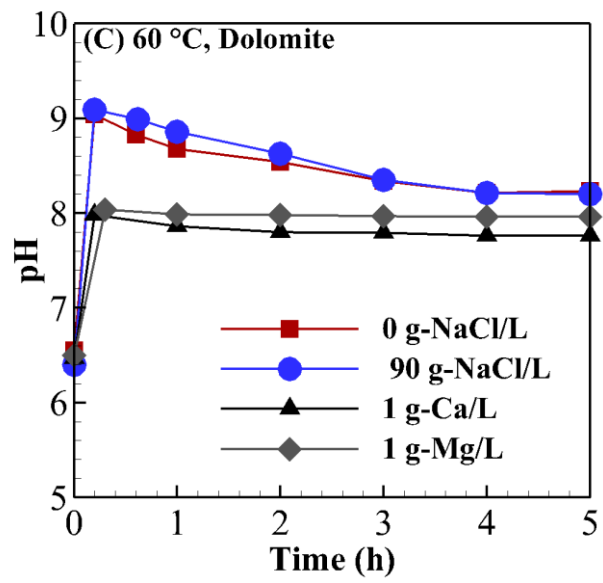
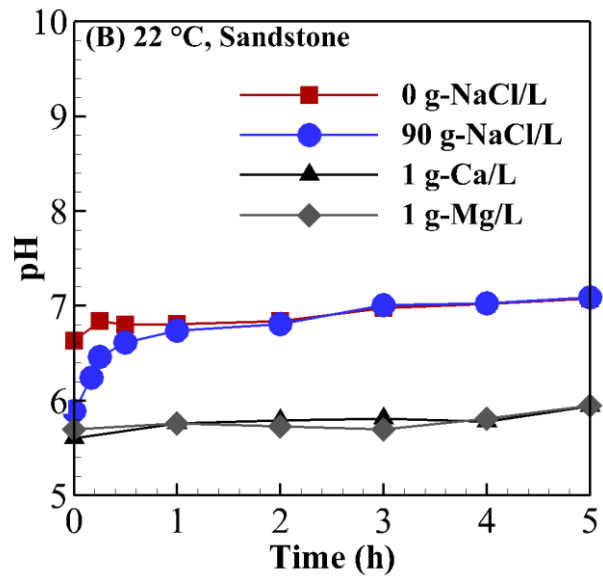
Table 3.5 summarizes all equilibrium Ba sorption on dolomite and sandstone obtained at 22 and 60 °C using zero salinity, saline water, water containing Ca and/or Mg, and guar gum. The large negative surface charge and specific surface area of clay minerals (e.g., kaolinite) commonly present in sandstones (Fig. 3.2), is expected to result in higher equilibrium Ba sorption levels in sandstone than in dolomite rocks. The opposite behavior was observed at all tested conditions in this study.

Fig. 3.6 shows representative pH profiles obtained at 22 and 60 °C using zero salinity, saline water (90 g-NaCl/L) and water containing Ca (1.0 g/L) or Mg (1.0 g/L). At both zero and 90 g-NaCl/L salinity and 22 °C, while pH increases from ~6 to ~9 in dolomite, pH increased from ~6.0 to just ~7.0 in sandstone. In general, an increase in pH due to the dissolution of minerals results in higher levels of metal sorption due to an increase in the number of negatively charged surface binding

sites of minerals (Tessier et al., 1989). Therefore, higher equilibrium Ba sorption levels in dolomite than in sandstone can be attributed to the greater chemical reactivity of dolomite relative to sandstone, rather than to a higher sorption capacity of dolomite over sandstone.

Lower levels of equilibrium Ba sorption is observed in both dolomite and sandstone at 90 g-NaCl/L salinity compared to zero salinity despite practically same pH profiles. This can be explained by the formation of $\text{Ba}(\text{Cl})^+$ complexes in solution which are subjected to less electrostatic attraction than Ba^{2+} by negatively charged complexation sites of minerals (Ebrahimi and Vilcáez, 2018). Apparently, the inhibitory effect of chloro-complexation reactions on Ba sorption is more dominant than the promotion effect of high pH levels on Ba sorption in both dolomites and sandstones.





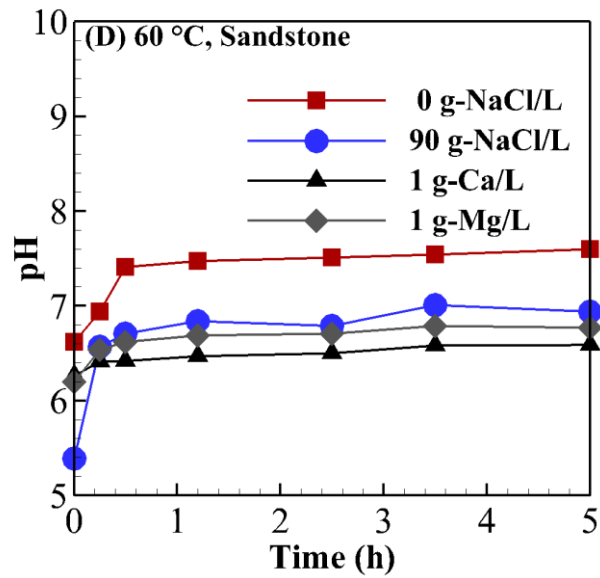


Fig 3. 6. Representative pH profiles of batch sorption experiments: Effect of temperature and rock type on pH.

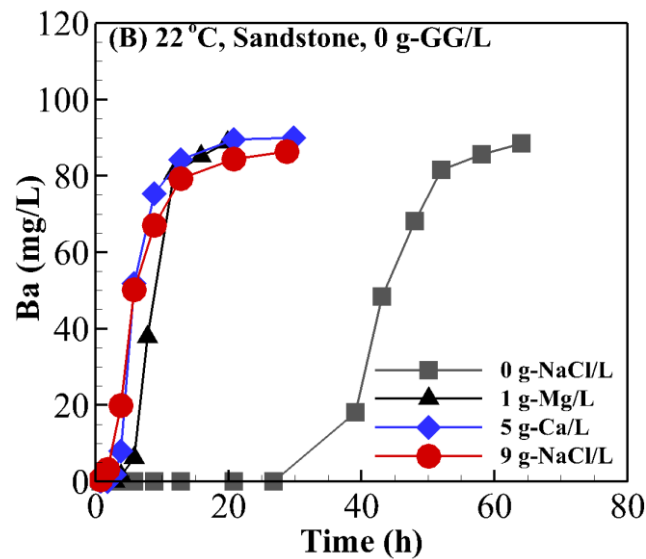
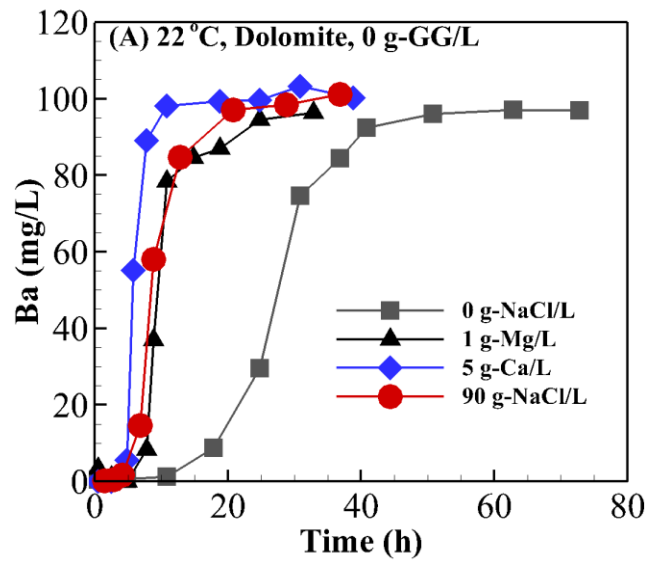
Using water containing Ca (1.0 g/L) or Mg (1.0 g/L), pH remains almost constant around ~6.0 with both dolomites and sandstones. This behavior can be attributed to the saturation of the solution with CaCO_3 and MgCO_3 which can attenuate the dissolution of both dolomites and sandstones. Hence, lower levels of equilibrium Ba sorption obtained using water containing Ca or Mg compared to using water with zero salinity, is due to the combined effect of competition of cations for binding sites of minerals and attenuation of minerals dissolution by the presence of relatively high concentrations of Ca and Mg in the solution.

Because high equilibrium Ba sorption levels were concomitant with high pH levels at 22 °C, higher pH levels at 60 °C (~6.5 pH for sandstone and ~7.9 pH for dolomite) than at 22 °C (~5.8 pH) was expected to result in higher Ba sorption levels at 60 °C than at 22 °C. Conversely, equilibrium Ba sorption levels in both rock types decreases with increasing temperature. This behavior which

contradicts the effect of pH observed at 22 °C, may be due to increased desorption as a result of the increase in thermal energy of the sorbate (Ba) (Mohamed et al., 2017; Shahwan et al., 1998).

3.4.2. Transport of Ba through sandstone and dolomite

Core-flooding experiments to determine the effect of sorption reactions on the transport of Ba through dolomite and sandstone were conducted using water solutions containing concentrations of NaCl/L, Ca, Mg, and guar gum representative of produced water from UOG reservoirs.



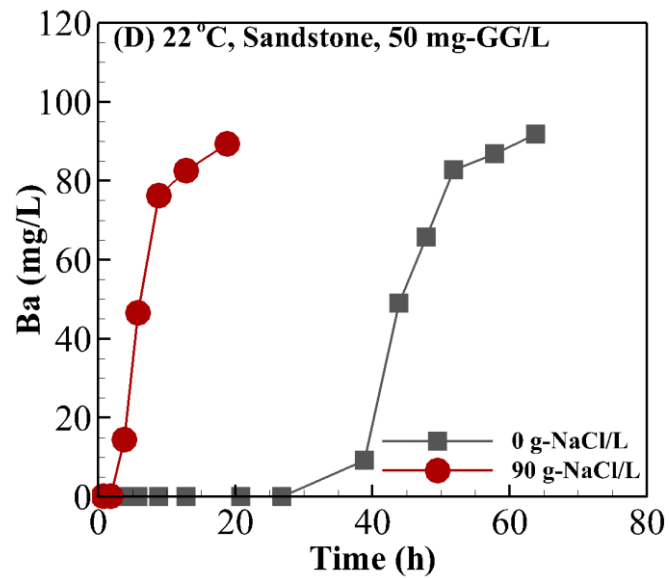
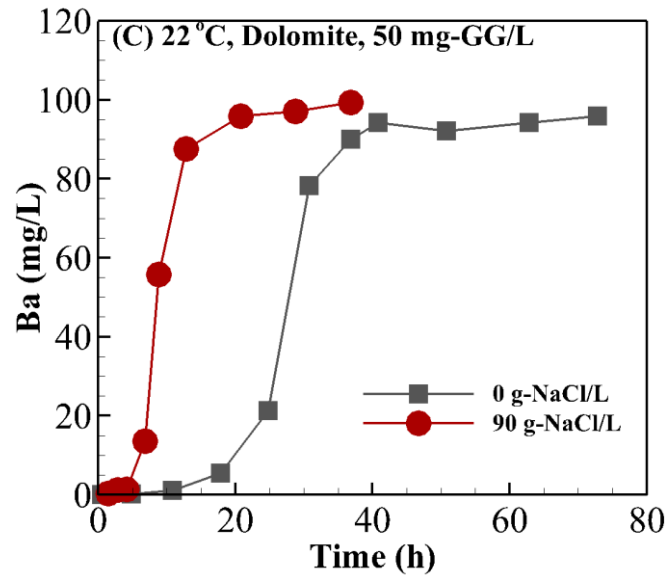


Fig 3. 7. Breakthrough curves of Ba through synthetic dolomite (P1) and sandstone (P2) cores (Table 3.1) at 22 °C. Injection flow rate of the solution of different compositions is 0.05 mL/min.

Figs. 3.7A&B compare the breakthrough curves of Ba through synthetic dolomite and sandstone cores of same flow properties (P1 and P2 in Table 3.1) using zero salinity water, saline water (90

g-NaCl), and water containing Ca (5.0 g/L) or Mg (1.0 g/L). At 22 °C, the respective breakthrough times of Ba using zero salinity and saline water are 41 and 15 hours for dolomite, and 43 and 11 hours for sandstone. The much shorter breakthrough time of Ba using saline water than using water with zero salinity for both rock core types confirms that salinity inhibits Ba sorption, hence facilitates its transport through both rock types.

Breakthrough times of Ba using water containing 5.0 g-Ca/L and 1.0 g-Mg/L are approximately 15 and 20 hours for dolomite (Fig. 3.7A), and approximately 20 and 19 hours for sandstone (Fig. 3.7B). These breakthrough times are similar to the breakthrough times of Ba using saline water (90 g-NaCl/L). This confirms that the competition of Ca, Mg, and Ba for binding sites of minerals combined with the attenuation of the dissolution of minerals results in the increase of the mobility of Ba through dolomites and sandstones almost as much as the formation of $Ba(Cl)^+$ complexes.

Figs. 3.7C&D compare the breakthrough curves of Ba through synthetic dolomite and sandstone cores of same flow properties (P1 and P2 in Table 3.1) using zero salinity and saline water (90 g-NaCl/L) containing guar gum (50 mg/L). The obtained breakthrough curves are virtually identical to those obtained without the addition of guar gum (Figs. 3.7A&B). This suggests that the presence of guar gum does not affect the transport of Ba through dolomite and sandstone under the condition of high flow properties (Table 3.1). These behavior is in accordance with results of our batch sorption experimental which show that guar gum has little effect on Ba sorption in both dolomites and sandstones.

Core-flooding experiments using dolomite were conducted at 22 and 60 °C. All breakthrough curves obtained at 60 °C for dolomite (Fig. 3.8) were almost the same to those obtained at 22 °C (Fig. 3.7). This reinforce the notion that brine salinity, together with competitions of cations for binding sites of minerals, and pH are the most important factors in controlling the sorption of Ba and thus its transport through dolomites and sandstones.

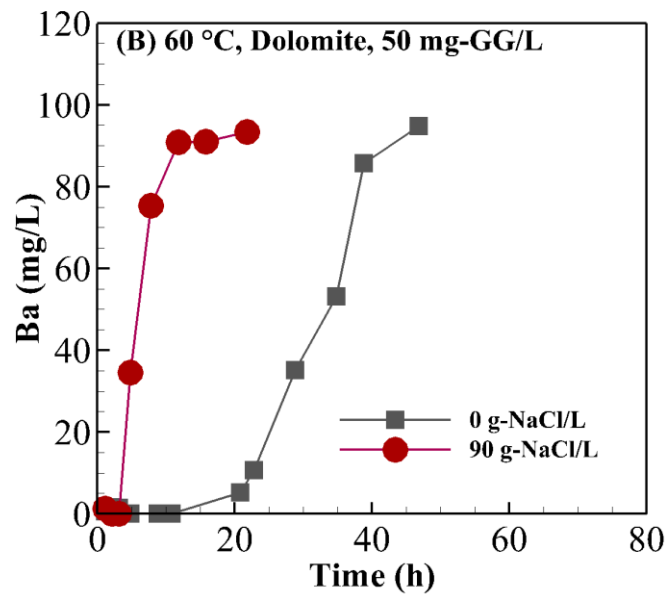
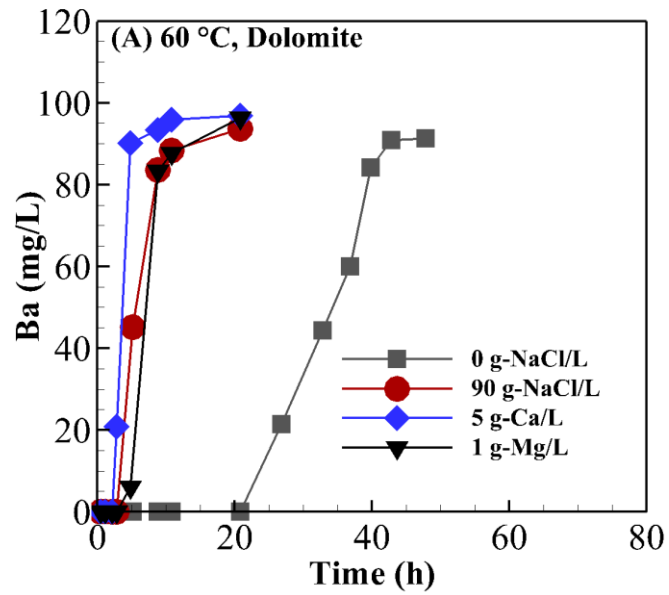


Fig 3. 8. Breakthrough curves of Ba through synthetic dolomite (P1) cores (Table 3.1) at 60 °C. Injection flow rate of the solution of different compositions is 0.05 mL/min.

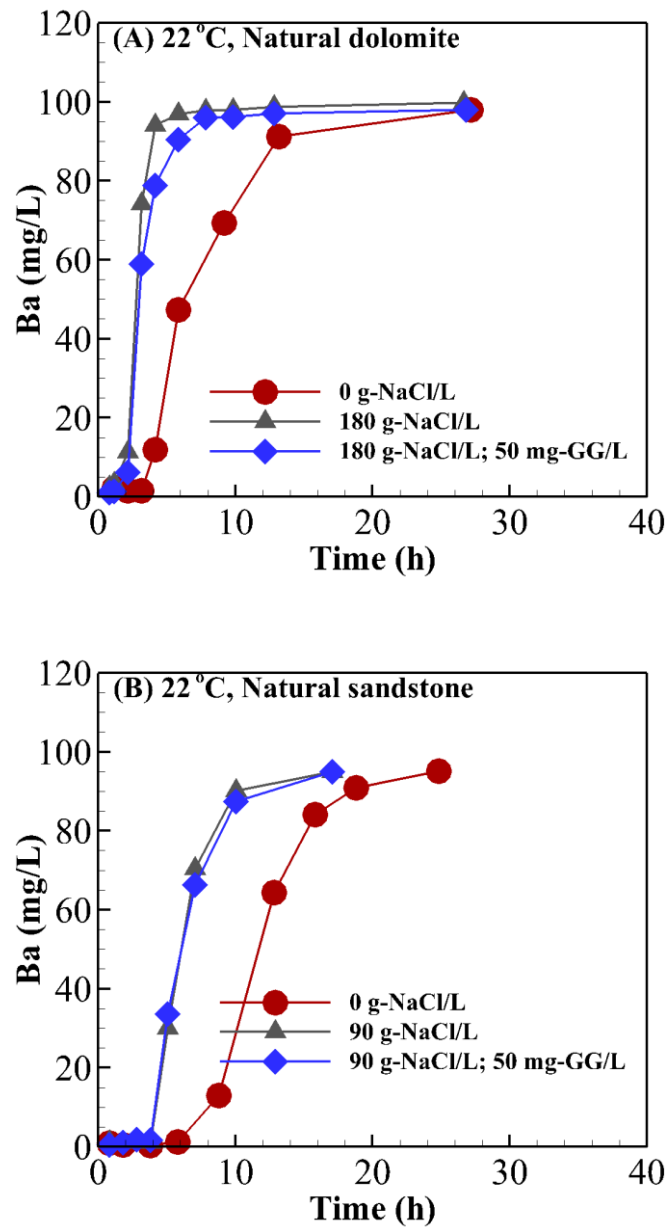


Fig 3. 9. Breakthrough curves of Ba through natural dolomite and sandstone cores at 22 °C. Injection flow rate of the solution of different compositions is 0.05 mL/min.

We conducted core-flooding experiments using natural dolomite and sandstone cores to evaluate whether or not guar gum affects the transport of Ba through these rock types. Figs. 3.9A&B compare the breakthrough curves of Ba through natural dolomite and sandstone cores (P3 and P4

in Table 3.1) using water with zero salinity and saline water (90, 180 g-NaCl/L) with and without guar gum (50 mg/L). Practically identical breakthrough curves were obtained with and without the addition of guar gum in both natural rock core types. This confirms that residual guar gum in produced water from conventional and UOG reservoirs play a secondary role in controlling the transport of Ba through dolomite and sandstone. The exception is that when the concentrations of guar gum are high enough to cause the plugging of pore throats (Ebrahimi and Vilcez, 2018). Our core-flooding experiments indicated that the Ba transport in natural dolomite and sandstone cores is faster under the conditions of saline water than water with zero salinity. This is similar to the results of the experiments conducted using synthetic rock cores when uniform properties were applied in both cases.

3.4.3. Modeling of Ba transport through dolomite and sandstone

We undertook numerical simulations to extend our experimental observations constraining conditions of USDW contamination by Ba into field-scale applications. This is done by solving the conservation of solute mass equation (Eq. 1) whose solution yields the spatial and temporal evolution of the concentration of solute i (C_i) due to the advection and dispersion transport mechanisms through porous media of porosity ϕ where solute i participates in N and M aqueous and mineral phase reactions.

$$\frac{\partial(\phi C_i)}{\partial t} = \nabla \cdot (\phi D \cdot \nabla C_i) - \nabla \cdot (q C_i) + q_s C_{i,s} \pm \sum_{n=1}^N R_{i,n}^{aq} \pm \sum_{m=1}^M R_{i,m}^{min} \quad (1)$$

$$R_i^{aq} = \rho_b \frac{\partial \bar{C}_i}{\partial t} = \rho_b \frac{\partial \bar{C}_i}{\partial C_A} \frac{\partial C_i}{\partial t} = \rho_b K_d \frac{\partial C_i}{\partial t} \quad (2)$$

$$-R_{i,m}^{min} = Ak_m [H^+]^{0.5} \left\{ 1 - \frac{IAP}{K_{eq}} \right\} \quad (3)$$

$R_{i,n}^{aq}$ and $R_{i,m}^{min}$ in Eq. (1) are the rate of aqueous and mineral phases reactions of solute i. Aqueous phase kinetic reactions ($R_{i,n}^{aq}$) include sorption reactions of solute i, whereas mineral phase kinetic reactions ($R_{i,m}^{min}$) include dissolution/precipitation reactions of solute i (e.g., Ca and Mg). D_i is the hydrodynamic dispersion coefficient of solute i which accounts for molecular diffusion, q is Darcy's flow velocity, q_s is the source/sink flow velocity, and $C_{i,s}$ is the concentration of solute i at source/sink points.

Equilibrium sorption reactions which are reflected by a decrease in the concentration of solute i in solution is represented by Eq. (2) where ρ_b is the density of the mineral, (C_i) is the concentration of solute i on the mineral surface, and K_d is the partition coefficient of solute i between the aqueous and minerals phases (g-i/kg-solid divided by g-i/L-solution). The kinetics of minerals (dolomite and sandstone) dissolution/precipitation is represented by Eq. (3), where k_m is the intrinsic rate constant, K_{eq} is the equilibrium constant, A refers to the surface area of the mineral which can be calculated from the diameter of the rock particle (d_i), and IAP is ion activity product.

Table 3.3 summarizes the composition of the injection and initial water solutions used to verify the applicability of Eqs. (1-3) to represent the transport of Ba in dolomite and saline aquifers. The concentrations of NaCl, Ba, Ca, and Mg correspond to those used to conduct the core-flooding experiments. The concentrations of HCO_3^- and H^+ correspond to calculated equilibrium conditions with atmospheric CO_2 at partial pressure of 3.15×10^{-4} atm. Table 3.4 summarizes the transport properties of dolomite and sandstone cores used for the simulations, and Table 3.5 lists all aqueous phase complexation reactions with its corresponding equilibrium constants used for the simulations.

Table 3. 3. Injection and initial conditions used to simulate the transport of Ba through dolomite and sandstone rock cores.

Species	Dolomite		Sandstone	
	Initial (mol/L)	Injection (mol/L)	Initial (mol/L)	Injection (mol/L)
H ⁺	0.197×10 ⁻⁸	0.145×10 ⁻⁵	0.145×10 ⁻⁵	0.145×10 ⁻⁵
Ca ²⁺	0.15×10 ⁻³	0.0 - 0.125	0.0	0.0 - 0.125
Mg ²⁺	0.134×10 ⁻³	0.0 - 4.17×10 ⁻²	0.0	0.0 - 4.17×10 ⁻²
Na ⁺	1.54 - 3.08	1.54 - 3.08	1.54 - 3.08	1.54 - 3.08
Cl ⁻	1.54 - 3.08	1.54 - 3.08	1.54 - 3.08	1.54 - 3.08
HCO ₃ ⁻	0.132×10 ⁻²	0.312×10 ⁻⁶	0.312×10 ⁻⁶	0.312×10 ⁻⁶
Ba ²⁺	0.0	7.281×10 ⁻⁴	0.0	7.281×10 ⁻⁴
SiO ₂ (aq)	0.0	0.0	0.0	0.0

Table 3. 4. Transport properties of the synthetic rock cores.

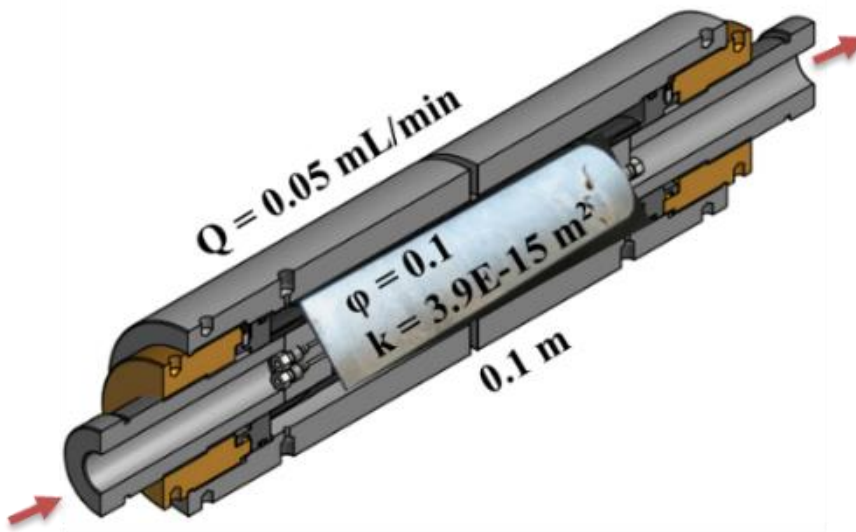
Parameters	Dolomite	Sandstone	Source
Volume %	97	94	Measured
k _m (mol/m ² /s)	2.951×10 ⁻⁸	1.023×10 ⁻¹³	Palandri (2004)
d _i (m)	1.51×10 ⁻⁴	5.50×10 ⁻⁴	Measured
ρ _b (kg/m ³)	2.84	2.65	Alden (2017)

Table 3. 5. Aqueous phase equilibrium complexation reactions.

Reaction	Log K (22°C)
OH ⁻ + H ⁺ ↔ H ₂ O	13.991

$\text{CO}_2(\text{aq}) + \text{H}_2\text{O} \leftrightarrow \text{H}^+ + \text{HCO}_3^-$	-6.342
$\text{CO}_3^{2-} + \text{H}^+ \leftrightarrow \text{HCO}_3^-$	10.325
$\text{CaOH}^+ + \text{H}^+ \leftrightarrow \text{Ca}^{2+} + \text{H}_2\text{O}$	12.852
$\text{CaCO}_3(\text{aq}) + \text{H}^+ \leftrightarrow \text{Ca}^{2+} + \text{HCO}_3^-$	7.009
$\text{MgCO}_3(\text{aq}) + \text{H}^+ \leftrightarrow \text{HCO}_3^- + \text{Mg}^{2+}$	7.356
$\text{CaHCO}_3^+ \leftrightarrow \text{Ca}^{2+} + \text{HCO}_3^-$	-1.043
$\text{MgHCO}_3^+ \leftrightarrow \text{HCO}_3^- + \text{Mg}^{2+}$	-1.033
$\text{CaCl}^+ \leftrightarrow \text{Ca}^{2+} + 2\text{Cl}^-$	0.701
$\text{MgCl}^+ \leftrightarrow \text{Mg}^{2+} + \text{Cl}^-$	0.139
$\text{CaCl}_2(\text{aq}) \leftrightarrow \text{Ca}^{2+} + 2\text{Cl}^-$	0.654
$\text{HCl}(\text{aq}) \leftrightarrow \text{H}^+ + \text{Cl}^-$	0.700
$\text{Mg}_4(\text{OH})_4^{4+} + 4\text{H}^+ \leftrightarrow 4\text{H}_2\text{O} + 4\text{Mg}^{2+}$	39.743
$\text{MgOH}^+ + \text{H}^+ \leftrightarrow \text{H}_2\text{O} + \text{Mg}^{2+}$	11.785
$\text{NaCO}_3^- + \text{H}^+ \leftrightarrow \text{HCO}_3^- + \text{Na}^+$	9.816
$\text{NaCl}(\text{aq}) \leftrightarrow \text{Na}^+ + \text{Cl}^-$	0.782
$\text{NaHCO}_3 \leftrightarrow \text{HCO}_3^- + \text{Na}^+$	-0.170
$\text{NaOH}(\text{aq}) + \text{H}^+ \leftrightarrow \text{H}_2\text{O} + \text{Na}^+$	14.154
$\text{CO}_2(\text{g}) + \text{H}_2\text{O} \leftrightarrow \text{H}^+ + \text{HCO}_3^-$	-7.809
$\text{CaH}_2\text{SiO}_4(\text{aq}) + 2\text{H}^+ \leftrightarrow \text{Ca}^{2+} + 2\text{H}_2\text{O} + \text{SiO}_2(\text{aq})$	18.562
$\text{CaH}_3\text{SiO}_4^+ + \text{H}^+ \leftrightarrow \text{Ca}^{2+} + 2\text{H}_2\text{O} + \text{SiO}_2(\text{aq})$	8.792
$\text{H}_2\text{SiO}_4^{2-} + 2\text{H}^+ \leftrightarrow 2\text{H}_2\text{O} + \text{SiO}_2(\text{aq})$	22.910
$\text{H}_3\text{SiO}_4^- + \text{H}^+ \leftrightarrow 2\text{H}_2\text{O} + \text{SiO}_2(\text{aq})$	9.812
$\text{H}_4(\text{H}_2\text{SiO}_4)_4^- + 4\text{H}^+ \leftrightarrow 8\text{H}_2\text{O} + 4\text{SiO}_2(\text{aq})$	35.746
$\text{MgH}_2\text{SiO}_4(\text{aq}) + 2\text{H}^+ \leftrightarrow 2\text{H}_2\text{O} + \text{Mg}^{2+} + \text{SiO}_2(\text{aq})$	17.482
$\text{MgH}_3\text{SiO}_4^+ + \text{H}^+ \leftrightarrow 2\text{H}_2\text{O} + \text{Mg}^{2+} + \text{SiO}_2(\text{aq})$	8.542
$\text{NaH}_3\text{SiO}_4(\text{aq}) + \text{H}^+ \leftrightarrow 2\text{H}_2\text{O} + \text{Na}^+ + \text{SiO}_2(\text{aq})$	8.622
$\text{NaHSiO}_3(\text{aq}) + \text{H}^+ \leftrightarrow \text{H}_2\text{O} + \text{Na}^+ + \text{SiO}_2(\text{aq})$	8.298
$\text{HSiO}_3^- + \text{H}^+ \leftrightarrow \text{H}_2\text{O} + \text{SiO}_2(\text{aq})$	9.942
$\text{Dolomite} + 2\text{H}^+ \leftrightarrow 2\text{HCO}_3^- + \text{Mg}^{2+} + \text{Ca}^{2+}$	2.524
$\text{Quartz} \leftrightarrow \text{SiO}_2(\text{aq})$	-3.745

To avoid excessive dispersion, D_i is assumed to be equal to the numerical dispersion introduced by the discretization scheme used to numerically solve Eq. (1). K_d values are available from the batch sorption experiments conducted in this study (Table 3.2). For practicality, K_d is assumed to remain constant. Fig. 3.10 shows a representative result of two-dimensional (2D) simulations of the core-flooding experiments obtained using constant K_d values. The formulated reactive transport model was solved using TOUGHREACT-EOS9 V3.0 multiphase reactive transport simulator (Xu et al., 2014, Shabani and Vilcáez, 2017, 2018). Radial coordinates were used to ensure that the simulation results account for the three-dimensional (3D) transport of Ba through the cylindrical-shaped dolomite and sandstone cores.



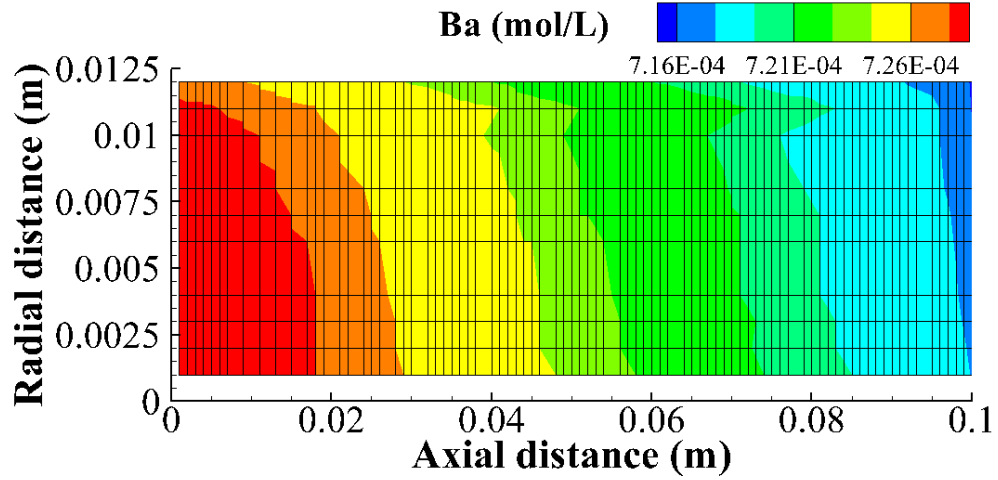
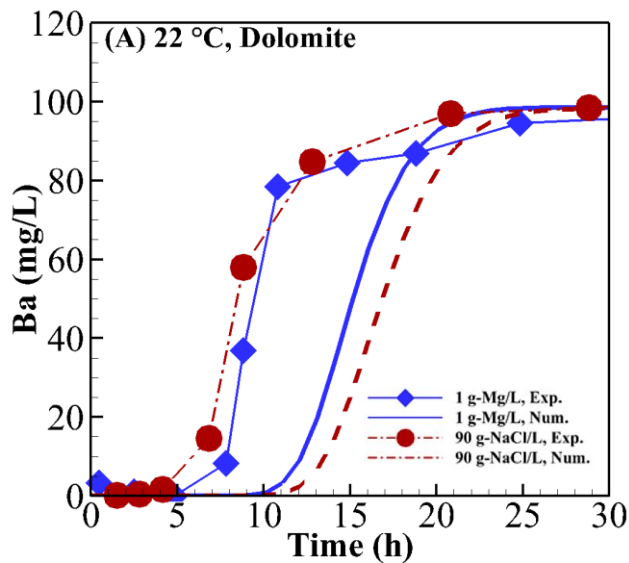


Fig 3. 10. Hassler type core-holder used for experiments, and simulation of the core-flooding experiments of Ba transport through a dolomite core: Equilibrium Ba sorption distribution.

Fig. 3.11 compares the measured and simulated breakthrough curves of Ba through synthetic dolomite and sandstone cores the properties of which are listed in Table 3.1. Simulated breakthrough curves of Ba exhibit reasonable agreement with the measured breakthrough curves of Ba through both dolomite and sandstone cores.



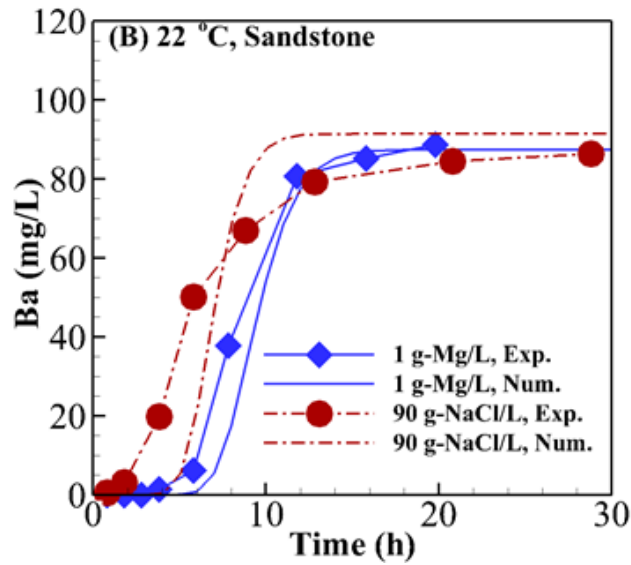


Fig 3. 11. Experimental versus numerical breakthrough curves of Ba transport through porous dolomite and sandstone cores.

These simulation results confirm that the transport of Ba in both dolomite and sandstone saline aquifers is largely controlled by its sorption to the rock types forming the aquifer. We observed that there is a better agreement between the measured and simulated breakthrough curves of Ba for the dolomite core compared to the sandstone core. This confirms that the reactivity of the rock types forming the aquifer plays an important role in controlling the transport of Ba. Apparently, high chemical reactivity minerals such as dolomite limits the use of constant K_d values to simulate Ba transport in dolomite saline aquifers. Therefore, our work highlights that the assumption of K_d constancy is more suitable for the numerical simulation of Ba transport in sandstone saline aquifers than in dolomite saline aquifers.

3.5. Conclusions

The following conclusions are withdrawn from the experimental and simulation studies conducted to assess the effect of salinity (NaCl), guar gum, competition of cations (Ca and Mg), and temperature on mobility of Ba in dolomite and sandstone and potential contamination of USDW:

Ba sorption is higher in highly pure dolomite than in quartz-dominated sandstone at both shallow (22 °C) and deep (60 °C) subsurface temperatures, and at both zero salinity and saline water containing NaCl Ca and Mg concentrations of petroleum produced water.

The difference in Ba sorption behavior between dolomite and sandstone significantly decreases with increasing salinity (NaCl) and/or the concentration of competing cations (Ca and Mg). At NaCl, Ca and Mg concentration levels of petroleum produced water, Ba sorption in both dolomite and sandstone is almost identical. This is due to the formation of $Ba(Cl)^+$ complexes as well as the competition of cations (Ca and Mg) for binding sites of minerals which results in the inhibition of Ba sorption.

Contrary to expectations, temperature does not play an important role in influencing the Ba sorption except under freshwater conditions represented by water with zero salinity. At NaCl, Ca and Mg concentration levels of petroleum produced water, temperature plays a minor role as observed from the similarity of Ba sorption levels in both the dolomite and sandstone when shallow and deep subsurface temperatures are considered.

Because high pH conditions are known to increase the number of negatively charged binding sites of minerals, and higher pH conditions occurred in the batch sorption experiments with dolomite than with sandstone, higher levels of Ba sorption in dolomite than in sandstone observed at all experiment scenarios is attributed to higher chemical reactivity of dolomite relative to sandstone.

The sorption and thus transport of Ba in dolomite and sandstone aquifers is controlled by salinity (NaCl), followed by the competition of cations for binding sites of minerals, pH, and temperature. The presence of fracturing organic polymers such guar gum at possible concentrations in produced water from UOG reservoirs has very little influence on the sorption and thus mobility of Ba in deep dolomite and sandstone aquifers.

Because of its low chemical reactivity compared to dolomite, the mobility of Ba in sandstone saline aquifers can be successfully simulated by a reactive transport model that accounts for the influence of dissolution of minerals, aqueous phase complexation reactions, and sorption reactions represented by a constant partition coefficient (K_d) value. However, to obtain accurate prediction of the transport of Ba in dolomite saline aquifers, the fact that K_d changes as function of pH needs to be taken into account.

3.6. Acknowledgements

We thank to the Society of Petrophysicists and Well Log Analysts (SPWLA) and Geological Society of America (GSA) for their financial support.

3.7. References

Acosta, J., et al., 2011. Salinity increases mobility of heavy metals in soils. *Chemosphere*. 85, 1318-1324.

Alden, A., 2017. Densities of Common Rocks and Minerals. ThoughtCo. [thoughtco.com/densities-of-common-rocks-and-minerals-1439119](https://www.thoughtco.com/densities-of-common-rocks-and-minerals-1439119).

Arias, F., Sen, T. K., 2009. Removal of zinc metal ion (Zn^{2+}) from its aqueous solution by kaolin clay mineral: A kinetic and equilibrium study. *Colloids and Surfaces A: Physicochemical and Engineering Aspects*. 348, 100-108.

Bradl, H. B., 2004. Adsorption of heavy metal ions on soils and soils constituents. *Journal of colloid and Interface Science*. 277, 1-18.

Ebrahimi, P., Vilcáez, J., 2018. Effect of brine salinity and guar gum on the transport of barium through dolomite rocks: Implications for unconventional oil and gas wastewater disposal *Journal of Environmental Management*.

EPA, Hydraulic Fracturing for Oil and Gas: Impacts from the Hydraulic Fracturing Water Cycle on Drinking Water Resources in the United States. United States Environmental Protection Agency, 2016.

Fan, Q., et al., 2009. Effect of pH, ionic strength, temperature and humic substances on the sorption of Ni (II) to Na-attapulgite. *Chemical Engineering Journal*. 150, 188-195.

Ghaemi, A., et al., 2011. Characterizations of strontium (II) and barium (II) adsorption from aqueous solutions using dolomite powder. *Journal of hazardous materials*. 190, 916-921.

Habibpour, M., Clark, P. E., 2017. Drag reduction behavior of hydrolyzed polyacrylamide/xanthan gum mixed polymer solutions. *Petroleum Science*. 14, 412-423.

Hamed, M. M., et al., 2016. Kinetics and thermodynamics studies of cobalt, strontium and caesium sorption on marble from aqueous solution. *Chemistry and Ecology*. 32, 68-87.

Hanes, R., et al., Analytical methods for maintaining quality assurance of recycled fracturing fluids. *International Symposium on Oilfield Chemistry*. Society of Petroleum Engineers, 2003.

Lajçi, N., et al., 2017. Assessment of Major and Trace Elements of Fresh Water Springs in Village Pepaj, Rugova Region, Kosova. *J. Int. Environmental Application & Science*. 12, 112-120.

Landry, C. J., et al., 2009. Surface complexation modeling of Co (II) adsorption on mixtures of hydrous ferric oxide, quartz and kaolinite. *Geochimica et Cosmochimica Acta*. 73, 3723-3737.

- Lester, Y., et al., 2013. Can we treat hydraulic fracturing flowback with a conventional biological process? The case of guar gum. *Environmental Science & Technology Letters*. 1, 133-136.
- Lutz, B. D., et al., 2013. Generation, transport, and disposal of wastewater associated with Marcellus Shale gas development. *Water Resources Research*. 49, 647-656.
- Ma, X., Pawlik, M., 2007. Role of background ions in guar gum adsorption on oxide minerals and kaolinite. *Journal of colloid and interface science*. 313, 440-448.
- McBroom, M., Study of the Potential Impacts of Hydraulic Fracturing on Drinking Water Resources. *The Effects of Induced Hydraulic Fracturing on the Environment: Commercial Demands vs. Water, Wildlife, and Human Ecosystems*. Apple Academic Press, 2013, pp. 141-228.
- Mohamed, A., et al., 2017. Removal of chromium (VI) from aqueous solutions using surface modified composite nanofibers. *Journal of colloid and interface science*. 505, 682-691.
- Murray, K. E., 2014. Class II underground injection control well data for 2010–2013 by geologic zones of completion, Oklahoma. *Oklahoma Geological Survey Open File Report OF1*. 32.
- Murray, K. E., 2015. Class II saltwater disposal for 2009–2014 at the annual-, state-, and county-scales by geologic zones of completion, Oklahoma. *Okla. Geol. Surv. Open-File Rept. OF5-2015*. 1-12.
- Palandri, J. L., A compilation of rate parameters of water-mineral interaction kinetics for application to geochemical modeling. In: Y. K. Kharaka, (Ed.). U.S. Dept. of the Interior, U.S. Geological Survey, Menlo Park, Calif. :, 2004.
- Reich, T. J., et al., 2010. Surface complexation modeling of Pb (II) adsorption on mixtures of hydrous ferric oxide, quartz and kaolinite. *Chemical Geology*. 275, 262-271.

- Rozell, D. J., Reaven, S. J., 2012. Water pollution risk associated with natural gas extraction from the Marcellus Shale. *Risk Analysis*. 32, 1382-1393.
- Sangiumsak, N., Punrattanasin, P., 2014. Adsorption Behavior of Heavy Metals on Various Soils. *Polish Journal of Environmental Studies*. 23.
- Shahwan, T., et al., 1998. Sorption studies of Cs⁺ and Ba²⁺ cations on magnesite. *Applied radiation and isotopes*. 49, 915-921.
- Strawn, D. G., Sparks, D. L., 2000. Effects of soil organic matter on the kinetics and mechanisms of Pb (II) sorption and desorption in soil. *Soil Science Society of America Journal*. 64, 144-156.
- Temminghoff, E., et al., 1995. Speciation and calcium competition effects on cadmium sorption by sandy soil at various pHs. *European Journal of Soil Science*. 46, 649-655.
- Tessier, A., et al., 1989. Partitioning of zinc between the water column and the oxic sediments in lakes. *Geochimica et Cosmochimica Acta*. 53, 1511-1522.
- Xing, S., et al., 2011. Removal of heavy metal ions from aqueous solution using red loess as an adsorbent. *Journal of Environmental Sciences*. 23, 1497-1502.
- Xu, T., et al., 2014. TOUGHREACT V3.0-OMP Reference manual: A parallel simulation program for non-isothermal multiphase geochemical reactive transport. Lawrence Berkeley Lab. Berkeley, California.
- Yost, E. E., et al., 2016. Overview of chronic oral toxicity values for chemicals present in hydraulic fracturing fluids, flowback, and produced waters. *Environmental science & technology*. 50, 4788-4797.

CHAPTER IV

TRANSPORT of BARIUM through FRACTURED SANDSTONE and DOLOMITE ROCKS in PETROLEUM PRODUCED WATER DISPOSAL

Pouyan Ebrahimi, Javier Vilcáez*

Boone Pickens School of Geology, Oklahoma State University, Stillwater, OK 74078, USA

4.1. Abstract

The disposed wastewater from conventional and unconventional petroleum reservoirs which contains heavy metals such as Ba may cause an environmental risk by migrating through fractured disposal sites toward the underground source of drinking water (USDW). In this paper we investigated the importance of mechanical and chemical transport of Ba through fractured sandstone and dolomite by conducting a set of core flooding experiments. A discrete fracture was generated by cutting the core plugs along their longitudinal axis. The experiments were conducted at different salinities (0 and 90,000 mg-NaCl/L), at the presence of the most common divalent cations (5000 mg-Ca/L and 1000 mg-Mg/L) of the wastewater, and the most common viscosities used for hydraulic fracturing purposes (guar gum). We applied a discrete fracture network model (DFN) using TOUGHREACT simulation to model the transport of Ba through intact/fractured sandstone and dolomite rocks by analyzing the role of (1) advection through a discrete fracture; (2) fluid dispersion in the matrix; and (3) Ba partition coefficient on sandstone/dolomite using different solutions. The main finding of this paper is that, although the sorption of Ba on surface of dolomite

is higher than the sandstone, the transport of Ba through intact and fractured dolomite is faster than sandstone. This is due to the fact that the dispersion in the sandstone matrix with a higher permeability ($\sim 10^{-14} \text{ m}^2$) is more than dolomite matrix with a lower permeability ($\sim 10^{-16} \text{ m}^2$). Hence by generating a synthetic fracture, the fluid disperses easily in the sandstone matrix and retards the transport of Ba.

* Corresponding author, Telephone: +1-405-744-6361. Email: vilcaez@okstate.edu

Keywords: Petroleum produced wastewater disposal, Mechanical and chemical transport, Fracture, Sandstone, Dolomite, Ba mobility, Core flooding experiment.

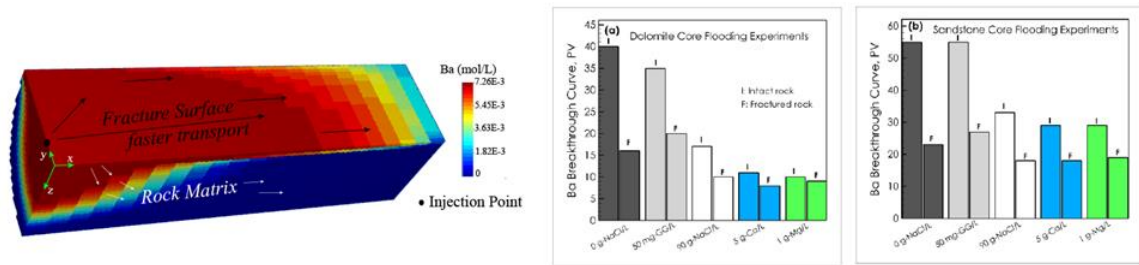


Fig. 4. 1. Graphical abstract.

4.2. Introduction

Millions of gallons of produced water from hydraulically fractured oil and gas wells have been managed through injection in Class II wells and reuse in other fracturing operations and various aboveground disposal practices (EPA., 2016a). In 2012, almost half of the produced water from onshore wells in the USA is injected into the disposal wells (Veil, 2015). For example, the number of active Class II disposal wells in Oklahoma is 3,837 by 2016 (EPA., 2016b). The produced wastewater contains a high level of salinities (18,000 to 300,000 mg/L), heavy metals (i.e. Ba, Sr), organics and in some cases radioactive materials (Veil et al., 2004). A recent EPA report notes that

for most people in the USA, approximately 42% of the drinking water comes from groundwater resources (Maupin et al., 2014). The possible environmental risks associated with the migration of disposed produced water from disposal sites toward the underground source of drinking water (USDW) have created public debate about the produced water disposal.

In the subsurface, the fluid flows through matrix of the rocks and through fractures. Hence, analyzing the flow transport through fractured porous media is an essential need for investigating the HFW migration from disposal sites toward USDW (Kumar, 2008). Flow and transport through a single fracture have been widely studied before. In most of the fracture analysis, a fracture is assumed as a single open space between two surfaces with a constant separation. The fracture aperture is bounded by the rock matrix and can play a significant role in the transport of solute and its mechanical and chemical retardation (Kumar, 2008; Rasmuson and Neretnieks, 1981). Mechanical retardation results from solute transfer by advective movement along the high permeability fractures to diffusion-controlled rock matrix with the lower permeability (Venture, 2004). Chemical retardation is due to sorption of solute which is basically a transfer of a solute from the liquid phase to the solid phase because of the multiple chemical reactions between transporting fluid and the fracture walls and/or the solid grain surfaces of rock matrix (Kumar, 2008). A higher sorption will cause a slower transport.

The chemical retardation could be represented by partition coefficient (K_d) values. K_d is mainly controlled by the type of sorbate (metal) and sorbent (soil, rock) and the pH. Janssen et al. (1997) show that the most significant factor on the distribution of “Cd, Cr, and Pb,” “As and Cu,” and Ni in the soil are respectively pH, Fe content and dissolved organic carbon. Ebrahimi and Vilcáez (2018b) found that the K_d of Ba is primarily controlled by salinity (NaCl, Ca and Mg) of the solution and type of rock (dolomite and sandstone). They also found that dissolution of dolomite which affects the pH of the solution can influence on K_d . However, for sandstone with a small amount of

dissolution in comparison with dolomite, the solution quickly reaches the equilibrium and K_d is not affected by sandstone dissolution.

Both diffusion and sorption influence the behavior of solute and subsequently complexes the spreading of solutes along the fracture (Kumar, 2008). To simplify simulation of reactive transport of contaminants in fractured rocks it is usually assumed that the solute transport is governed by a linear sorption isotherm and could be represented by distribution coefficient, K_d (Fetter et al., 2017; Tang et al., 1981). Batch experiments are a simple and quick way to empirically identify K_d values and investigate the sorption of solute on an adsorbent. In this study we used the results of batch experiments parented by Ebrahimi and Vilcez (2018b) and conducted a series of simplistic core flooding experiments to:

- find the actual breakthrough curve of Ba through fractured sandstone and dolomite core plugs and provide direct evidence of Ba mobilization/retardation as a function of K_d .
- understand how the presence of synthetic fractures may affect the Ba transport through sandstone and dolomite rocks with different mechanical dispersions
- test the accuracy of reactive transport codes in predicting breakthrough curves of Ba through intact and fractured sandstone and dolomite.

The experiments are conducted on salinities relevant to the salinities of produced water in Oklahoma. Core flooding experiments using intact core plugs provide information on the effects of advective/dispersive flow on sorption behavior in the sandstone and dolomite. Flooding experiment is a means to quantify some effects (K_d and mechanical dispersion) of coupled fluid transport under simulated flow conditions. We conducted core flooding experiments on intact and fractured plugs to demonstrate retardation in Raton sandstone and Arbuckle dolomite. Three parameters that may influence Ba transport were varied in the experiments: type of rock, brine and

fracture. We tested five different solutions on two type of rocks (sandstone and dolomite) in presence and absence of synthetic fractures.

4.3. Materials

4.3.1. Natural Porous Rocks with/without Synthetic Fractures

Sandstone and dolomite rocks represent the characteristic sedimentary rocks that are primarily used for wastewater disposal in the state of Oklahoma. Sandstone is prepared from <300 depth of Raton Formation from Las Animas County, Colorado and dolomite is collected from Arbuckle Group, McDonald County, Missouri. Experiments were conducted to study the transport of Ba during flow of a fracturing wastewater into these rocks. The sandstone and dolomite in this study respectively comprise “a fine grain lithology, low porosity (~3-5%) and low permeability ($1-3 \times 10^{-16} \text{ m}^2$)” and “a fine grain lithology, low porosity (~5-8%) and low permeability ($1.1 \times 10^{-15}-6.3 \times 10^{-14} \text{ m}^2$).” Although the dolomite contain vuggy pores (<3mm), they are isolated and because of that they do not have high permeability.

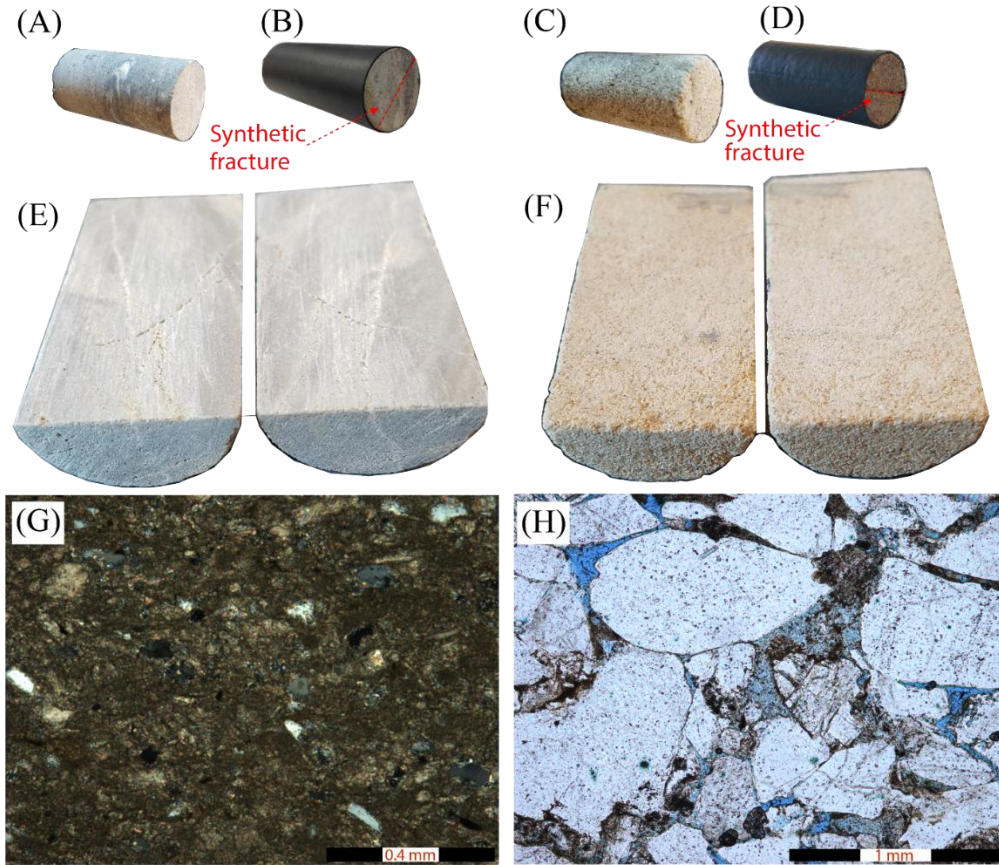


Fig. 4. 2. Representative core plug, synthetic fractures and photomicrograph analysis of sandstone and dolomite

Cylindrical plugs, with diameter of 2.54 cm and length of ~5 cm were cut from collected rocks (Fig. 4.2A&C). The plugs were cut into two equal semi-cylinder along their longitudinal axis for the purpose of creating synthetic fractures (Fig. 4.2E&F). To increase the reactivity of the smooth surface of synthetic fractures in dolomite rocks, they are uniformly roughened by a half round wood rasp file. After cutting rocks and abrading them, there is no distinct differences on surface of synthetic fractures for each type of rock. Two semi-cylinders were hold together by using a heat-shrink rubber sleeve (Fig. 4.2B&D). The fracture aperture of the sandstone and dolomite is ~180-400 μ m and ~150-300 μ m, respectively as indicated by digital microscope (20x-800x Magnification). Fig. 4.2G&H represent the photomicrograph analysis conducted on the collected

sandstone and dolomite. The grain sizes of sandstone and dolomite are respectively ~100-2000 μm and ~50-150 μm . The XRD analysis the sandstone is mainly composed of quartz (>98%) and <2% is clay minerals; and the dolomite is mainly composed of dolomite minerals (>99%) and <1% carbonate and silt (Ebrahimi and Vilcáez, 2018b).

4.3.2. Synthetic Petroleum Produced Water

Inductively coupled plasma-atomic emission spectroscopy (ICP-OES) analysis conducted on HFW near Stillwater, OK, confirmed that produced water in Oklahoma contains high TDS ranging from 90,000 to 180,000 mg/L, with TDS mainly composed of NaCl (>93.5%), Ca (~5%) and Mg (~1%), and <0.5% of other elements (e.g., Fe, S, N). pH ranges from 5.9 to 6.9. Based on this information and given the relevance of divalent cations (e.g., Ca and Mg) on the competition for surface binding sites and surface charge of minerals, which affects the sorption of Ba, we used a synthetic produced water composed of NaCl, $\text{CaCl}_2 \cdot 2\text{H}_2\text{O}$, $\text{MgCl}_2 \cdot 6\text{H}_2\text{O}$ and $\text{BaCl}_2 \cdot 2\text{H}_2\text{O}$ (all from Fisher Scientific with >99% purity). Concentrations corresponded to the analyzed produced water from HFW reservoirs in Oklahoma. The synthetic produced water composition included guar gum, which was provided by PfP Industries LLC that supplies additives to hydraulic fracturing and oilfield completion companies in the USA. To ensure that guar gum molecules have been hydrated properly in the synthetic brine, guar gum was added to the synthetic brine 24 hours prior to its utilization (Habibpour and Clark, 2017).

4.4. Experimental Setup

Core-flooding experiments were conducted to assess the effect of fracture on the transport of Ba through sandstone and dolomite rocks at 22 °C and a confining pressure of 6,894 MPa. To emulate petroleum produced water injection into a saline aquifer, prior to the injection of the synthetic petroleum produced water solution containing Na, Cl, Ca, Mg, Ba and/or guar gum, the core plug was saturated with a brine solution composed of NaCl and deionized water. The synthetic

petroleum produced water was injected using a dual piston Chrom Tech-HPLC pump at constant rate of 0.05 ml/min in all core-flooding experiments. For the plugs with synthetic fracture, the synthetic solution was injected from the center of the plug and the effluent line was placed at the center of other end. The injection and production are from a combination of advective transport through synthetic fractures and diffusive transport of the porous media. The inlet pressure of the core holder was measured using a Rosemount pressure transducer with a scale resolution of 0.48 kPa and the effluent was collected in 0.5 ml volumes every 10 minutes for 60 hours using an automatic fraction collector. Collected samples were analyzed for their Ba content by ICP-OES analysis. Experimental set-up are shown in Fig. 4.3.

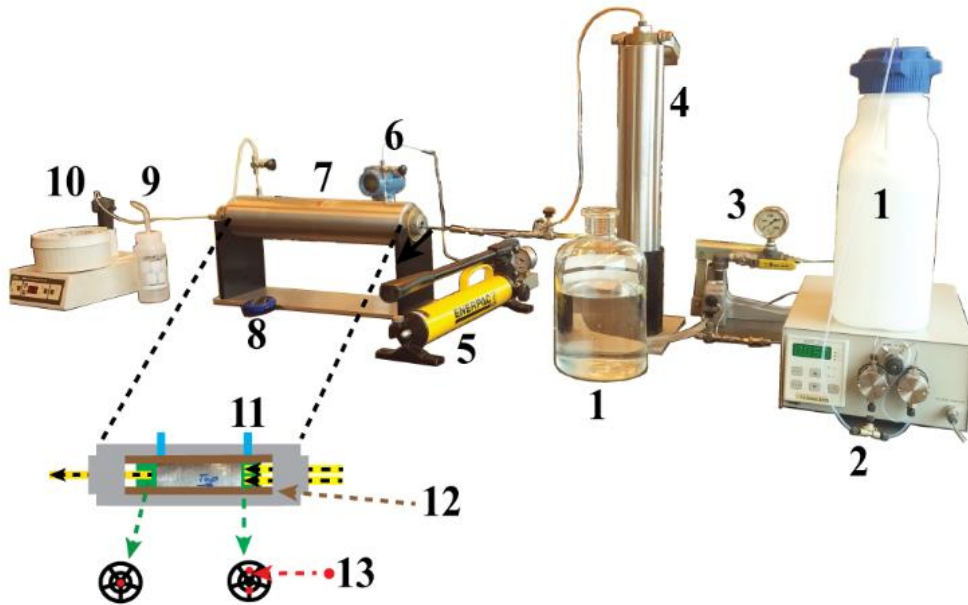


Fig. 4. 3. Core-flooding experimental setup: (1) Water tank, (2) Dual piston Chrom Tech-HPLC pump, (3) Hand pump, (4) Floating piston accumulator containing brine, (5) Confining pump, (6) Pressure transducer, (7) Hassler type core holder, (8) Chronometer, (9) Water tank, (10) Fraction collector, (11) Confining pressure port, (12) Viton sleeve, (13) Fluid injection/production port.

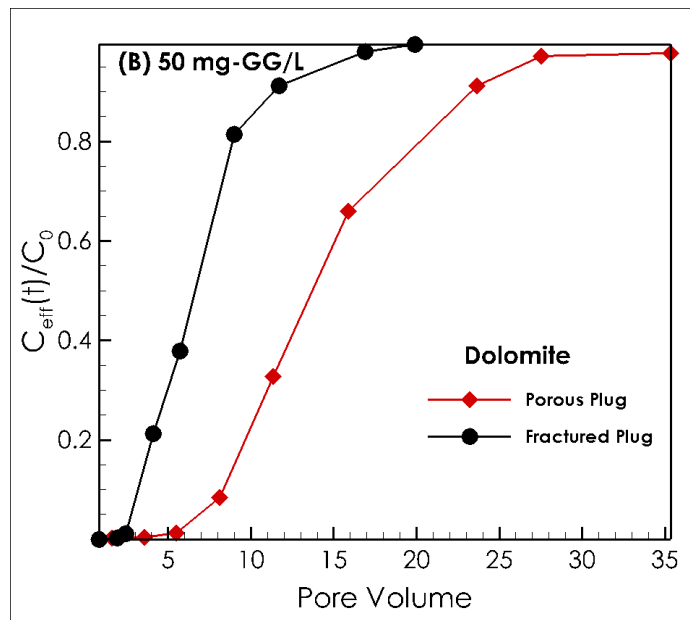
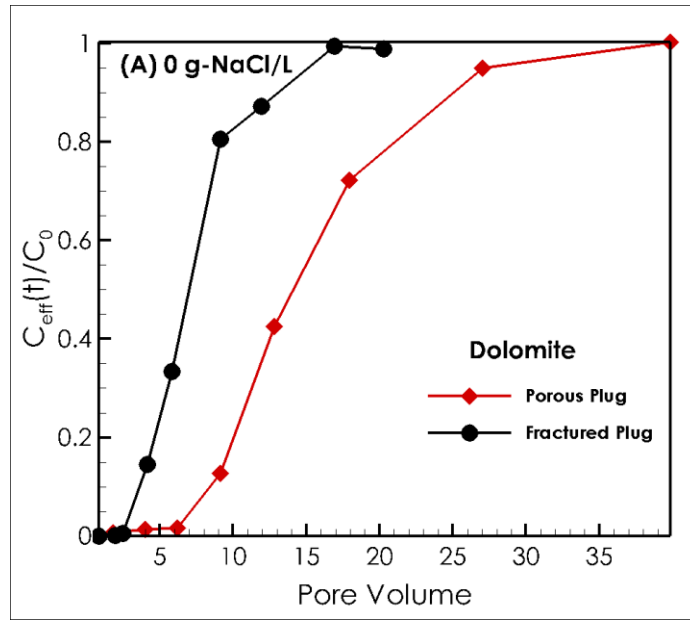
4.5. Results and Discussion

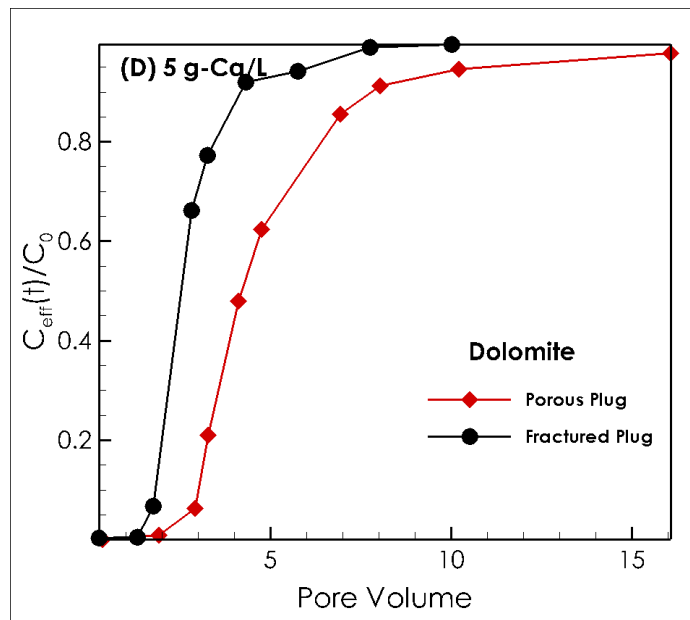
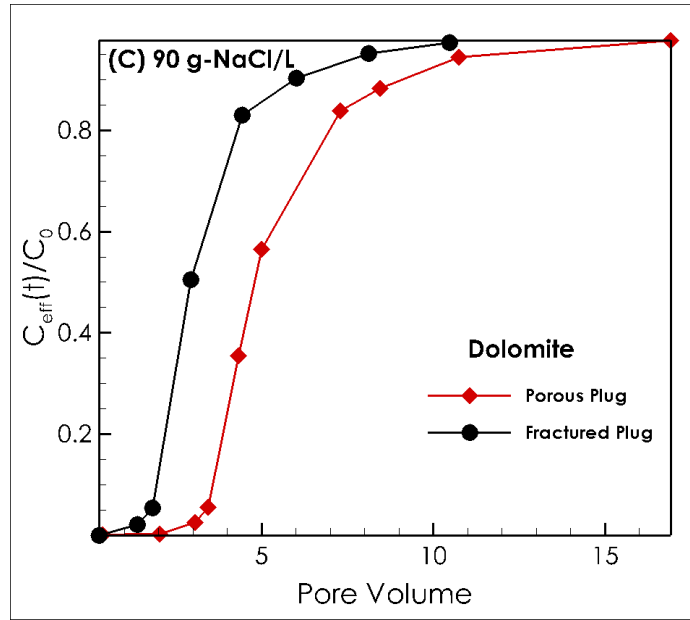
Core plug properties and applied solutions' composition are shown in the Table 4.1. Solutions in Table 4.1 are representative of produced HFW. In this study, the term “salinity” refers to the amount of NaCl in the solution.

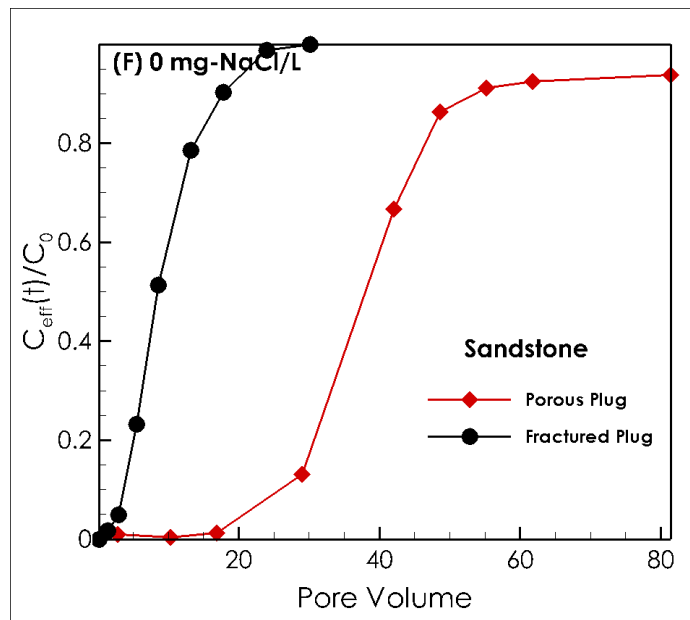
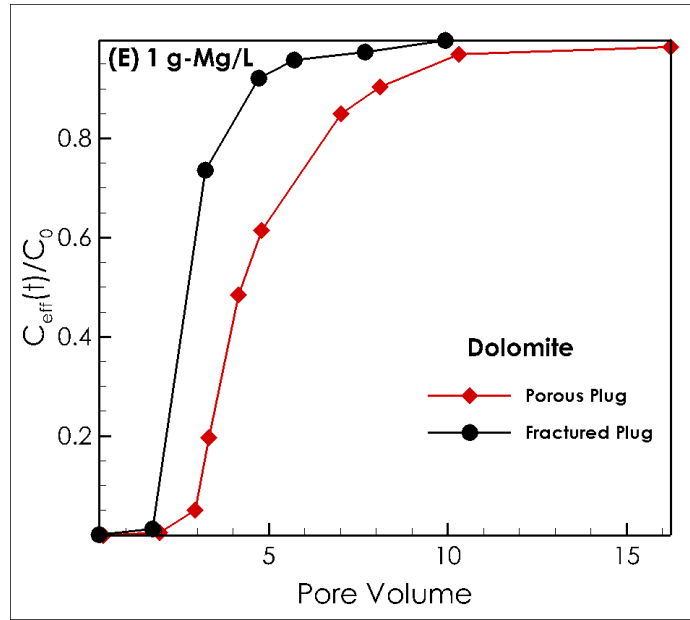
Table 4. 1. Core plug properties and solution composition used in core flooding experiments. Ba concentration kept constant at 100 mg/L.

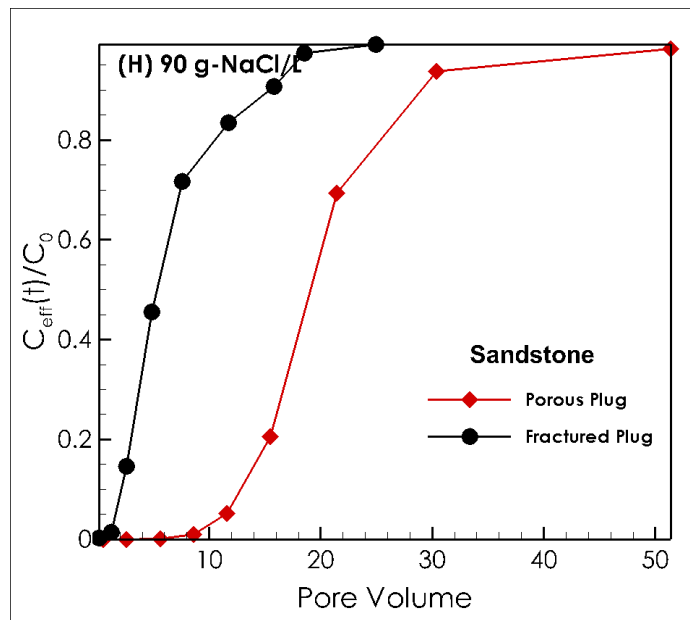
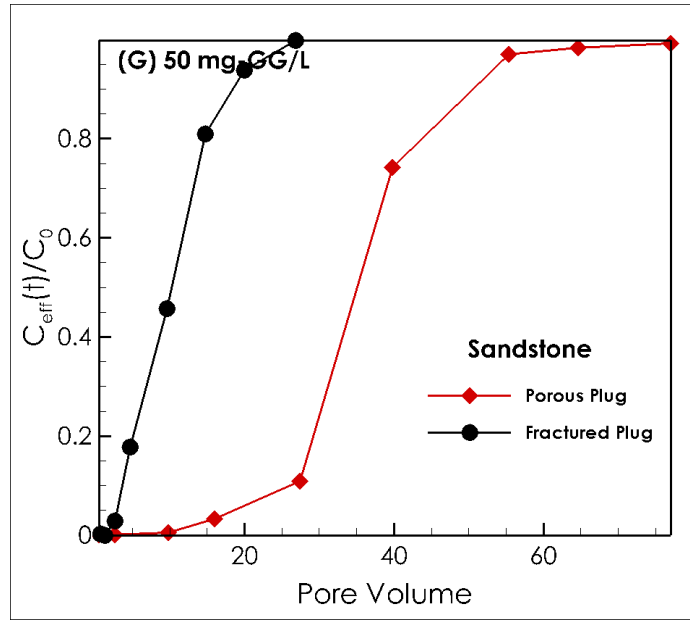
#	Rock Type	ϕ^a (%)	K^b (m^2)	L^c (cm)	PV^d	GG (mg/L)	NaCl (mg/L)	Ca (mg/L)	Mg (mg/L)
1	Intact Dol	5.3	1.0E-16	5.1	1.4	0	0	0	0
2	Intact Dol	6.2	1.8E-16	4.9	1.5	50	0	0	0
3	Intact Dol	5.4	3.0E-16	4.8	1.3	0	90,000	0	0
4	Intact Dol	5.4	2.3E-16	5.0	1.4	0	0	5,000	0
5	Intact Dol	5.4	2.8E-16	5.0	1.4	0	0	0	1,000
6	Fractured Dol	7.1	3.1E-13	5.0	1.8	0	0	0	0
7	Fractured Dol	7.2	1.4E-14	5.0	1.8	50	0	0	0
8	Fractured Dol	7.5	2.9E-13	5.0	1.9	0	90,000	0	0
9	Fractured Dol	7.9	2.1E-13	5.0	2.0	0	0	5,000	0
10	Fractured Dol	8.1	1.1E-13	4.9	2.0	0	0	0	1,000
11	Intact S.S.	3.6	6.3E-14	5.0	0.9	0	0	0	0
12	Intact S.S.	3.8	2.8E-15	5.1	1.0	50	0	0	0
13	Intact S.S.	3.9	1.1E-15	5.1	1.0	0	90,000	0	0
14	Intact S.S.	4.1	6.3E-14	5.0	1.0	0	0	5,000	0
15	Intact S.S.	5.1	2.4E-15	5.0	1.3	0	0	0	1,000
16	Fractured S.S.	15.3	1.9E-13	5.0	3.9	0	0	0	0
17	Fractured S.S.	13.2	1.2E-13	5.2	3.5	50	0	0	0
18	Fractured S.S.	17.0	9.7E-14	5.1	4.4	0	90,000	0	0
19	Fractured S.S.	18.1	9.4E-14	4.9	4.5	0	0	5,000	0
20	Fractured S.S.	16.9	1.2E-14	4.9	4.2	0	0	0	1,000

^aPorosity (%), ^bPermeability, ^cLength (cm), ^dPore Volume, ^eDolomite (Dol), ^fSandstone (S.S.)









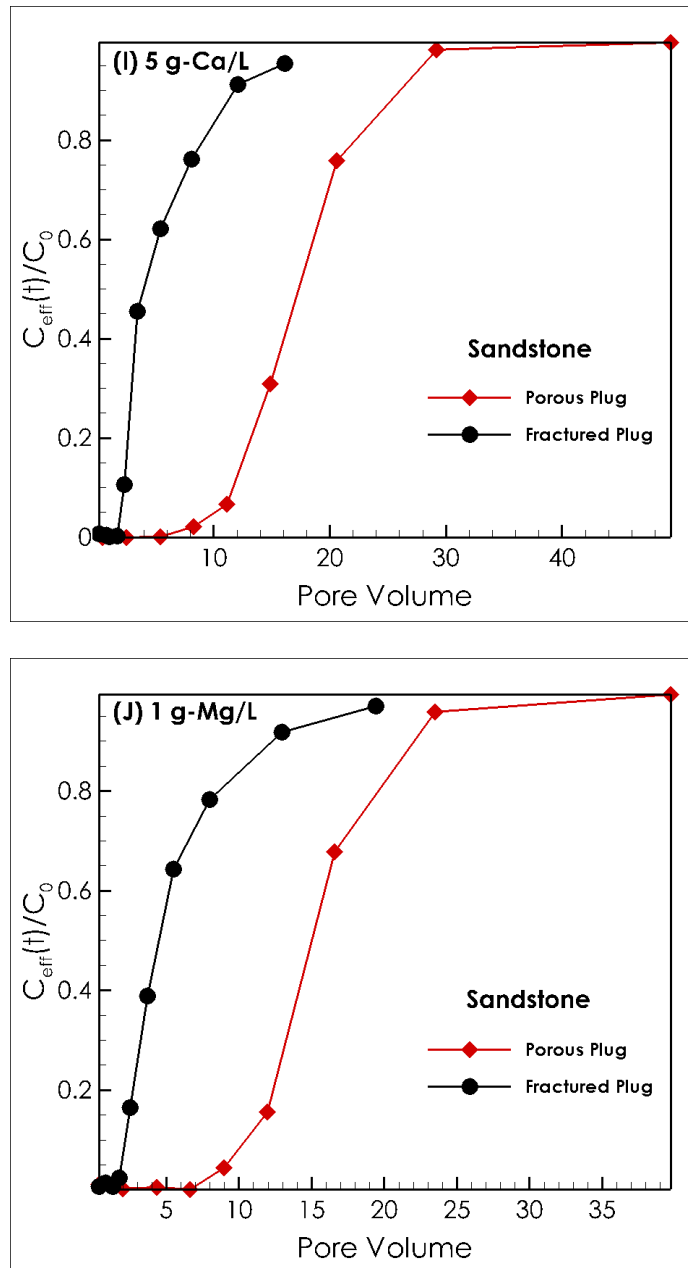


Fig. 4. 4. Core flooding experiments results using intact and fractured sandstone and dolomite plugs.

Fig. 4.4 compares the breakthrough curves of Ba through intact and fractured sandstone and dolomite core plugs. The figure shows the results of relative Ba concentration at the effluent side ($C(t)/C_0$) versus the pore volume (PV). Here C_0 and $C(t)$ stand for inlet initial concentration and

concentration at the time of measurement at the outlet and PV is defined as the ratio of total volume of extracted effluent per pore volume of the core plug. The rock properties are listed in Table 4.1. The flow rate kept constant at 0.05 ml/min for comparison purpose of experiments using different plugs and solutions. All experiments are conducted at an ambient temperature of 22°C and a constant confining pressure of 6894 kPa.

Overall, increasing salinity decreases the breakthrough curve of Ba through both intact/fractured sandstone and dolomite (Fig. 4.1 and Fig. 4.4). It is also observed that adding guar gum to the solution does not significantly affect the breakthrough curve of Ba. These results are along with the results of batch and core flooding experiments conducted by Ebrahimi and Vilcáez (2018a, 2018b) where increasing salinity decreases Ba sorption on both sandstone and dolomite.

Ebrahimi and Vilcáez (2018b) found that Ba sorption (partition coefficient) on dolomite is more than two times larger than on sandstone at zero salinity. Subsequently one may conclude that transport of Ba through dolomite is slower than sandstone due to higher sorption on dolomite. However, by comparing results of sandstone and dolomite in Fig. 4.1 and Fig. 4.4, the breakthrough curve of all experiments using dolomite is faster than sandstone using a similar solution. Thus, besides the chemical retardation, the mechanical retardation is significantly controlling the transport of Ba. It is noteworthy to mention that, the PV of both intact sandstone and dolomite is around 0.9-1.6 mL³. Hence, having a larger breakthrough curve in sandstone is not because of higher PV in sandstone.

Presence of fracture decreases breakthrough curves in both sandstone and dolomite. The amount of the reduction is different at different salinities. The maximum decrease in the breakthrough curve is at 0 salinity for sandstone which decreases by 32 PV (from 55 to 23 PV) at 0 guar gum, and by 28 PV (from 55 to 27 PV) at 50 mg-guar/L. It means that at 0 salinity, the fractures play a significant role in reducing the breakthrough curve of intact sandstone at zero salinity. The same reduction

trend was observed for dolomite rocks at zero salinity where the breakthrough curve of Ba decreases by 24 PV (from 40 to 16 PV) at 0 mg-guar/L and by 6 PV (from 26 to 20 PV) at 50 mg-guar/L. On the other hand, the amount of breakthrough curve reduction at high salinity solutions ranges 10 and 15 PV for sandstone and ranges between 1 and 7 PV for dolomite. It could be concluded that at high salinity, the presence of fractures plays a secondary role in increasing the transport of Ba through a porous media especially in dolomite rocks. It is important to mention that the presence of fractures in sandstone has more impact on reducing the breakthrough curve of sandstone than dolomite. This could be due to the fact that, distribution of the fluid from fracture aperture into a rock with higher permeability (i.e. sandstone) is more than a rock with lower permeability (i.e. dolomite). Indeed, in presence of the fractures, the retardation of high permeable rocks will be higher than low permeable ones.

Investigating the fluid flow through fractures is critical, especially for low permeable rocks (such as dolomite) as the fluid transport may significantly rely on fracture network (Cai, 2014). A number of modeling methods has been devolved to deal with flow through fractured systems which can account for different parameters including fracture distributions, hydraulic characteristics, rock matrix properties, and flow and transport processes (Bordas, 2005). In general, these models are divided into two categories: continuum models and discrete fracture network models (DFN) (Berkowitz, 2002). The continuum models rely on the assumption that within each continuum an approximate equilibrium exists at a given location and for all times (Wu et al., 2004). On the other hand, the central motivation of DFN model is due to the fact that at every scale, the flow through fractured porous media is dominated by a limited number of discrete pathways formed by fractures (Dershowitz et al., 2004). The DFN model can quantify many flow and transport pathways which are not effectively taken into account by continuum models. DFN can explicitly capture the effects of each fracture on fluid flow (Berkowitz, 2002).

Since there is only one single fracture in the core plugs, in this paper we use the DFN model to capture the effect of generated discrete fracture on Ba transport through sandstone and dolomite. The DFN model is applied by using a parallel plate model which is broadly applied to simulate fluid flow through a fracture due to its simplicity of idealizing a fracture. Then later, the simulation could be up-scaled to a field scale. In a parallel plate model, the fluid is evenly distributed over the fracture plate and it can access to all interfaces between the fracture and the matrix (Erwinsyah and Yan, 1999). The corresponding transport equation of each component k can be written as follows (Wu et al., 2004):

$$\begin{aligned} \frac{\partial}{\partial t} \{ \phi \sum_{\beta} (\rho_{\beta} S_{\beta} X_{\beta}^k) + (1 - \phi) \rho_s \rho_L X_L^k K_d^k \} + \lambda_k \{ \phi \sum_{\beta} (\rho_{\beta} S_{\beta} X_{\beta}^k) + (1 - \phi) \rho_s \rho_L X_L^k K_d^k \} = \\ - \sum_{\beta} \nabla \cdot (\rho_{\beta} X_{\beta}^k v_{\beta}) + \sum_{\beta} \nabla \cdot (\rho_{\beta} D_{\beta}^k \cdot \nabla X_{\beta}^k) + q^k \end{aligned} \quad \text{Eq. 1}$$

where subscript β is an index for fluid phase ($\beta=L$ for liquid and g for gas), and k is an index for mass components, ϕ is the porosity, ρ_{β} is the density of phase β at in situ conditions (kg/m³), S_{β} is the fluid saturation of phase β , X_{β}^k is the mass fraction of component k in phase β , ρ_s is the density of rock grain (kg/m³), K_d^k is the distribution coefficient of component k between the liquid phase and rock solids of fractures and matrix (m³/kg), λ_k is the radioactive decay constant of the chemical species k (s⁻¹), v_{β} is the darcy's velocity of phase β (m/s), D_{β}^k is the effective hydrodynamic dispersion tensor accounting for both molecular diffusion and mechanical dispersion for component k in phase β (m²/s), and q^k is source/sink or fracture–matrix interaction of mass for component k (kg/s m³) which includes the aqueous phase kinetic reactions such as sorption reactions of solute k and mineral phase kinetic reactions such as dissolution/precipitation reactions of solute (Ebrahimi and Vilcez, 2018a, b).

The fluid flow models are discussed in detail by Pruess (1987, 1991). Aqueous species not only are subject to transport in the liquid phase, but also interact with chemical interactions with the solid

and gaseous phases (Xu et al., 2014). Chemical transport is explained by advection and diffusion processes and is also subject to sorption and partitioning between phases (Wu and Fakcharoenphol, 2011). The diffusion coefficients are assumed to be the same for all aqueous species (Xu et al., 2014).

The applicability of DFN method is tested by simulating the transport of Ba through fractured sandstone and dolomite. K_d values are available from the batch sorption experiments conducted by Ebrahimi and Vilcáez (2018b). We are using TOUGHREACT-EOS3 multiphase reactive transport to simulate the results of fluid flow and transport through fractured core plugs (Xu et al., 2014). We used a radial coordinates to ensure that the simulation results account for the three-dimensional (3D) transport of Ba through the cylindrical-shaped dolomite and sandstone cores (Fig. 4.4). The dispersion of fluid within the porous media is assumed to be the same as the numerical dispersion introduced by Eq. 1. The permeability of rock matrix is equal to the permeability of intact plugs and the permeability of synthetic fracture is assumed to be equal to the measured permeability of fractured rocks. The porosity of rock matrix is equal to the measured porosities before cutting the rock along its axial axis and the porosity of fracture is assumed to be equal to 90%. For the fractured rocks, a layer of meshes is assigned to the fracture spacing (Fig 4.5). In this study, we kept the K_d constant for simulation of each specific experiment. The initial and injection conditions kept the same as used one by Ebrahimi and Vilcáez (2018b). The grain size of the dolomite is assigned as 150 μm for dolomite and 500 μm for sandstone.

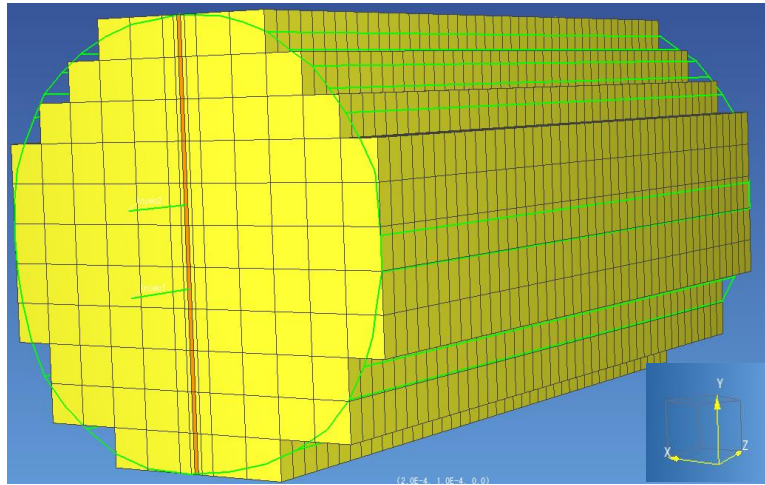
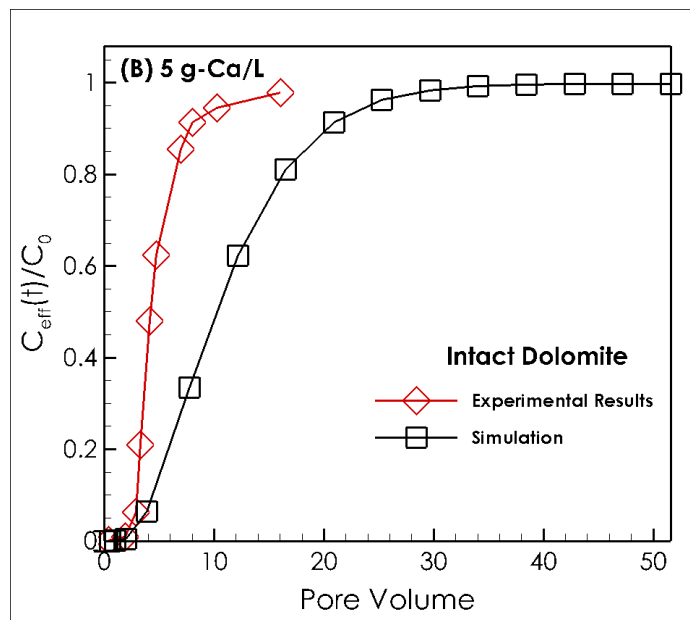
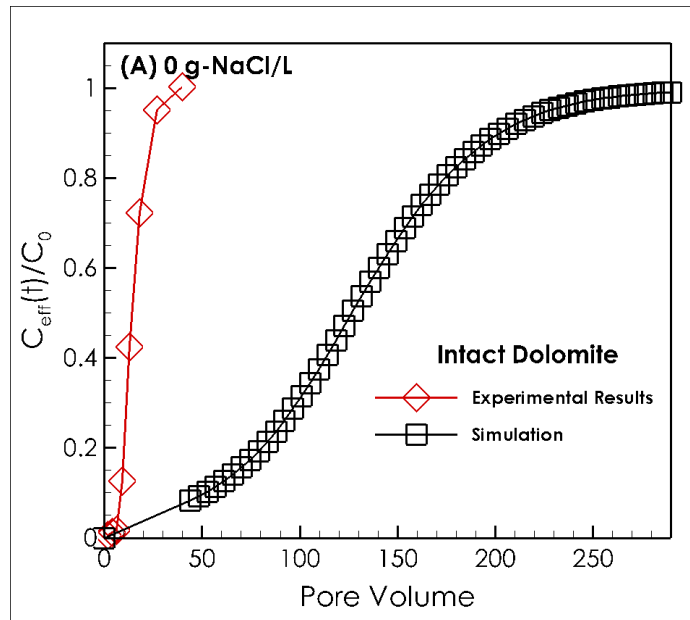
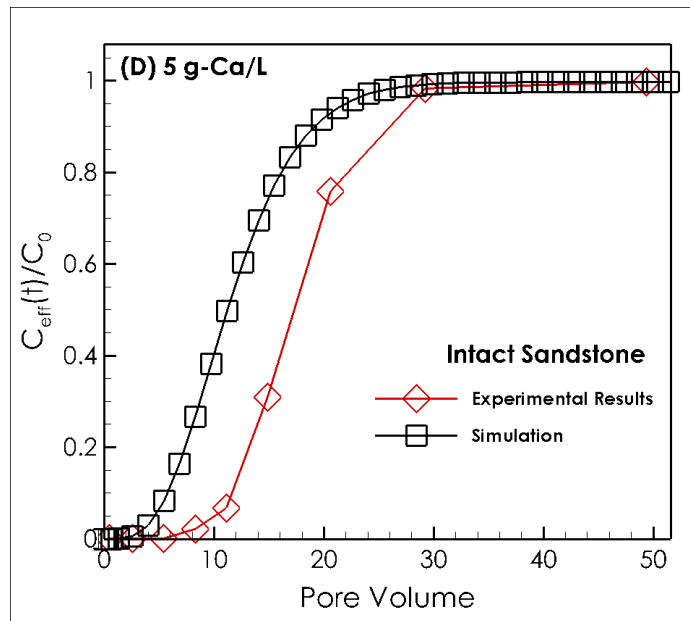
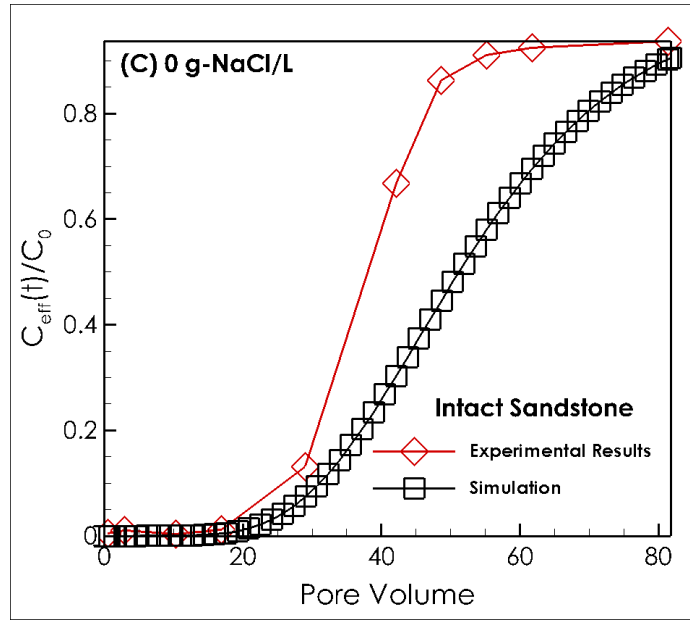


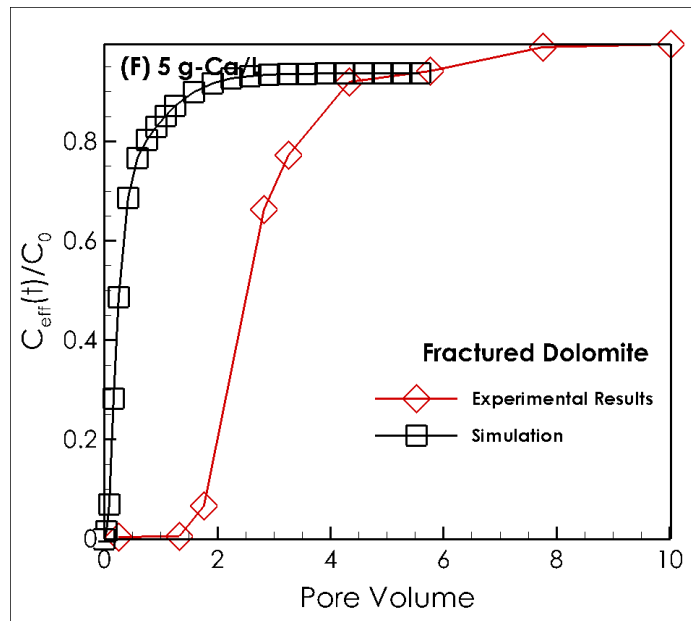
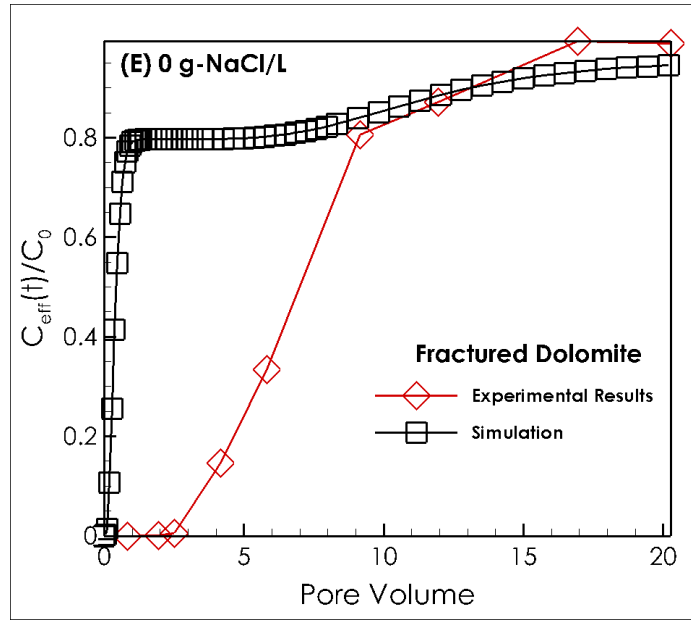
Fig. 4. 5. Discretization of the fractured core plug. The central mesh (orange color) is representative of a fracture line with permeability and porosity of fracture.

Two injection points with flow rate of 4.17×10^{-7} kg/s are located at inlet side and one production point with flow rate of 8.33×10^{-7} kg/s is located on the opposite side as it was in the conducted experiments. The block is discretized into 15, 11, and 22 grid blocks in x, y and z direction. A layer along the z axis at $x=1.27$ cm is assigned to the fracture layer and the rest are matrix layers. The mesh size for the fracture layer represents the thickness of the synthetic fracture in the flooding experiment. The mesh size around the fracture layer is increase gradually to avoid numerical errors while modeling the core plug.

Fig. 4.6 compares the measured and simulated breakthrough curves of Ba through intact and fractured sandstone and dolomite cores at 0 salinity and at high concentration of a divalent ion (Ca^{2+}). The properties of cores are listed in Table 4.1.







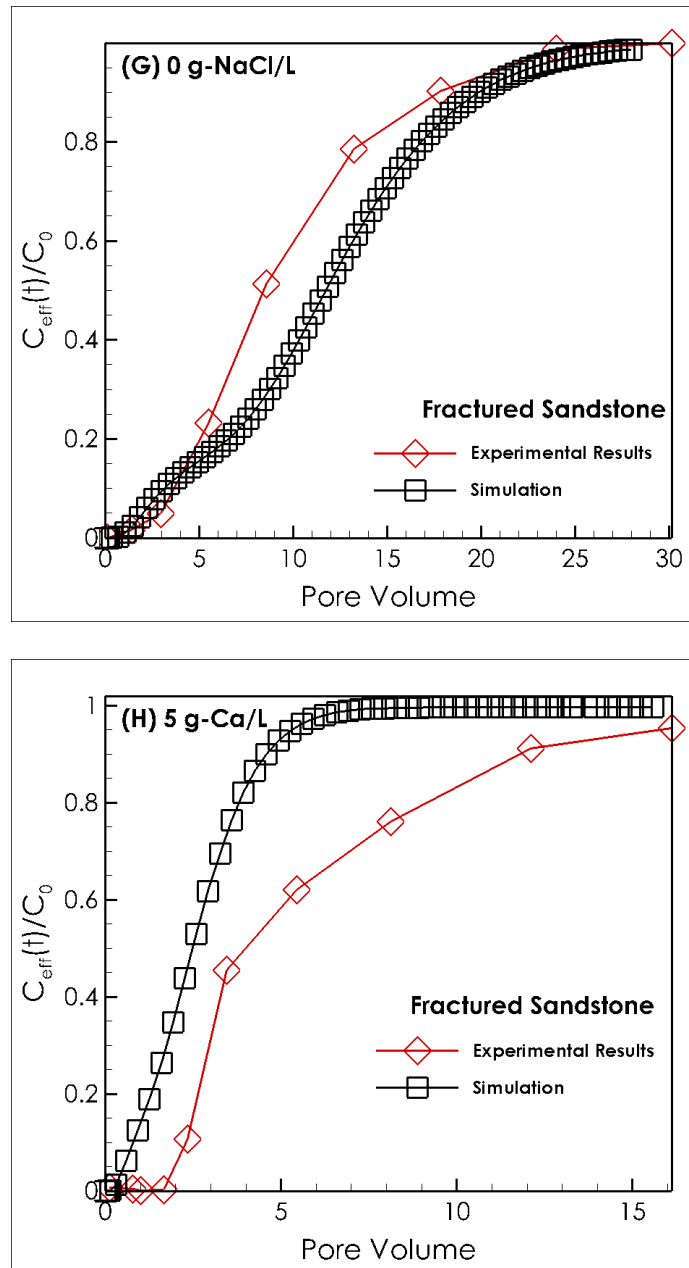


Fig. 4. 6. Experimental versus numerical breakthrough curves of Ba transport through intact/fractured dolomite and sandstone cores.

It is assumed that the sorption on the surface of fracture is equal to the sorption within the porous media. The graphical abstract shows a representative result of three-dimensional (3D) simulations of the core-flooding experiments obtained using constant K_d values for a fractured core plug. The

Graphical Abstract also illustrates how the distribution of Ba is faster through the fractured spacing with a higher permeability compare to the rest of the rock.

Although the model over-predict the sorption of Ba on dolomite and predicts a slower breakthrough curve for the dolomite, the simulated breakthrough curves of Ba exhibit reasonable agreement with the measured breakthrough curves of Ba through both intact (Fig. 4.6C&D) and fractured (Fig. 4.6G&H) sandstone cores. This is in agreement with the findings of Ebrahimi and Vilcáez (2018b) who suggested using an adjustable K_d for the simulation of core flooding experiments in dolomite rocks. The reason is due to the fact that the reactivity of dolomite is higher than sandstone. The pH of the solution within a highly reactive rock such as dolomite continuously changes with the injection of a new solution with a constant initial pH. Subsequently the pH variation affects the K_d of the experiments which is in contrast with the assumption of a constant K_d value in the simulation. It illustrated by Ebrahimi and Vilcáez (2018b) the batch experiments of Ba solutions with powdered dolomite and sandstone needs around 5 hours to reach the equilibrium. In case of core flooding experiments using short core plugs, where the solution is continuously injected into the core plugs, reaching to an equilibrium is very difficult.

4.6. Conclusions

We have described a study of the Ba transport through intact and fractured sandstone and dolomite. The transport of Ba not only is dependent to its chemical interactions with the surface of the rocks, but also is under significant influence of its mechanical transport through porous media. Although the chemical sorption of Ba on dolomite is higher than sandstone, the results of this study shows that it cannot be concluded that the Ba transport through sandstone is faster than dolomite. The experimental results of this study shows that, in general, the transport of Ba through sandstone was slower than through dolomite. This is because of the fact that the mechanical dispersion of solute through a high permeable rock such as sandstone was higher than a low permeable rock such as

dolomite. Hence, the distribution of Ba through sandstone is easier than dolomite which delays its transport. In case of having a fracture, the Ba flows faster through dolomite. This can be explained by easier distribution of Ba through sandstone matrix compare to the dolomite.

The ability of a reactive chemical transport model to predict Ba transport through the sandstone and dolomite is critically dependent upon availability of the data to characterize partition coefficient and the variation of available surface charge with pH. For the simple flooding experiment investigated here, the simulation proved relatively effective for sandstone. However for the dolomite which is dissolved by transporting the fluid through it, the pH of the solution changes by time. As a result the, simulation of Ba through dolomite is not as good as sandstone.

4.7. Acknowledgment

We thank to the Society of Petrophysicists and Well Log Analysts (SPWLA) and Geological Society of America (GSA), Unconventional Resources Special Interest Group (URSIG) for their financial support.

4.8. References

Berkowitz, B., 2002, Characterizing flow and transport in fractured geological media: A review: Advances in water resources, v. 25, no. 8-12, p. 861-884.

Bordas, J. M., 2005, Modeling Groundwater Flow and Contaminant Transport in Fractured Aquifers: AIR FORCE INST OF TECH WRIGHT-PATTERSON AFB OH SCHOOL OF ENGINEERING AND MANAGEMENT.

Cai, L., 2014, Matrix-fracture interaction analysis in fractured unconventional gas reservoir, Colorado School of Mines.

Dershowitz, W., La Pointe, P., and Doe, T., Advances in discrete fracture network modeling, in Proceedings Proceedings of the US EPA/NGWA fractured rock conference, Portland2004, p. 882-894.

Ebrahimi, P., and Vilcáez, J., 2018a, Effect of brine salinity and guar gum on the transport of barium through dolomite rocks: Implications for unconventional oil and gas wastewater disposal: Journal of environmental management, v. 214, p. 370-378.

-, 2018b, Petroleum produced water disposal: Mobility and transport of barium in sandstone and dolomite rocks: Science of The Total Environment, v. 634, p. 1054–1063.

EPA., U. S., 2016a, Hydraulic Fracturing for Oil and Gas: Impacts from the Hydraulic Fracturing Water Cycle on Drinking Water Resources in the United States (Final Report): U.S. Environmental Protection Agency, EPA/600/R-16/236F.

-, 2016b, Technical development document for the effluent limitations guidelines and standards for the oil and gas extraction point source category, EPA-820-R-16-003.

Erwinsyah, P., and Yan, F., 1999, STUDY OF WATERFLOODING PROCESS IN NATURALLY FRACTURED RESERVOIRS FROM STATIC AND DYNAMIC IMBIBITION EXPERIMENTS: ITB/New Mexico of Mining and Technology and David S. Schechter, New Mexico PRRC.

Fetter, C. W., Boving, T., and Kremer, D., 2017, Contaminant hydrogeology, Waveland Press.

Habibpour, M., and Clark, P. E., 2017, Drag reduction behavior of hydrolyzed polyacrylamide/xanthan gum mixed polymer solutions: Petroleum Science, v. 14, no. 2, p. 412-423.

Janssen, R., Peijnenburg, W. J., Posthuma, L., and Van Den Hoop, M. A., 1997, Equilibrium partitioning of heavy metals in Dutch field soils. I. Relationship between metal partition coefficients and soil characteristics: *Environmental Toxicology and Chemistry*, v. 16, no. 12, p. 2470-2478.

Kumar, G. S., 2008, Effect of sorption intensities on dispersivity and macro-dispersion coefficient in a single fracture with matrix diffusion: *Hydrogeology journal*, v. 16, no. 2, p. 235-249.

Maupin, M. A., Kenny, J. F., Hutson, S. S., Lovelace, J. K., Barber, N. L., and Linsey, K. S., 2014, Estimated use of water in the United States in 2010: US Geological Survey, 2330-5703.

Pruess, K., 1987, TOUGH user's guide, Nuclear Regulatory Commission: report NUREG/CR-4645 (also Lawrence Berkeley Laboratory Report LBL-20700, Berkeley, California).

-, 1991, Simulator, TOUGH2-A General-Purpose Numerical for Multiphase Fluid and Heat Flow: LBL Report, Berkeley, CA.

Rasmuson, A., and Neretnieks, I., 1981, Migration of radionuclides in fissured rock: The influence of micropore diffusion and longitudinal dispersion: *Journal of Geophysical Research: Solid Earth*, v. 86, no. B5, p. 3749-3758.

Tang, D., Frind, E., and Sudicky, E. A., 1981, Contaminant transport in fractured porous media: Analytical solution for a single fracture: *Water resources research*, v. 17, no. 3, p. 555-564.

Veil, J., 2015, US produced water volumes and management practices in 2012: Oklahoma City, OK: Ground Water Protection Council.

Veil, J. A., Puder, M. G., Elcock, D., and Redweik Jr, R. J., 2004, A white paper describing produced water from production of crude oil, natural gas, and coal bed methane: Argonne National Lab., IL (US).

Venture, S.-N. J., 2004, The Role of Dispersion in Radionuclide Transport-Data and Modeling Requirements: Revision No. 1: Stoller-Navarro Joint Venture; Nevada Test Site, Mercury, NV (US).

Wu, Y.-S., and Fakcharoenphol, P., A unified mathematical model for unconventional reservoir simulation, in Proceedings SPE EUROPEC/EAGE Annual Conference and Exhibition 2011, Society of Petroleum Engineers.

Wu, Y.-S., Liu, H., and Bodvarsson, G., 2004, A triple-continuum approach for modeling flow and transport processes in fractured rock: Journal of Contaminant Hydrology, v. 73, no. 1-4, p. 145-179.

Xu, T., Sonnenthal, E., Spycher, N., and Zheng, L., 2014, TOUGHREACT V3.0-OMP Reference manual: A parallel simulation program for non-isothermal multiphase geochemical reactive transport, Lawrence Berkeley Lab. Berkeley, California.

CHAPTER V

CONCLUSIONS AND RECOMMENDATIONS

The main objective of this dissertation was to provide a thorough understanding of the mobility and transport of Ba in deep saline aquifers where petroleum produced water (PPW) is commonly disposed in the USA. This research is important because PPW in the USA contains many organic and inorganic contaminants including heavy metals which could cause environmental risks. To reach the main objective of this dissertation, batch experiments were conducted to understand the chemical factors that control Ba sorption in sandstones and dolomites of saline aquifers, and core-flooding experiments were conducted to understand combined physical and chemical factors that control Ba transport in porous and fractured dolomites and sandstones. Experiments were performed at high salinities of PPW and at subsurface high pressure and temperature conditions. The experimental results were used to 1) formulate a surface complexation model to predict Ba sorption in dolomites, and 2) develop a reactive transport model to simulate the mobility and transport of Ba in dolomite and sandstone saline aquifers. This was achieved through the use of CrunchFlow and TOUGHREACT reactive transport simulators as frameworks.

The dissertation results were presented as three journal papers. In the following the main conclusions of these journal papers are provided followed by recommendations for future work.

5.1. Conclusions

5.1.1. Effect of brine salinity and guar gum on the transport of barium through dolomite rocks: implications for unconventional oil and gas wastewater disposal

Batch and core-flooding experiments were conducted to assess the effect of brine salinity and guar gum on the sorption and transport of Ba in dolomite rocks collected from the Arbuckle formation in Oklahoma, US.

At brine salinities of UOG wastewater, Ba sorption on dolomite is controlled by chloro-complexation reactions between Ba and Cl ions, and pH changes that results from dolomite dissolution. Chloro-complexation reactions between Ba and guar gum, competition of Ba with common cations (Ca and Mg) for hydration sites of dolomite, play a secondary role. Ba sorption on dolomite decreases with increasing brine salinity and increases with increasing pH. This mechanism of Ba sorption on dolomite can be represented by a sorption model that accounts for both surface complexation reactions on three distinct hydration sites ($>CaOH_o$, $>MgOH_o$, and $>CO_3H_o$), and the kinetic dissolution of dolomite.

Although, guar gum does not affect the transport of Ba through dolomite rocks of high flow properties, guar gum can retard the transport of Ba through tight dolomite rocks of low flow properties by clogging the pore throats of dolomite.

Collectively, the results of these research indicate that as a consequence of high brine salinities of UOG wastewater, the mobility of heavy metals such as Ba in deep dolomite saline aquifers might be much higher than the mobility of heavy metals observed in shallow aquifers where brine salinity is <500 mg/L. Contrary to shallow aquifers where organic polymers such as guar gum increases the mobility of heavy metals (Mittal et al., 2015; Pal et al., 2014; Thakur et al., 2014), in deep dolomite saline aquifers injected with UOG wastewater of high brine salinities (18,000-180,000

mg/L), depending on the flow properties of the dolomite rock, organic polymers might play a secondary role on the transport of heavy metals through porous dolomite rocks.

These results have large implications toward the elucidation of the physical feasibility of USDW contamination with heavy metals present in UOG wastewater disposed into deep dolomite saline aquifers. Studies on the effect of temperature and transport of heavy metals through fractures will follow.

5.1.2. Petroleum produced water disposal: mobility and transport of barium in sandstone and dolomite rocks

The following conclusions are withdrawn from the experimental and simulation studies conducted to assess the effect of salinity (NaCl), guar gum, competition of cations (Ca and Mg), and temperature on mobility of Ba in dolomite and sandstone and potential contamination of USDW:

Ba sorption is higher in highly pure dolomite than in quartz-dominated sandstone at both shallow (22 °C) and deep (60 °C) subsurface temperatures, and at both zero salinity and saline water containing NaCl Ca and Mg concentrations of petroleum produced water.

The difference in Ba sorption behavior between dolomite and sandstone significantly decreases with increasing salinity (NaCl) and/or the concentration of competing cations (Ca and Mg). At NaCl, Ca and Mg concentration levels of petroleum produced water, Ba sorption in both dolomite and sandstone is almost identical. This is due to the formation of $Ba(Cl)^+$ complexes as well as the competition of cations (Ca and Mg) for binding sites of minerals which results in the inhibition of Ba sorption.

Contrary to expectations, temperature does not play an important role in influencing the Ba sorption except under freshwater conditions represented by water with zero salinity. At NaCl, Ca and Mg concentration levels of petroleum produced water, temperature plays a minor role as observed from

the similarity of Ba sorption levels in both the dolomite and sandstone when shallow and deep subsurface temperatures are considered.

Because high pH conditions are known to increase the number of negatively charged binding sites of minerals, and higher pH conditions occurred in the batch sorption experiments with dolomite than with sandstone, higher levels of Ba sorption in dolomite than in sandstone observed at all experiment scenarios is attributed to higher chemical reactivity of dolomite relative to sandstone.

The sorption and thus transport of Ba in dolomite and sandstone aquifers is controlled by salinity (NaCl), followed by the competition of cations for binding sites of minerals, pH, and temperature. The presence of fracturing organic polymers such guar gum at possible concentrations in produced water from UOG reservoirs has very little influence on the sorption and thus mobility of Ba in deep dolomite and sandstone aquifers.

Because of its low chemical reactivity compared to dolomite, the mobility of Ba in sandstone saline aquifers can be successfully simulated by a reactive transport model that accounts for the influence of dissolution of minerals, aqueous phase complexation reactions, and sorption reactions represented by a constant partition coefficient (K_d) value. However, to obtain accurate prediction of the transport of Ba in dolomite saline aquifers, the fact that K_d changes as function of pH needs to be taken into account.

5.1.3. Transport of Barium through Fractured Sandstone and Dolomite Rocks in Petroleum Produced Water Disposal

I have described a study of the Ba transport through intact and fractured sandstone and dolomite. The transport of Ba not only is dependent to its chemical interactions with the surface of the rocks, but also is under significant influence of its mechanical transport through porous media. Although the chemical sorption of Ba on dolomite is higher than sandstone, the results of this study shows

that it cannot be concluded that the Ba transport through sandstone is faster than dolomite. The experimental results of this study shows that, in general, the transport of Ba through sandstone was slower than through dolomite. This is because of the fact that the mechanical dispersion of solute through a high permeable rock such as sandstone was higher than a low permeable rock such as dolomite. Hence, the distribution of Ba through sandstone is easier than dolomite which delays its transport. In case of having a fracture, the Ba flows faster through dolomite. This can be explained by easier distribution of Ba through sandstone matrix compare to the dolomite.

The ability of a reactive chemical transport model to predict Ba transport through the sandstone and dolomite is critically dependent upon availability of the data to characterize partition coefficient and the variation of available surface charge with pH. For the simple flooding experiment investigated here, the simulation proved relatively effective for sandstone. However for the dolomite which is dissolved by transporting the fluid through it, the pH of the solution changes by time. As a result the, simulation of Ba through dolomite is not as good as sandstone.

5.2. Recommendations for Future Studies

In this dissertation I was able to develop an understanding of the mobility and transport of Ba in porous and fractured sandstones and dolomites at high salinities of produced water and at high pressure and high temperature of disposal sites. In this section, I would like to introduce some of the questions whose investigation was beyond the scope and time limit of this PhD dissertation.

- In this study, I only focused on Ba, as the most common heavy metal found in produced water. However there are other frequent heavy metals in produced water such as As, Se and Sr. The same experimental and computational analysis done for Ba can be done in the future for As, Se and Sr.
- Many experiments were conducted using synthetic, intact and fractured rocks. The employed approach allows the investigation of solute transport under controlled

conditions. I suggest conducting more core-flooding experiments using similar approach using sandstone and dolomite rocks of different mineral composition and flow properties.

- Ba transport through fractured rocks was analyzed by generating one single discrete fracture along the longitudinal axis of core plugs. However, in reality fractures can be distributed in all three directions. I suggest conducting core-flooding experiments on core plugs with fractures in the three directions.
- More studies are needed to investigate the effect of hydration site densities (pores and fractures) on Ba sorption.
- The concentration of clay minerals in the dolomite and sandstones used in this study was <1%. Clay minerals can greatly increase the availability of hydration (binding) sites of dolomites and sandstones. More studies are needed using dolomites and carbonates containing higher concentrations of clay minerals.
- Reactive transport modeling and simulations were used to interpret the batch and core-flooding experimental results. I recommend the application of the developed surface complexation and reactive transport models to simulate the mobility and transport of Ba at the field-scale.

VITA

Pouyan Ebrahimi Lialekol

Candidate for the Degree of

Doctor of Philosophy

Thesis: STUDIES ON THE MOBILITY AND TRANSPORT OF BARIUM PRESENT IN UNCONVENTIONAL PETROLEUM PRODUCED WATER DISPOSED INTO SALINE AQUIFERS

Major Field: Geology

Biographical:

Education:

Completed the requirements for the Doctor of Philosophy in Geology at Oklahoma State University, Stillwater, Oklahoma in May, 2018.

Completed the requirements for the Master of Science in Geology at Oklahoma State University, Stillwater, Oklahoma in 2015.

Completed the requirements for the Master of Science in Petroleum Exploration Engineering at Sahand University of Technology, Sahand, Iran in 2011.

Completed the requirements for the Bachelor of Science in Petroleum Exploration Engineering at Petroleum University of Technology, Abadan, Iran in 2008.

Experience: Graduate Teaching and Research Associate at Oklahoma State University, Petrophysicist at Iranian Central Oil Fields Company, Tehran, Iran, Seismic Interpreter at Iranian Central Oil Fields Company, Geophysicist Intern at Research Institute of Petroleum Industry, Mud Logging Intern at National Iranian Oil Company

Professional Memberships: Society of Petrophysicists and Well Log Analysts, Society of Exploration Geophysicists, Geological Society of America, American Geophysical Union, American Association of Petroleum Geologists, National Association of Black Geoscientists Society of Petroleum Engineers, American Petroleum Professionals of Iranian Heritage